

Copyright Warning & Restrictions

The copyright law of the United States (Title 17, United States Code) governs the making of photocopies or other reproductions of copyrighted material.

Under certain conditions specified in the law, libraries and archives are authorized to furnish a photocopy or other reproduction. One of these specified conditions is that the photocopy or reproduction is not to be “used for any purpose other than private study, scholarship, or research.” If a user makes a request for, or later uses, a photocopy or reproduction for purposes in excess of “fair use” that user may be liable for copyright infringement,

This institution reserves the right to refuse to accept a copying order if, in its judgment, fulfillment of the order would involve violation of copyright law.

Please Note: The author retains the copyright while the New Jersey Institute of Technology reserves the right to distribute this thesis or dissertation

Printing note: If you do not wish to print this page, then select “Pages from: first page # to: last page #” on the print dialog screen

The Van Houten library has removed some of the personal information and all signatures from the approval page and biographical sketches of theses and dissertations in order to protect the identity of NJIT graduates and faculty.

ABSTRACT

SEPARATION OF VARIOUS ORGANIC-ORGANIC AND AQUEOUS-ORGANIC SOLUTIONS VIA PERVAPORATION

by
John Tang

Pervaporation, an energy saving separation process, can be useful in pharmaceutical processing. However, the organic solvents involved in pharmaceutical product synthesis are chemically demanding; very few polymers are able to withstand them. An ideal membrane would be polymeric having a high thermal, chemical and mechanical stability. Such a membrane is made of a copolymer of polydimethyldioxole and tetrafluoroethylene known as PDD-TFE of the CMS-3 variety with a very high free volume. This novel membrane is used to separate a variety of organic-organic and aqueous-organic mixtures. An earlier study based on water-ethanol-isopropanol has shown evidence that the membrane selectivity may be based on size exclusion. Thus, solvents with larger molecular dimensions may not be able to penetrate the membrane and remain in the feed; the permeate is enriched in the molecularly smaller solvent. Separation systems of methanol-toluene, ethyl acetate-toluene, tetrahydrofuran (THF)-toluene, N,N-dimethylformamide (DMF)-water, N,N-dimethylacetamide (DMAc)-water and N,N-dimethylsulfoxide (DMSO)-water are explored using a 25 μm thick PDD-TFE membrane at various temperatures and feed compositions. Depending on the system, a wide range of separation factors (α_{ij}) are achieved.

The highest water-organic solvent separation factors are obtained in the dehydration of aprotic solvents. A feed containing of 99 wt% DMAc and 1 wt% water would yield an α_{ij} of 12,373 for water at 50°C. For mixtures of DMSO and water, similar

performance has been observed resulting in an α_{ij} of 8,834. For systems of DMF and water, the highest α_{ij} of 12,514 is achieved at 50°C with a feed containing 90 wt% DMF and 10 wt% water. Separation of a 95 wt% THF and 5 wt% water feed at 50°C results in a separation factor of 497. Compared to the results for aprotic solvent systems with water, separation of the organic-organic mixtures yielded limited performance. The PDD-TFE membrane is selective for methanol over toluene with an α_{ij} of 7.8 at 30°C for a 72.6 wt%–27.4 wt% toluene-methanol feed. Very poor separation is observed for THF–toluene mixtures. The maximum α_{ij} is 1.6 at 50°C using a 25 wt%–75 wt% toluene–THF feed. For mixtures of ethyl acetate and toluene, an almost constant α_{ij} of 6 is found at all temperatures and compositions. For water for systems of DMAc and DMSO, water fluxes range from 4.0 to 9.8 g/(m²-h). In DMF-water mixtures, water exhibits significantly higher flux at 77 g/(m²-h). For most other solvents, permeation through the membrane is relatively small, 5 g/(m²-h) at maximum.

Overall permeability coefficients for solvents studied correlate a relationship with the longest molecular solvent size. Such a correlation describes permeation of highly polar solvents such as methanol only when methanol dimerization in the highly hydrophobic membrane is postulated. Analysis of the permeability coefficient shows a decreasing trend with temperature, unlike that of traditional glassy polymers. This is affected by Langmuir sorption of all solvents onto the membrane including water.

Dehydration of this novel membrane has also been explored for other solvent mixtures such as water–ethylene glycol, and acetone–butanol–ethanol–water. Very high α_{ij} values have been determined; 12,800 for water–ethylene glycol, 7,180 for water–butanol, 900 for water–ethanol, and 235 for water–acetone have been observed at 30°C.

**SEPARATION OF VARIOUS ORGANIC-ORGANIC AND
AQUEOUS-ORGANIC SOLUTIONS VIA PERVAPORATION**

**by
John Tang**

**A Dissertation
Submitted to the Faculty of
New Jersey Institute of Technology
in Partial Fulfillment of the Requirements for the Degree of
Doctor of Philosophy in Chemical Engineering**

Department of Chemical, Biological, and Pharmaceutical Engineering

January 2013

Copyright © 2013 by John Tang

ALL RIGHTS RESERVED

APPROVAL PAGE

**SEPARATION OF VARIOUS ORGANIC-ORGANIC AND
AQUEOUS-ORGANIC SOLUTIONS VIA PERVAPORATION**

John Tang

Dr. Kamalesh K. Sirkar, Dissertation Advisor Date
Distinguished Professor of Chemical, Biological, and Pharmaceutical Engineering, NJIT

Dr. Piero Armenante, Committee Member Date
Distinguished Professor of Chemical, Biological, and Pharmaceutical Engineering, NJIT

Dr. Somenath Mitra, Committee Member Date
Distinguished Professor of Chemistry, NJIT

Dr. Boris Khusid, Committee Member Date
Professor of Chemical, Biological, and Pharmaceutical Engineering, NJIT

Dr. Xianqin Wang, Committee Member Date
Assistant Professor of Chemical, Biological, and Pharmaceutical Engineering, NJIT

BIOGRAPHICAL SKETCH

Author: John Tang
Degree: Doctor of Philosophy
Date: January 2013

Undergraduate and Graduate Education:

- Doctor of Philosophy in Chemical Engineering,
New Jersey Institute of Technology, Newark, NJ, 2012
- Bachelor of Engineering,
The Cooper Union, New York, NY, 2006

Major: Chemical Engineering

Presentations and Publications:

Tang, J., Sirkar, K.K., Majumdar, S., Permeation and sorption of organic solvents and separation of their mixtures through an amorphous perfluoropolymer membrane in pervaporation, submitted for publication.

Tang, J., Sirkar, K.K., Perfluoropolymer membrane behaves like a zeolite membrane in dehydration of aprotic solvents, *J. Membr. Sci.* 421 – 422 (2012) 211 – 216.

Tang, J., Sirkar, K.K., Perfluorinated Membranes for Pharmaceutical Processing, Presented at North American Membrane Society Annual Meeting, Session: Pervaporation/Vapor Separation, Paper #26b. Louisiana, New Orleans. 2012 June 13th.

Roy, S., Thongsukmak A., Tang, J., Sirkar, K., Concentration of aqueous hydrogen peroxide solution by pervaporation, *J. Membr. Sci.* 389 (2012) 17 – 24.

Tang, J., Sirkar, K.K., Perfluorinated Membranes for Pervaporation Separation of Organic Solvent Mixtures in Pharmaceutical Processing, Presented at American Institute of Chemical Engineers (AIChE) Annual Meeting, Session 576: 02D07 Characterization and Simulation of Novel Membranes and Simulations, Minneapolis, Minnesota. 2011 October 19th.

To my family and friends

ACKNOWLEDGMENT

I would like to thank, first and foremost, Professor Sirkar for being my advisor and providing me with much support so my research may be on the forefront of membrane science and technology. Without his knowledge and guidance, I would not be able to even begin my foray into higher level study. His reputation in research often overshadows his equally great ability to create opportunities and motivate his students to pursue far reaching goals.

Additionally, I would like to thank Dr. Boris Khusid, Dr. Somenath Mitra, Dr. Piero Armenante and Dr. Xianqin Wang who were gracious enough to act as my committee members. Each of them was able to utilize their expertise and background to provide constructive criticism and invaluable recommendations throughout different stages of this work. I would also like to thank Dr. Reginald Tomkins for his guidance during my early career at the New Jersey Institute of Technology.

Further thanks are needed to given to the Center of Membrane Technology at NJIT, Lynntech Corporation, National Science Foundation, Membrane Science, Engineering & Technology Center and Compact Membrane Systems Incorporated. All of these organizations, in concert, have helped generate the opportunity as well as provide a sustainable environment in which I may contribute to the scientific community with my research and complete my graduate degree.

Finally, I would like to thank all of my colleagues and co-workers for their technical support, but not limited to Dr. Atsawin Thongsukmak, Dr. Gordana Obuskovic, Dr. Dhananjay Singh, Jose Sousa, and George Barnes.

TABLE OF CONTENTS

Chapter	Page
1 INTRODUCTION.....	1
1.1 Pervaporation Process.....	2
1.2 Applications of Pervaporation	3
1.2.1 Organic Solvent Dehydration.....	3
1.2.2 Dilute Organic Removal from Aqueous Solutions.....	3
1.2.3 Organic – Organic Separation.....	4
1.3 Desirable Properties of a Membrane System for Pervaporation Process.....	4
1.4 Previous Studies for Membranes Used for Pervaporation Process.....	4
1.4.1 Polymeric Membranes.....	5
1.4.2 Ceramic Membranes and Non-Metallic Membranes.....	8
1.4.3 Liquid Membranes.....	10
1.5 Objectives of This Thesis	12
1.6 Approach.....	13
2 EXPERIMENTAL.....	17
2.1 Membranes, Chemicals and Instruments.....	17
2.1.1 Membranes.....	17
2.1.2 Chemicals.....	17
2.1.3 Instruments Used.....	17
2.2 Fabrication of Flat Membrane Cell.....	18

TABLE OF CONTENTS
(Continued)

Chapter	Page
2.3 Experimental Procedure for Pervaporation.....	19
2.4 Permeate Sampling.....	20
2.5 Permeate Analysis.....	21
2.6 Solubility Analysis of Pure Components.....	26
2.7 Solubility Analysis of Mixtures.....	26
2.8 Definitions of Flux and Separation Factor.....	29
3 RESULTS AND DISCUSSION OF THE PERVAPORATION PERFORMANCE OF PDD-TFE MEMBRANE FOR APROTIC SOLVENT-WATER SYSTEMS.....	32
3.1 Performance of PDD-TFE Membrane for Pure Aprotic Solvents.....	38
3.2 Performance of PDD-TFE Membrane on Dehydration of Aprotic Solvents.....	39
4 RESULTS AND DISCUSSION OF THE PERVAPORATION PERFORMANCE OF PDD-TFE MEMBRANE FOR ORGANIC-ORGANIC SYSTEMS.....	57
4.1 Performance of PDD-TFE Membrane on Pure Organic Solvents.....	59
4.1.1 Sorption of Pure Components onto PDD-TFE Membrane.....	59
4.1.2 Pervaporation Results of Pure Organic Solvents using PDD-TFE Membrane.....	60
4.2 Performance of PDD-TFE Membrane to Separate Organic-Organic Systems...	72
4.2.1 Sorption of Organic-Organic Mixtures onto PDD-TFE Membrane.....	72
4.2.2 Pervaporation Results Separating Organic-Organic Systems using PDD-TFE Membrane.....	73
5 ALTERNATIVE USES OF PDD-TFE MEMBRANE IN DEHYDRATION.....	85
5.1 Dehydration of Volatile Organic Compounds (VOCs)	85

TABLE OF CONTENTS
(Continued)

Chapter	Page
5.2 Dehydration of Ethylene Glycol.....	90
6 GENERAL CONCLUSIONS AND RECOMMENDATION FOR FUTURE STUDIES.....	93
APPENDIX A ESTIMATION OF SOLUBILITY PARAMETERS IN GLASSY POLYMERS.....	97
APPENDIX B EXPERIMENTAL DATA.....	103
APPENDIX C SAMPLE CALCULATIONS.....	110
REFERENCES.....	116

LIST OF TABLES

Table	Page
3.1 Structural Dimensions and Physical Properties of Various Aprotic Solvents, and Water Used as a Comparison.....	34
3.2 Activity Coefficients for N,N-Dimethylformamide and Water at Various Temperatures and Compositions.....	37
3.3 Activity Coefficients for N,N-Dimethylacetamide and Water at Various Temperatures and Compositions.....	37
3.4 Activity Coefficients for N,N-Dimethylsulfoxide and Water at Various Temperatures and Compositions.....	37
3.5 Gas Sorption Parameters of Teflon AF 2400 by Merkel et al.....	56
4.1 Various Properties and Structural Dimensions of a Few Organic Solvents.....	58
4.2 Solubility of Pure Components by Weight at Room Temperature.....	60
4.3 Solubility of Mixtures by Composition.....	73
4.4 Solvent Activity Coefficients at Varying Compositions and Temperatures.....	76
5.1 Molecular Dimensions of ABE Solvents and Water.....	88
B.1 Experimental Data for DMAc (99 wt%) – Water (1 wt%) Systems.....	104
B.2 Experimental Data for DMAc (95 wt%) – Water (5 wt%) Systems.....	104
B.3 Experimental Data for DMAc (90 wt%) – Water (10 wt %) Systems.....	105
B.4 Experimental Data for DMF (10 wt%) – Water (90 wt%) Systems.....	105
B.5 Experimental Data for DMF (95 wt%) – Water (5 wt%) Systems.....	105
B.6 Experimental Data for DMF (99 wt%) – Water (1 wt%) Systems.....	106
B.7 Experimental Data for DMSO (90 wt%) – Water (10 wt%) Systems.....	106
B.8 Experimental Data for DMSO (95 wt%) – water (5 wt%) Systems.....	106

LIST OF TABLES
(Continued)

Table	Page
B.9 Experimental Data for DMSO (99 wt%) – Water (1 wt%) Systems.....	107
B.10 Experimental Data for Methanol (25 wt%) – Toluene (75 wt%) Systems.....	107
B.11 Experimental Data for Methanol (50 wt%) – Toluene (50 wt%) Systems.....	107
B.12 Experimental Data for Methanol (75 wt%) – Toluene (25 wt%) Systems.....	108
B.13 Experimental Data for THF (25 wt%) – Toluene (75 wt%) Systems.....	108
B.14 Experimental Data for THF (50 wt%) – Toluene (50 wt%) Systems.....	108
B.15 Experimental Data for THF (75 wt %) – Toluene (25 wt%) Systems.....	109
B.16 Experimental Data for Ethyl Acetate (25 wt%) – Toluene (75 wt%) Systems.....	109
B.17 Experimental Data for Ethyl Acetate (50 wt%) – Toluene (50 wt%) Systems.....	109
B.18 Experimental Data for Ethyl Acetate (75 wt%) – Toluene (25 wt%) Systems.....	110
B.19 Experimental Data for a Synthetic ABE Feed Containing Water.....	110
C.1 Activity Coefficients for a 72.6 – 26.4 wt% Methanol-Toluene Mixture.....	111

LIST OF FIGURES

Figure	Page
1.1 Schematic drawing of the pervaporation process	3
2.1 Top view schematic of the flat membrane cell.....	19
2.2 Side view schematic of the flat membrane cell.....	19
2.3 Schematic diagram of the experimental pervaporation set up.....	20
2.4 Calibration curve of toluene in n-butanol.....	22
2.5 Calibration curve of tetrahydrofuran in n-butanol.....	23
2.6 Calibration curve of methanol in n-butanol.....	23
2.7 Calibration curve of ethyl acetate in n-butanol.....	24
2.8 Calibration curve of N,N-dimethylformamide in N,N-dimethylsulfoxide.....	24
2.9 Calibration curve of N,N-dimethylsulfoxide in N,N-dimethylformamide.....	25
2.10 Calibration curve of N,N-dimethylacetamide in N,N-dimethylformamide.....	25
2.11 Headspace calibration curve of toluene in n-butanol.....	27
2.12 Headspace calibration curve of tetrahydrofuran in n-butanol.....	27
2.13 Headspace calibration curve of ethyl acetate in n-butanol.....	28
2.14 Headspace calibration curve of methanol in n-butanol.....	28
3.1 Vapor pressure of aprotic solvents and water versus temperature.....	33
3.2 Reduction of diffusion coefficient with increasing critical volume of gases for Hyflon AD.....	35
3.3 Size dependent permeability of organic solutes through Teflon AF films.....	36
3.4 Comparison of aprotic solvent fluxes as a function of temperature for 90 wt% solvent and 10 wt% water solution.....	40
3.5 Solvent flux for N,N-dimethylacetamide and water with respect to temperature..	42

LIST OF FIGURES
(Continued)

Figure	Page
3.6 Solvent flux for N,N-dimethylsulfoxide and water with respect to temperature...	43
3.7 Solvent flux for N.N-dimethylformamide and water with respect to temperature.	43
3.8 Separation factor of water over aprotic solvent plotted against feed composition.	45
3.9 Separation factor of water over N,N-dimethylformamide plotted against feed composition.....	46
3.10 Calculations of permeance of PDD-TFE membrane compared to NaA zeolite data from Shah et al. for DMF-water systems.....	48
3.11 Separation factor of THF-water systems varying with feed concentration.....	49
3.12 Flux values for THF-water systems as a function of temperature.....	50
3.13 Permeability coefficient of water and DMF plotted against temperature for a 90 wt % DMF-10 wt% water feed.....	51
3.14 Typical behavior of solubility coefficient as a function of temperature.....	52
3.15 Typical behavior of diffusion coefficient as a function of temperature.....	53
3.16 Typical behavior of overall permeability coefficient as a function of temperature.....	53
3.17 Methane solubility into a polymeric membrane as a function of temperature and pressure.....	55
3.18 Langmuir sorption parameter as a function of increasing temperature.....	55
4.1 Vapor pressure of common organic solvents and water versus temperature.....	58
4.2 Flux of pure methanol through the PDD-TFE membrane as a function of temperature.....	61
4.3 Overall permeability coefficient of methanol as a function of temperature.....	62
4.4 Flux of pure ethyl acetate through the PDD-TFE membrane as a function of temperature.....	63

**LIST OF FIGURES
(Continued)**

Figure	Page
4.5 Overall permeability coefficient of ethyl acetate as a function of temperature.....	64
4.6 Flux of pure tetrahydrofuran through the PDD-TFE membrane as a function of temperature.....	65
4.7 Overall permeability coefficient of tetrahydrofuran as a function of temperature.	66
4.8 Flux of pure toluene through the PDD-TFE membrane as a function of temperature.....	67
4.9 Overall permeability coefficient of toluene as a function of temperature.....	67
4.10 Increasing flux observed with temperature for pure organic solvents between 30 to 70°C.....	68
4.11 Decreasing permeability coefficient with temperature for pure solvent components through a PDD-TFE membrane.....	69
4.12 Permeability coefficient as a function of a single dimension, longest molecular diameter.....	70
4.13 Permeability coefficients for pure solvents calculated on a per gram mole basis as a function longest molecular diameter.....	71
4.14 A plot of the natural log of the permeability coefficient to determine the permeation energy of pure solvents e.g., toluene, THF, ethyl acetate and methanol.....	72
4.15 Flux behavior of toluene and ethyl acetate at varying compositions with respect to temperature.....	75
4.16 Separation factor of the PDD-TFE membrane as a function of feed composition for systems of ethyl acetate and toluene at varying temperatures.....	78
4.17 Decreasing permeability coefficient with temperature for ethyl acetate-toluene systems through a PDD-TFE membrane.....	78
4.18 Separation factor of the PDD-TFE membrane as a function of feed composition for systems of methanol and toluene at varying temperatures.....	79

**LIST OF FIGURES
(Continued)**

Figure	Page
4.19 Flux behavior of toluene and methanol at varying compositions with respect to temperature.....	80
4.20 Decreasing permeability coefficient with temperature for methanol-toluene systems through a PDD-TFE membrane.....	81
4.21 Separation factor of the PDD-TFE membrane as a function of feed composition for systems of tetrahydrofuran and toluene at varying temperatures.....	82
4.22 Flux behavior of toluene and THF at varying compositions with respect to temperature.....	82
4.23 Decreasing permeability coefficient with temperature for THF-toluene systems through a PDD-TFE membrane.....	83
5.1 Flux of acetone, n-butanol, ethanol and water through a PDD-TFE membrane as a function of temperature.....	87
5.2 Separation factor of the PDD-TFE membrane of water over VOCs as a function of temperature.....	89
5.3 Separation factor of a PDD-TFE membrane for ethylene glycol-water systems...	91
5.4 Flux across a PDD-TFE membrane for ethylene glycol-water system.....	92
A.1 Retention diagrams for n-alkanes in (a) AF1600 and (b) AF2400.....	100

LIST OF SYMBOLS

©	Copyright
Å	Angstrom (10^{-10} meters)
≈	Approximately
A_m	Effective area of membrane
C_i	Concentration of solvent i by mass
J_i	Flux of i in $\text{g}/(\text{m}^2\text{-h})$
P_{perm}	Pressure on the permeate side
P_i^{sat}	Saturated vapor pressure of solvent i at a given temperature
x_i	Mole fraction of solvent i, in feed
y_i	Mole fraction of solvent i, in permeate
y_{if}	Weight fraction of solvent i in the feed
Q_i	Permeability coefficient of solvent i in $\text{g}\cdot\text{m}/(\text{m}^2\text{-h}\cdot\text{mm Hg})$
R	Ideal gas constant ($8.314 \text{ J}\cdot\text{K}^{-1}\cdot\text{mol}^{-1}$)
T	Operating temperature
E_p	Energy of permeation, kJ/mol
K_w	Permeance of water
C_{im}	Concentration of species i in the membrane
S_{im}, k_D	Henry's Law sorption parameter

LIST OF SYMBOLS
(Continued)

C'_{Hi}	Langmuir sorption capacity
b_i	Langmuir sorption parameter
C_D, C_H	Concentration due to Henry's Law or Langmuir sorption
N	Molar flux
a_i	Activity of species i
T_g	Glass transition temperature of a polymer
K_{ij}	Binary interaction parameter between a solute and solvent.

Greek Symbols

γ	Activity coefficient
δ	Membrane thickness in meters
ρ	Density, g/cm^3
α_{ij}	Separation factor by weight fraction
α^*	Separation factor by mole fraction
$\Delta\mu_i$	Chemical potential of dissolution of solute i
χ	Flory-Huggins interaction parameter
χ^∞	Flory-Huggins interaction parameter at infinite dilution
φ_i	Volume fraction of species i

LIST OF DEFINITIONS

GPU

$$10^{-6} \frac{cm^3}{cm^2 \cdot sec \cdot cmHg}$$

Barrer

$$10^{-10} \frac{cm^3(STP) \cdot cm}{sec \cdot cm^2 \cdot cmHg}$$

CHAPTER 1

INTRODUCTION

The pharmaceutical industry synthesizes drugs in mass quantities using a wide variety of organic solvents. The characteristics of solvents can be simple organic compounds such as alcohols as well as harsh ones such as N,N-dimethylsulfoxide. Separation of organic solvents is desired in the industry to optimize production economically. Re-use or reclaiming pure solvent from mixtures are viable alternatives when compared to acquiring pure solvent from other sources and proceeding with the necessary protocols for the disposal of mixed solvents. Several separation techniques are available for organic-organic mixtures like distillation, solvent extraction, adsorption and other membrane-based processes. Still, initial capital and continued operating costs of these processes may exceed that of replacement and disposal of the said mixtures. Thus, discovering a cost-effective and efficient means of separation is of great importance. For example, distillation is able to achieve high performance as well as being able to produce large amounts of highly pure solvents. At the same time, it is unable to handle azeotropes that may occur in mixtures and is associated with significantly higher costs compared to other methods. Membrane-based separation techniques involving zeolites often are characterized by having high chemical resistant properties with high performance as well as low operational costs. This approach seems more relevant than distillation, however, zeolite membranes typically introduce economical issues when scaling up to commercial sized processes [1].

Developing a polymeric membrane-based solution has great potential in separating mixtures found in the pharmaceutical industry. A polymeric material would avoid high manufacturing costs often associated with ceramic membranes or zeolites. Specifically, pervaporation is such a technique that can utilize these membranes and accommodate numerous solvents present in the process of drug synthesis. However, the polymeric membrane must be able to handle chemically demanding solvents as well as possess high selectivity and large capacity for flux.

1.1 Pervaporation Process

Pervaporation can be described as a process in which a liquid mixture undergoes a phase change while simultaneously separating its components through a membrane. A liquid feed mixture contacts the membrane. At the same time, a vacuum is pulled on the opposite face of the membrane known as the permeate side. As this occurs, solvent molecules, in which the membrane is more preferential for, may be sorbed onto the membrane upon contact. These molecules then diffuse through the matrix of the membrane. As they approach the permeate side of the membrane, solvent molecules desorb from the membrane and are then condensed into a lower energy state by way of rapid cooling. Permeation through the membrane is driven by the difference in the partial pressure of the liquid feed component and that of the corresponding vapor on the permeate side.

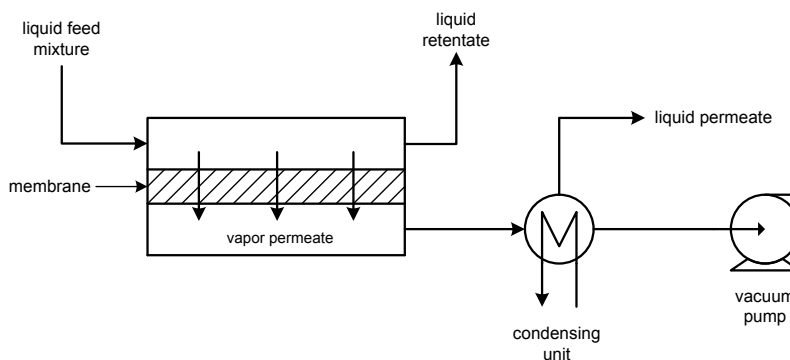


Figure 1.1 Schematic drawing of the pervaporation process.

1.2 Applications of Pervaporation

1.2.1 Organic Solvent Dehydration

Pervaporation can be used to remove small quantities of water from solutions largely composed of organic solvent. Numerous studies have been done to separate water from ethanol for fuel production. Typically, membranes selected for this purpose have been hydrophilic. This allows for water to be preferentially adsorbed by the membrane and prevents other insoluble solvents from entering the permeate side stream. Materials such as polyvinylalcohol (PVA) and modified membranes of PVA have been used for dehydration [2].

1.2.2 Dilute Organic Removal from Aqueous Solutions

Another use for pervaporation is to separate small amounts of organic solvents from aqueous solutions. A popular field of study is the recovery of volatile organic compounds such as ethanol, butanol and acetic acid. Membranes that are highly hydrophobic have produced desirable results for this application. Polydimethylsiloxane (PDMS) is one such membrane that is able to selectively remove organics from aqueous solutions.

1.2.3 Organic – Organic Separation

Particular membranes may demonstrate a strict preference for one solvent over another. Selectivity, in this case, is beyond simple solubility of hydrophilic and hydrophobic solvents. Separation occurs when the preferred solvent absorbs, diffuses and desorbs quicker than the other solvents present in the mixture.

1.3 Desirable Properties of a Membrane System for Pervaporation Process

- Has high stability to retain membrane transport characteristics for separation
- Exhibits high selectivity for the compounds of interest
- Demonstrates large flux for the desired solvent(s)

1.4 Previous Studies of Membranes Used for Pervaporation Process

The main objective of this thesis is to develop a high performing, polymeric pervaporation system for separating various solvents used in the pharmaceutical industry. A viable system would emphasize the application of a polymeric membrane able to withstand these industrial solvents that are often detrimental to a majority of membranes currently available. To understand the specific need to develop such a system, one must also know the different types of materials used to manufacture membranes. Two branches of membranes exist, organic and synthetic. Organic membranes can be described as those that occur naturally; cellulose can be considered an organic membrane. However, for commercial applications, synthetic membranes have found greater success due to ease of production and higher stability. Subsets of these types include polymeric, ceramic, and liquid membranes. Of the three, polymeric and ceramic membranes are

significantly more popular to separate organic-organic and organic-aqueous systems via pervaporation.

1.4.1 Polymeric Membranes

Polymeric membranes are known for their great processing ability. This, in turn, makes them the most cost-effective membrane from a manufacturing standpoint. Polymeric membranes are polymers whose structure and characteristics are tailored towards separation processes. Polymers consist of long chains of repeating units known as monomers. Side groups present on the monomers, nature of the monomers, and the overall length of the chains are factors that ultimately determine physical characteristics such as the degree of hydrophilicity or hydrophobicity, fractional free volume, and glass transition temperature. Some physical characteristics that are important for use as a membrane include porosity, thermal and chemical resistance. Molecular transport through porous membranes heavily depends on pore size, tortuosity and membrane thickness. For non-porous membrane materials, this is typically defined by solution-diffusion across the membrane. Advancements in polymer chemistry and processing have significantly increased the variety of polymers for a wide range of uses. Traditional polymers, or homopolymers, utilize a single molecule as their monomers. Composites of these can be formed by melting, mixing and cooling polymers together at various concentrations. In this way, their physical attributes can be altered for higher performance. This method of devising unique membranes has been furthered with the development of co-polymers. Co-polymers are able to incorporate two or more different molecules as monomers. Being able to utilize different combinations of molecules as monomers greatly enhances the number of possible of polymers and their applications.

Panek and Konieczny [3] have studied composite polydimethylsiloxane (PDMS) membranes containing varying amounts of carbon black. This is used to separate aqueous mixtures of toluene, acetone and ethyl acetate in pervaporation. Flux values for toluene, acetone, ethyl acetate and water are 5.59, 2.30, 5.04 and 286.40 g/(m²-h), respectively. Selectivity values for organic solvents are rather high for toluene and ethyl acetate, about 105 and 75.

Villaluenga et al. [4] have utilized coextruded linear low-density polyethylene to separate mixtures of methanol, ethanol and propanol with toluene. These membranes have been found to be preferentially selective for toluene instead of lower molecular weight alcohols. The maximum selectivity value is 66 for mixtures of methanol and propanol with lower concentrations of toluene. Toluene flux has been reported as being between 0.1 and 1.4 kg/(m²-h).

Lue et al. [5] have synthesized composites of polyurethane (PU) and polydimethylsiloxane (PDMS) to separate azeotropic mixtures of methanol and toluene. Using pervaporation, this has resulted in very high flux for toluene, 113.14 kg μm/(m²-h), but also very poor separation. The selectivity factor reaches a maximum value of about 12 for mixtures with around 10% toluene in the feed. For a feed concentration of 32% toluene, the selectivity factor dramatically decreases to 3.66. This has been attributed to swelling of the membrane caused by toluene. The swollen membrane allows more permeation of methanol through, reducing separation of the feed mixture.

Zhou et al. [6] have had early success in using composites of polypyrrole (PPy) membranes for the removal of methanol from organic solvents. These organic selected solvents are toluene, isopropyl alcohol and methyl tert-butyl ether (MTBE). Polypyrrole

membranes doped with hexafluorophosphate demonstrate high selectivity for methanol for mixtures of toluene and methanol, 560 for a feed concentration of 5% methanol. Methanol flux is considerably large as well, 230 g/(m²-h), under the same conditions. As for toluene, flux remains significantly lower, having values between 6 to 7.5 g/(m²-h).

Ray and Ray [7] have modified natural rubber (NR) and poly(styrene-co-butadiene) rubber (SBR) with sulfur and crosslinked with high abrasion carbon black filler at varying doses. These are used to separate solely mixtures of methanol and toluene heavily concentrated in methanol, at least 89 wt%. Both rubbery membranes exhibit moderate flux, 20.814 g/(m²-h) for SBR and 10.26 g/(m²-h) for natural rubber. The membrane shows the highest performance when separating mixtures with very small quantities of toluene in the feed. At 0.55 wt%, toluene-methanol selectivity factors have been determined to be 183.7 for a SBR-based membrane and 286.4 for a natural rubber one.

Mandal et al. [8] have looked at pervaporation to separate mixtures of methanol-benzene and methanol-toluene. A wide range of membranes, both hydrophilic and hydrophobic, are used to compare the performance for this application. These membranes include cellulose, poly (vinyl alcohol) PVA, cellulose acetate (CA), cellulose tri-acetate (CTA), poly (dimethylsiloxane) and linear low density polyethylene (LLDPE). For hydrophilic membranes, cellulose is found to be highest performing membrane, having selectivity factors of ~1,200 and ~145 for methanol-toluene and methanol-benzene separation, respectively. These membranes have been preferential for methanol over organic solvents. For hydrophobic membranes, it has been concluded that PDMS was more suitable to separate these mixtures than LLDPE.

Aminabhavi and Naik [9] have explored the separation of N,N-dimethylformamide-water mixtures using a poly (vinyl alcohol)-g-polyacrylamide (PVA-g-AAm) copolymer membrane. It should be noted that PVA, by itself, is unable to resist dimethylformamide chemically. The grafting of polyacrylamide allows it to withstand harsher solvents. These mixtures have been selective for water at lower concentrations of water in the feed. Still, the water-DMF separation factor is only moderate, ranging between 15 and 22. The highest permeation rate, or flux, has been found to be 0.459 kg/(m²-h) at 90% water in the feed mixture.

A later study in 2006 by Devi et al. [10] has focused on a similar membranes, poly (vinyl alcohol)/poly (acrylic acid) blends, for the dehydration of N,N-dimethylformamide-water systems. This membrane performs better than the previous one, producing a selectivity factor of 275 and water flux of 0.0125 kg/(m²-h). This has been achieved at feed water concentrations less than 10 wt%.

1.4.2 Ceramic Membranes and Non-Metallic Membranes

Ceramic membranes exhibit very high thermal, mechanical and chemical stability. However, when compared to polymeric membranes, ceramic membranes are more brittle, cannot be processed as easily, and typically more expensive to manufacture. Despite this, researchers continue to study these membranes due to their ability achieve significantly high selectivity factors in various separations techniques. In general, ceramic membranes are created by forming a nitride, carbide or an oxide. Other non-metallic membranes utilize different formulations, and are still able to achieve significant selectivities and flux values. A prime example of a high performing non-metallic membrane is an aluminosilicate material known as zeolite. Zeolites are microporous membranes that are

often characterized as being molecular sieves. Porosity and size of the pores depend on the ratio of alumina to silica present. Zeolites have been used to separate mixtures containing water. The pores are highly selective for water and have been known to block out other solvents even in mixtures with small concentrations of water. Zeolite, as a membrane material, possesses very desirable qualities; however, the feasibility of scaling up a zeolite-based process can be tenuous. For this reason, efforts have been made to incorporate zeolites into mixed matrix membranes to potentially create high performing, economical membranes.

Shah et al. [11] have used hydrophilic zeolite NaA membranes for organic solvent dehydration. Separation of alcohol-water systems, involving methanol, ethanol and isopropanol, has achieved very high water-alcohol selectivity factors. The separation factor for methanol-water mixtures ranges from 500 to 1,000. Mixtures of ethanol-water and isopropanol-water has greater separation factors between 1,000 to 5,000. Despite this, separating mixtures of N,N-dimethylformamide produces a separation factor of 330. Total flux through the membrane has been determined to be 1.6 kg/(m²-h). It has been concluded that molecules of N,N-dimethylformamide competed against water for micropores in the zeolite membrane. The permeate sample contains 0.13 wt% N,N-dimethylformamide, starting with a 30 wt% solvent feed.

Kolsch et al. [12] have modified alumina membranes by depositing SiO_x networks inside the γ -Al₂O₃ layer of the membrane. With these enhanced membranes, the separation of water from various organic solvents begins. The solvents of interest are acetonitrile, tetrahydrofuran (THF), 2-propanol, ethyl alcohol, N,N-dimethylsulfoxide, N,N-dimethylformamide, and phenol. Different temperatures and feed concentrations have

been investigated for each solvent pair. For THF-water systems, the water-THF separation factor is 9,860 at 25°C for a feed highly concentrated in THF. Separating mixtures of N,N-dimethylsulfoxide and water is poor. Using a 50-50 vol% feed of DMSO and water has resulted in a water-DMSO separation factor of only 2. Flux is also relatively small, 0.02 kg/(m²-h). The reported performance of the membrane is higher for mixtures of N,N-dimethylformamide and water. However, the temperature has increased from 25°C to 95°C. This gives a separation factor of 95; the overall flux value is 0.40 kg/(m²-h).

1.4.3 Liquid Membranes

Pervaporation is typically studied using polymeric and ceramic membranes. This is due to the reliable performance and costs associated with the process. However, they are not very selective for a variety of polar volatile organic compounds (VOCs). This leads to low concentrations of these compounds in the permeate stream and must be removed using another separation process downstream.

Liquid membranes provide an alternative to fill this gap. As a technique that is based on solvent extraction, the selectivity of a liquid membrane would be dependent upon solubility of a particular solvent present in the feed side while excluding others. For example, a liquid membrane may be chosen as an organic compound, having a high molecular weight. This would be optimal in extracting dilute organic solvents in aqueous solutions. An application for such a liquid membrane would be to extract VOCs from fermentation broths as a source for energy purposes.

At the same time, liquid membranes are not without shortcomings. From a materials aspect, a compatible support for the liquid membrane must be found. Related to

this issue, a means of properly immobilizing the membrane onto the support must also be developed. Also, the support should be able to withstand the operating pressures and temperatures required by the process. The support itself may prove to be a limiting factor in terms of performance. In addition, continual loss of the liquid membrane is another obstacle that must be addressed. Typically, the feed solution comes into direct contact with the liquid membrane. Compounds within the feed solution are then selected by the membrane via molecular interactions. However, as these compounds diffuse through the membrane and desorb, some liquid membrane may also escape from the support material and become present in the permeate. This later affects the long term performance and overall operation costs if the membrane has to be continually immobilized at timely intervals. Another issue arises in the particular case when live media such as bacteria or yeast cells are involved. Interaction between the feed solution and the liquid membrane can potentially render the retentate toxic to the live media and must be disposed of. A desirable process would allow for the retentate to be recycled to promote greater efficiency and sustainability.

Matsumara et al. [13] have looked at oleyl alcohol for the removal of volatile organic compounds such as acetone, butanol and ethanol. In this study, the liquid membrane is immobilized on a porous flat sheet polymeric membrane of polypropylene. It achieves relatively high selectivity for these organic compounds, 40 for acetone, 180 for butanol and 14 for ethanol. Since the feed solution is in direct contact with the liquid membrane, continual loss of oleyl alcohol has been found to be problematic. Constant re-immobilization of the liquid membrane is necessary to achieve consistent results.

Qin et al. [14] have focused on trioctylamine (TOA) as a liquid membrane supported by polymeric hollow fibers in pervaporation. This is used to separate aqueous solutions of acetic acid. The highest separation factor of 33 achieved is at 60 °C. Again, this process suffers similar setbacks observed by Matsumara with loss of the liquid membrane into the permeate. However, an automatic method of liquid membrane regeneration had been developed to overcome this obstacle.

Thongsukmak and Sirkar [15] have applied TOA as a liquid membrane for the removal of acetone, butanol and ethanol in dilute aqueous solutions. Using a similar methodology employed by Qin et al. [14] they have observed high selectivity values for these three organic compounds. Hollow fibers with a nanoporous, fluorosilicone coating prevent direct contact of the feed solution and the liquid membrane. Thus, loss of the liquid membrane is able to be avoided. Additionally, a thin liquid membrane is created in the hollow fibers immobilizing a solution of TOA and hexane. Hexane is primarily used as diluent and then is evaporated from the pores. The remainder TOA on the hollow fiber support creates a thin layer that provided the needed selectivity and greater flux than immobilized TOA alone.

1.5 Objectives of This Thesis

1. Investigate a novel polymeric membrane for the separation of organic-organic and organic-aqueous systems.
2. Demonstrate high selectivity for removal of molecularly small solvents from larger ones.
3. Establish a model to describe the mass transfer of solvent molecules that permeate through the membrane

1.6 Approach

Polymeric membranes are selected based on previous performance published in literature. Membranes with unique properties that exhibit good gas/vapor separation may also be good candidates in pervaporation. The polymeric membrane chosen in this study is poly(2,2,-dimethyl-1,1,3,dioxole)-co-tetrafluoroethylene of the CMS-3 variety. Previous studies have shown excellent performance of the CMS-3 membrane in regards to gas/vapor separation [16 – 17]. In these papers, gases such as nitrogen, oxygen, and water vapor are used as a standard. Oxygen flux is reported as high as 1,500 GPUs for CMS-3 and 9,900 for CMS-7, a related membrane. Competing membranes, such as ethyl cellulose and silicone rubber, offer permeances of 100 and 500 GPUs, respectively. These perfluoro membranes by Compact Membrane Systems also have been able to separate mixtures of nitrogen and oxygen. O₂-N₂ Selectivity values for CMS-3 and CMS-7 are respectively 2.6 and 2. Water vapor permeability has been reported to be as high as 4,500 Barrer [16 – 17]. The high capacity of flux for perfluoro polymers has been attributed to the high fractional free volume on the material. Traditional glassy polymers, like polytetrafluoroethylene (PTFE) only have a fractional free volume of about 15%. Copolymers of dioxole and tetrafluoroethylene are able to reach fractional free volumes of 36% depending on the composition. Further, there are reports of these types of membranes being resistant to all solvents except perfluoro solvents [18].

Due to the potential use of hazardous chemical solvents, an experimental pervaporation set up is constructed entirely out of PTFE. The flat membrane cell is being made in-house at the New Jersey Institute of Technology using PTFE rods, blocks, and o-rings purchased from McMaster-Carr. A positive displacement pump is used to transport

solvent mixtures to contact the membrane housed in the flat membrane cell under laminar flow conditions. This pump must also support the use of PTFE tubing to avoid degradation over time and the introduction of impurities into the feed stream. This is also true for the vacuum pump on the permeate side. Oil-based vacuum pumps are known to degrade when exposed to even small amounts of organic solvents. Rotary-based vacuum pumps, though less effective than oil-based vacuum pumps, are available with PTFE coatings if solvent appears too far downstream.

Pure component permeation experiments take place before analyzing mixtures of solvents. In many cases, permeation of the different components in the feed across the membrane is considered not to be coupled. By running these experiments, the validity of this assumption and the expected amount of permeate sample can be determined. For each pure solvent, experiments operate at various temperatures, specifically, 30°C, 50°C, 60° C or 70°C. Observing the transport properties of the membrane at increasing temperature allows for comparison to other glassy polymer membranes. For high boiling aprotic solvents, pure component permeation tests are run for 60°C or higher. N,N-dimethylformamide (DMF), N,N-dimethylacetamide (DMAc) and N,N-dimethylsulfoxide (DMSO) have very low vapor pressures near room temperature. DMF possesses the highest vapor pressure at 50°C with 29.2 mm Hg. DMSO, on the other hand, has a vapor pressure of only 5.5 mm Hg at the same temperature. Since pervaporation is driven by the difference in partial pressure on the feed and permeate sides of the membrane, a collectable permeate sample can be obtained if the initial vapor pressure of the component is reasonably large.

Mixtures of solvents can commence after initial runs of pure component permeation have finished. It is difficult to predict needs in the pharmaceutical industry as different formulations of drugs may require different concentrations of solvents. For this reason, performance studies are made over the entire composition range when separating organic-organic mixtures. Three pre-determined concentrations are prepared for each mixture pair. In mixtures of methanol and toluene, for example, the three selected concentrations are 25 wt% methanol with 75 wt% toluene, 50 wt% methanol and 50 wt% toluene and 75 wt% methanol with 25 wt% toluene. These concentrations remain the same for all of the organic-organic mixtures. In addition to varying concentration, the effect of temperature is an area of interest. Similarly to that of pure component permeation, the temperatures of 30°C, 50°C, and 60°C are selected. For aprotic solvents, water contamination is often an issue in the pharmaceutical industry. To simulate this condition, concentrations of 90 wt% aprotic solvent and higher are used. Temperatures selected are the same for mixtures of organic-organic mixtures.

Since sorption is the first step in the pervaporation process, solubility measurements of each solvent into the membrane are invaluable. Using a microbalance, pure solvent sorption onto the PDD-TFE membrane can be measured. A membrane sample can be soaked in the desired solvent overnight to ensure sorption equilibrium. By removing excess liquid on the surface of the sample, it can be placed in a microbalance to determine the amount of weight gain compared to that of a dry membrane sample. Furthermore, to test the solubility of mixtures, headspace gas chromatography can be used. This information would be important to understand solvents competing for free volume regions in the membrane.

Ultimately, an analysis based on various molecular size dimensions would be desirable. Separation using the PDD-TFE membrane has been hypothesized to be based on size exclusion. However, in pervaporation, a number of additional process variables affect permeation through the membrane. These factors include vapor pressure, solubility, and activity coefficients. If a particular molecular dimension or property can be teased out as the overall deciding factor for separation, a greater understanding of the membrane transport and selectivity can be gained. Thus, use of this membrane in specific applications can be selected with greater ease.

CHAPTER 2

EXPERIMENTAL

2.1 Membranes, Chemicals and Instruments

2.1.1 Membranes

Flat membrane sheets of PDD-TFE of the CMS-3 variety are obtained from Compact Membrane Systems Inc. (Wilmington, DE). This membrane is available in two thicknesses, 110 micrometers and 25 micrometers. From the sheets, membranes are cut out with 2.5 inch diameters to be placed in the flat membrane cell.

2.1.2 Chemicals

The solvents used in pervaporation experiments for aprotic solvent dehydration include N,N-dimethylformamide ($\geq 99.8\%$ ACS reagent), and N,N-dimethylacetamide (anhydrous, 99.8%) (purchased from Sigma Aldrich) and N,N-dimethylsulfoxide (certified) (from Fisher Scientific). Deionized water is processed from a Barnstead E-pure water purification unit.

The solvents used in pervaporation experiments for organic-organic separation include toluene (ACS reagent, $> 99.5\%$), tetrahydrofuran (ChromaSOLV Plus for HPLC, $> 99.9\%$), and ethyl acetate (ACS Reagent, $> 99.5\%$) (purchased from Sigma Aldrich) and methanol (histological grade) (from Fisher Scientific).

2.1.3 Instruments Used

- Gas chromatograph (model CP 3800 ,Varian Walnut Creek, CA) equipped with DB 5ms column (Agilent, Wilmington, DE)
- CTC Analytics CombiPAL autosampler in concert with the gas chromatograph (Zwingen, Switzerland)

- Cahn C-31 microbalance (Cerritos, CA)

2.2 Fabrication of Flat Membrane Cell

The flat membrane cell is modeled in AutoCAD 2009 by Autodesk (San Rafael, CA). The design is based off of a pre-existing flat membrane cell. However, due to size and material compatibility issues, a new membrane cell has to be fabricated. Schematic diagrams of the flat membrane cell can be seen in the Figures 2.1 and 2.2. The previous cell has an outer diameter of 2 inches, making the effective membrane area approximately 9 cm^2 . It is manufactured from stainless steel which is known to degrade in the presence of certain organic solvent liquids and vapors. The new cell is designed to be made from polytetrafluoroethylene (PTFE). This is selected as the material for its strong chemical resistance. It is designed to have an outer diameter of 2.5 inches, with an effective membrane area of 11.4 cm^2 . The increase in area seems only moderate. However, as the membrane area increases, sealing becomes a larger problem. This is an important issue when running pervaporation where a vacuum must be pulled on one side of the membrane. The o-rings used to seal the cell are also made from PTFE. Being a rigid polymer, PTFE is fairly easy to machine. Still, ideal o-rings must possess an ability to compress and form a tight seal. PTFE o-rings present a limiting factor to the overall size of the flat membrane cell. Thus, a conservative design is chosen to ensure proper sealing for pervaporation experiments.

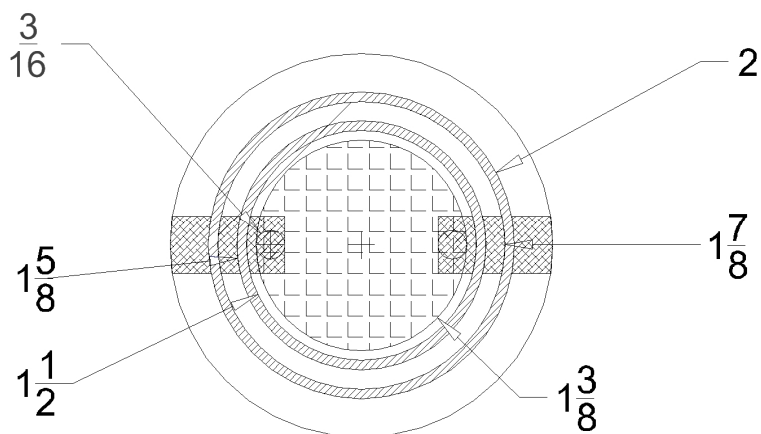


Figure 2.1 Top view schematic of the flat membrane cell with dimensions in inches.

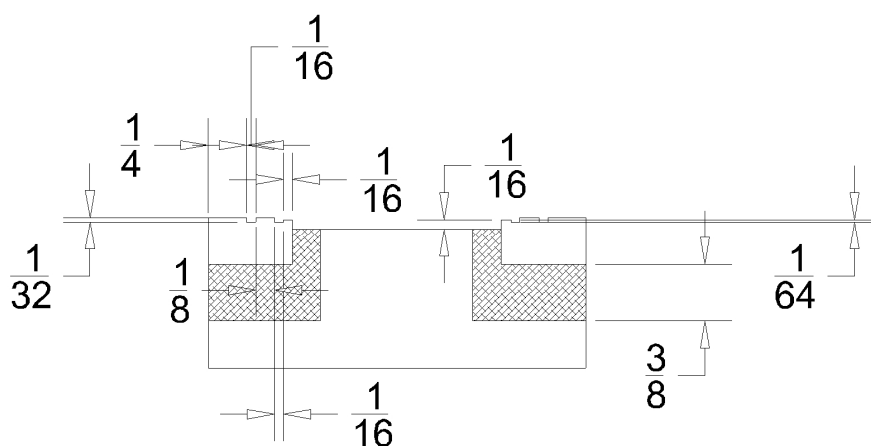


Figure 2.2 Side view schematic of the flat membrane cell with dimensions in inches.

2.3 Experimental Procedure for Pervaporation

Feed solution is introduced to the membrane using a Masterflex L/S PTFE-tubing peristaltic pump from a reservoir. This feed is then circulated back to the reservoir. At the same time, the reservoir is heated to the desired temperature in a Fisher Isotemp 3013HP water bath. This process of heating and circulating continues until the temperature of the reservoir reaches steady state. For higher temperatures, this typically can take up to 2 hours. After this is completed, the vacuum pump is initiated and draws against the

permeate side of the membrane. Some time is needed before the pressure becomes stable at about 7 – 9 Torr (mm Hg). When this is achieved, the vacuum trap is placed in a silvered dewar flask and submerged in liquid N₂.

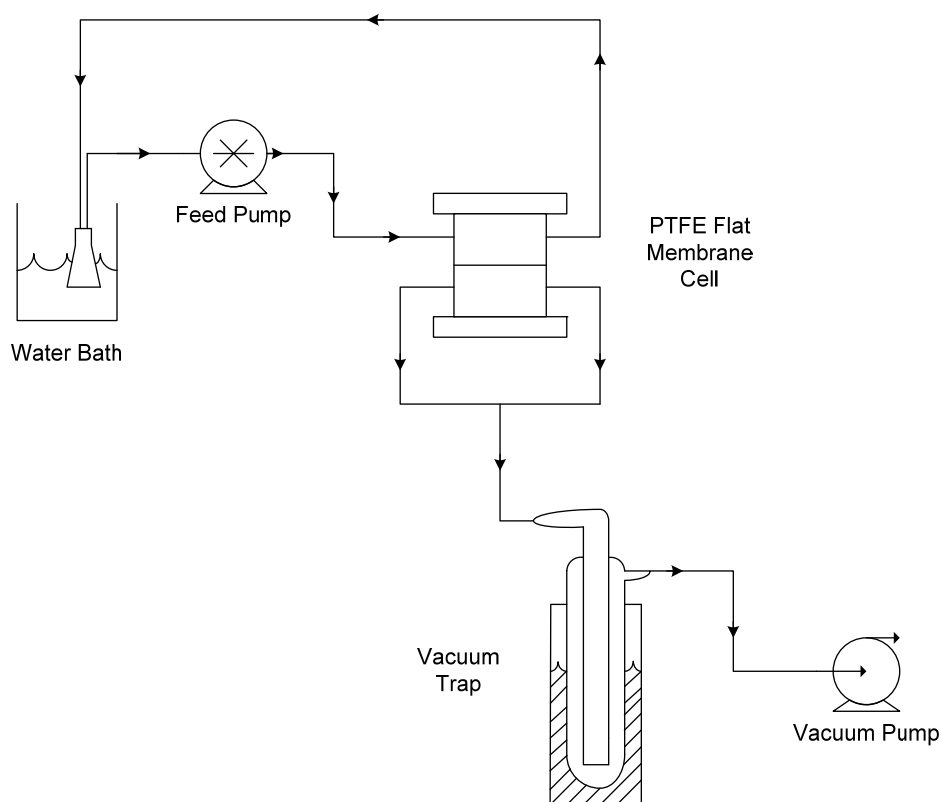


Figure 2.3 Schematic diagram of the experimental pervaporation set up.

2.4 Permeate Sampling

Permeate vapors are collected for a fixed period of time, usually 7 hours in a vacuum trap. The trap itself is then placed in a silvered dewar flask and is submerged in liquid N₂. The temperature of the vacuum trap is low enough to solidify the permeate vapors. The vacuum trap is then removed from the liquid nitrogen and gradually brought to room temperature. A diluent is passed through the finger of the vacuum trap to capture the

small amount of permeate sample that would condense onto the sides of the glass. Selection of this diluent is important and dependent upon the solvents present in the feed solution. Ideally, this diluent solvent must be soluble in all of the components of the feed, and has relatively low vapor pressure at room temperature. In pure component permeation tests involving methanol and tetrahydrofuran, water had been initially used as the diluent solvent; but finally, it has changed to n-butanol. Runs of ethyl acetate are diluted with toluene and then later with n-butanol. For toluene, n-butanol is selected as a reliable diluent. However, organic-organic mixtures add an additional condition for solubility of the diluent solvent. n-Butanol was chosen as a diluent since it is independent of the other solvents and has reasonable organic solubility and is relatively stable at room temperature. Similarly for aprotic solvent mixtures, N,N-dimethylsulfoxide is used to dilute mixtures of N,N-dimethylformamide and water. Alternately, N,N-dimethylformamide is used to dilute systems of N,N-dimethylsulfoxide-water and N,N-dimethylacetamide-water.

2.5 Permeate Analysis

A gas chromatograph manufactured by Varian, model CP-3800 (Walnut Creek, CA), equipped with a DB 5ms column (Agilent, Wilmington, DE) is used to analyze the liquid permeate samples. The conditions of analysis are: 100°C for 5 minutes, the oven temperature is raised to 140°C at rate 35°C/minute then temperature is kept at 140°C for 10 minutes.

Using this method, calibrations curves are generated by analyzing known concentrations of samples. These samples would reflect the composition of the permeate

samples obtained experimentally. For example, if the solvent mixture consists of methanol, and toluene, and the diluent is n-butanol, then calibration curves would be generated for small amounts of methanol in n-butanol and toluene in n-butanol separately. This is done for aqueous-organic systems as well. However, it is known that gas chromatography cannot detect water; peaks of curves do not appear for water specifically. To overcome this issue, a calibration curve for water is created by analyzing samples of the diluent solvent with known concentrations of water. This is essentially performed by subtraction, where the decreasing area of the diluent corresponds to increasing concentration of water.

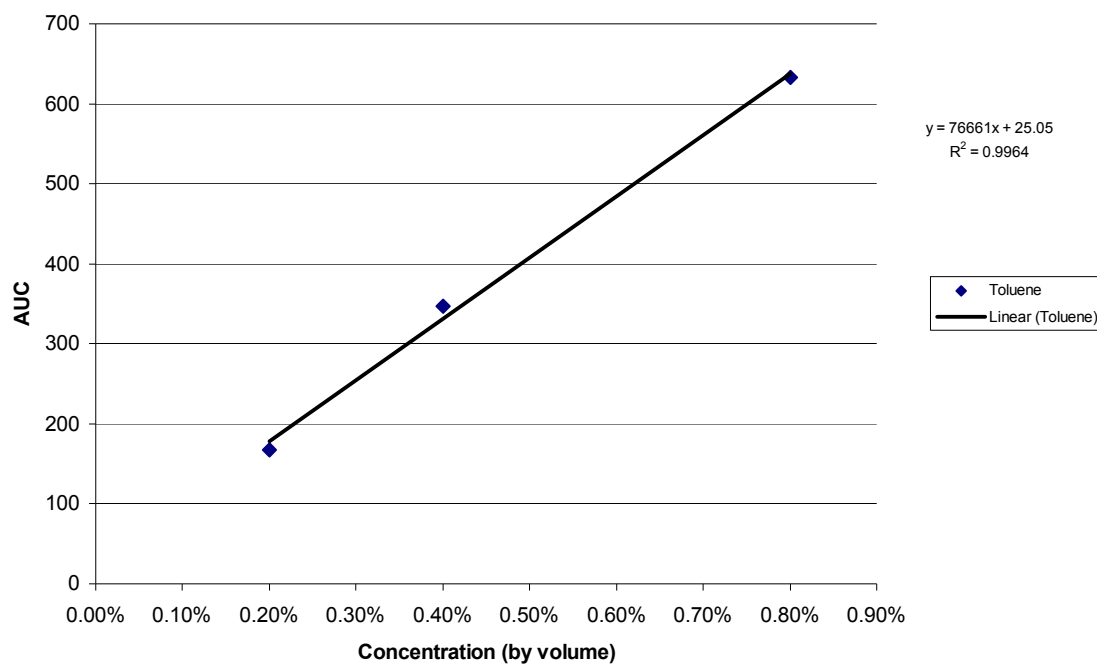


Figure 2.4 Calibration curve of toluene in n-butanol.

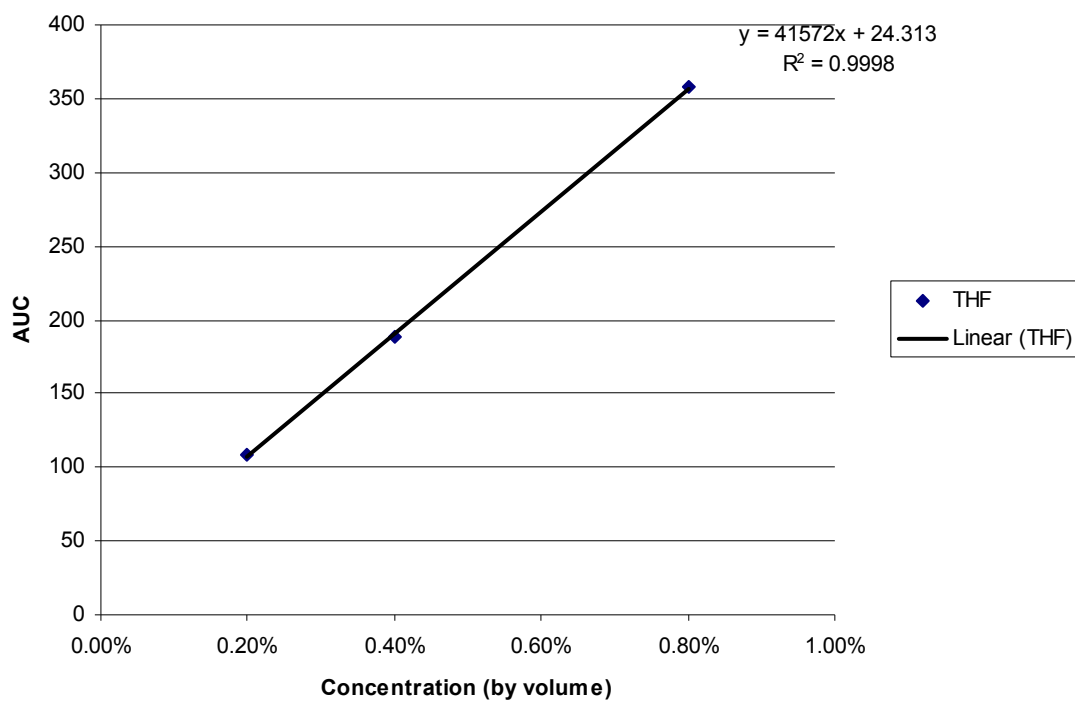


Figure 2.5 Calibration curve of tetrahydrofuran in n-butanol.

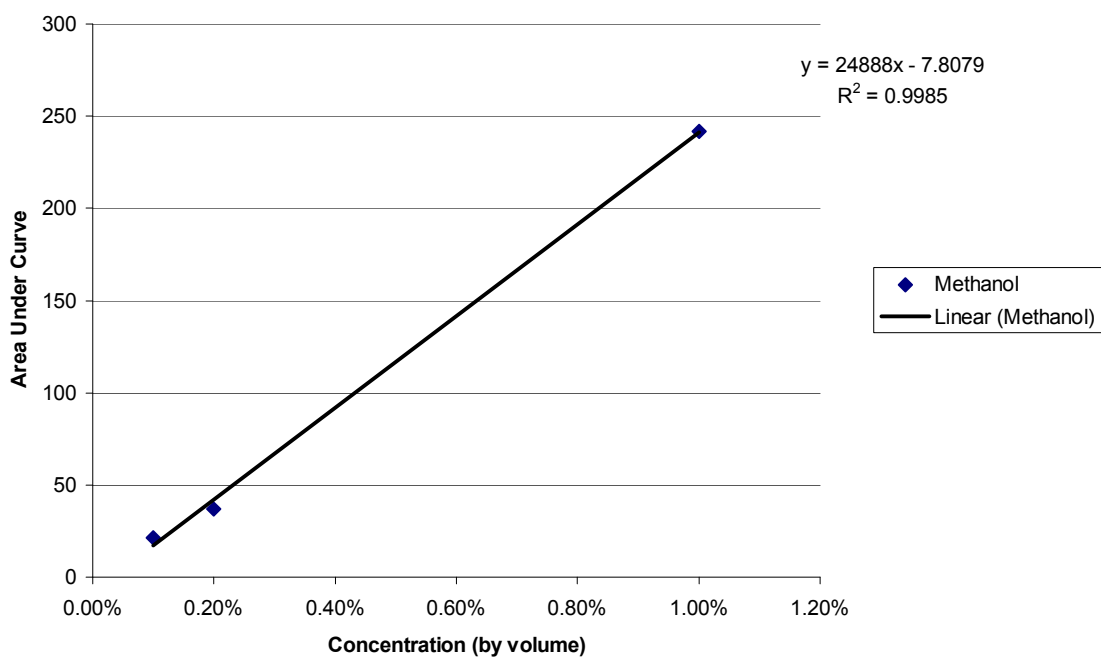


Figure 2.6 Calibration curve of methanol in n-butanol.

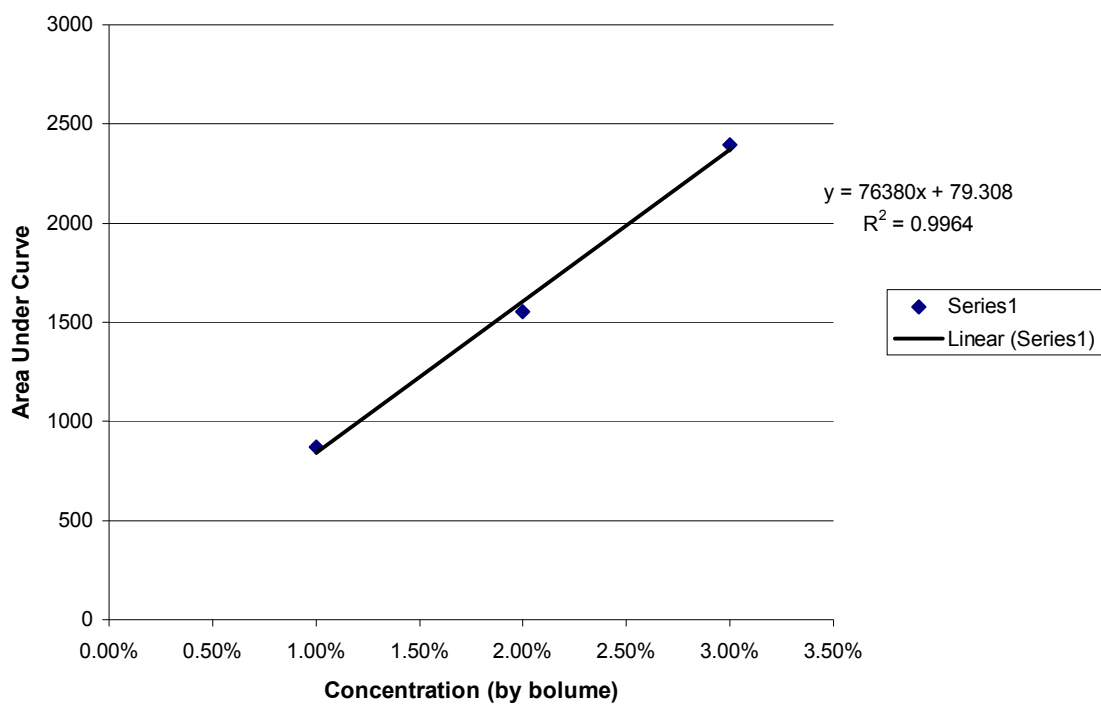


Figure 2.7 Calibration curve of ethyl acetate in n-butanol.

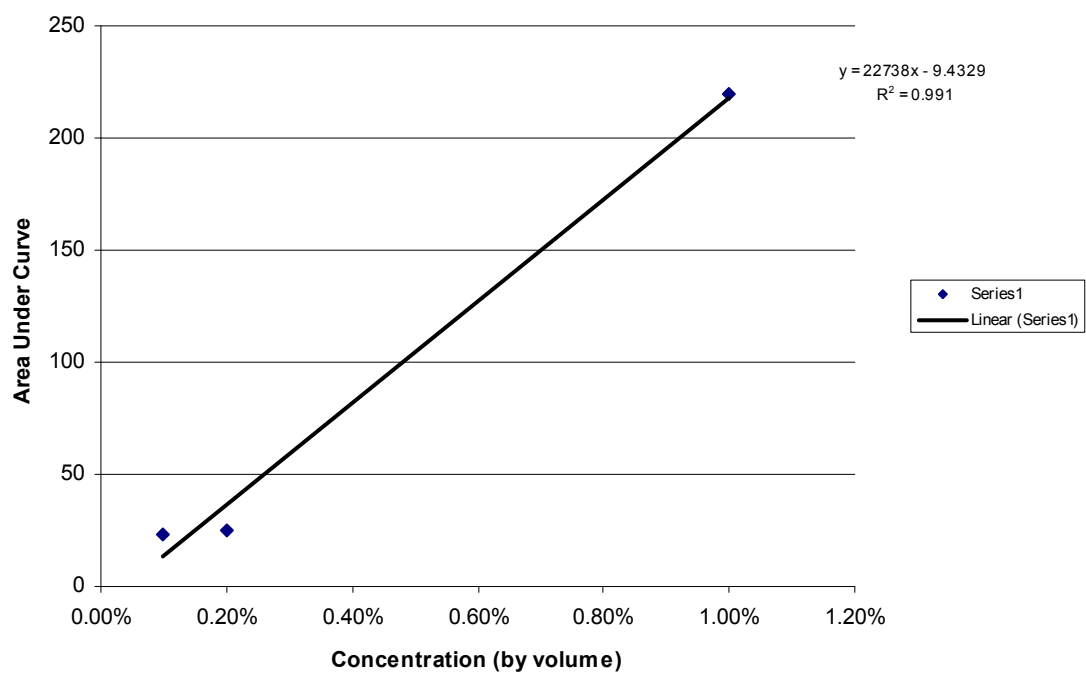


Figure 2.8 Calibration curve of N,N-dimethylformamide in N,N-dimethylsulfoxide.

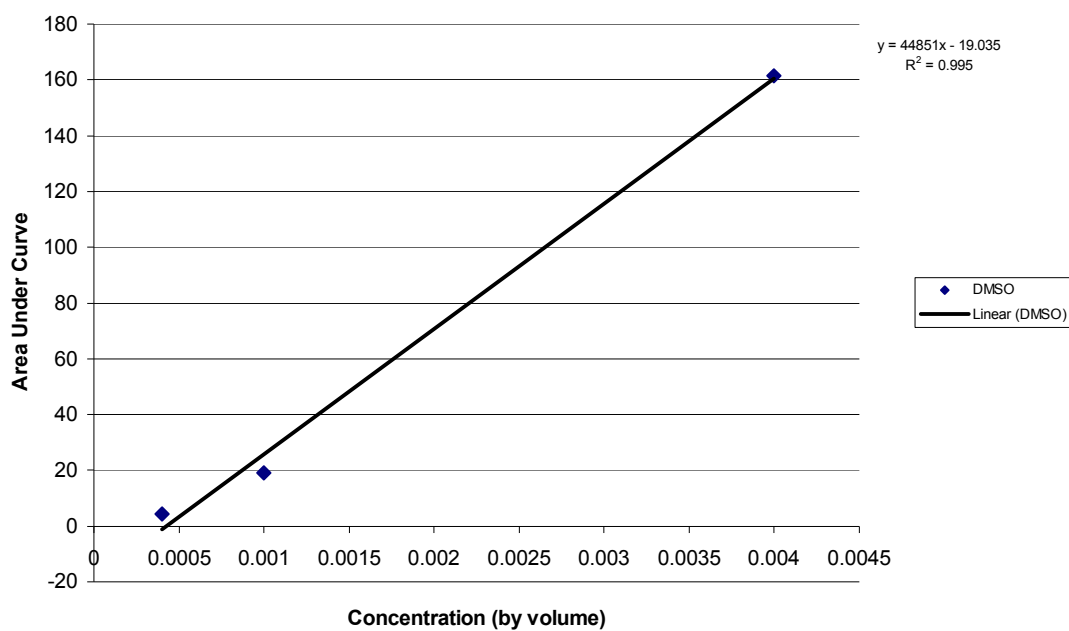


Figure 2.9 Calibration curve of N,N-dimethylsulfoxide in N,N-dimethylformamide.

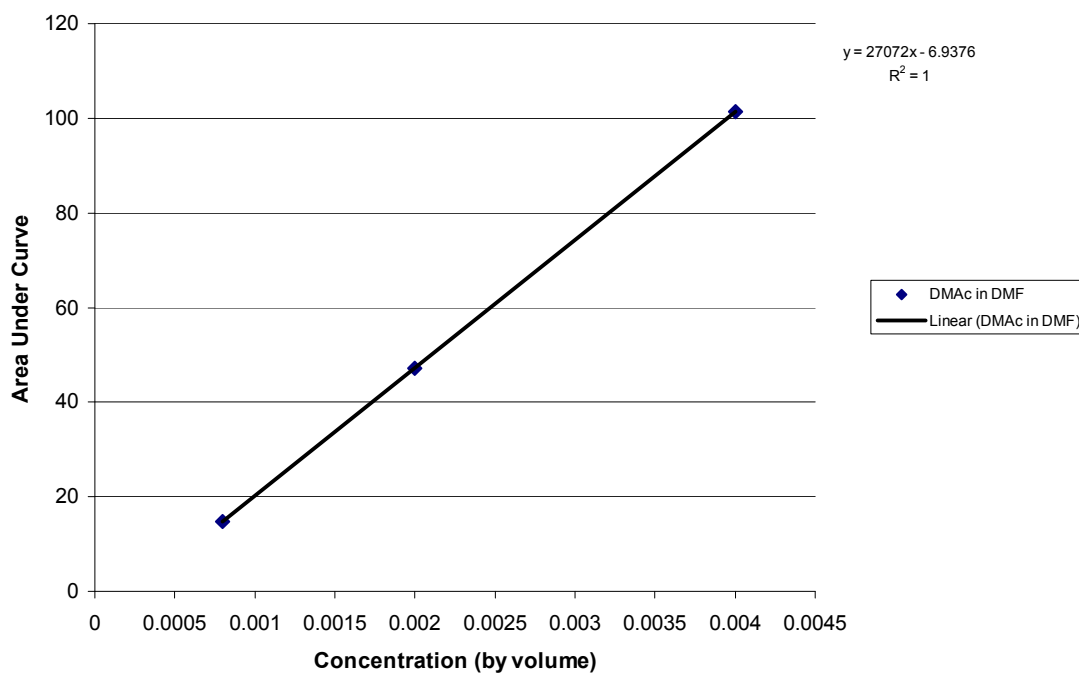


Figure 2.10 Calibration curve of N,N-dimethylacetamide in N,N-dimethylformamide.

2.6 Solubility Analysis of Pure Components

Measurements are made using a Cahn C-31 microbalance (Cerritos, CA). A membrane sample is dried in an oven at approximately 60°C for over 12 hours. This sample is then weighed using the microbalance. To measure solvent sorption, the same membrane sample is soaked in the desired solvent for at least 8 hours or overnight. It is removed from the liquid and any remaining excess solvent is carefully removed using a Kimwipe. The weight of the sorbed membrane is measured. The difference in weight gain from the sorbed membrane to the dried membrane represents the amount of solvent absorbed by the membrane.

2.7 Solubility Analysis of Mixtures

Sorption measurements are made using headspace analysis via a Varian, model CP-3800, gas chromatograph (Walnut Creek, CA). It is enabled through the use of a CombiPAL autosampler manufactured by CTC Analytics (Zwingen, Switzerland). A membrane sample is submerged in a desired organic-organic solvent mixture of a known composition. This is done at 25°C for a minimum of 8 hours. Excess liquid is removed from the surface with a Kimwipe. The sample is then placed into a vial and heated to approximately 100°C for 15 minutes. Vapor in the vial is then withdrawn and injected into the gas chromatograph for analysis.

Due to the presence of two species sorbed into the membrane, additional calibration curves are generated for headspace analysis. Since the sample analyzed is in a vapor phase rather than liquid, calibration curves made for permeate sample analysis could not be used. In addition, small amounts of solvent are sorbed by the membrane give

rise to proportionally smaller concentrations, several magnitudes of order found in the permeate sample.

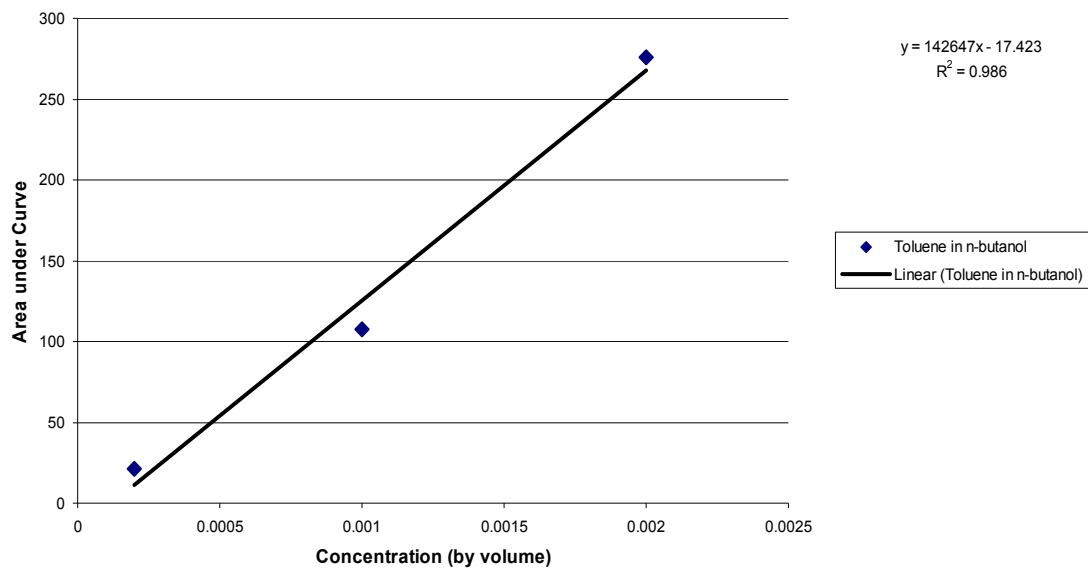


Figure 2.11 Headspace calibration curve of toluene in n-butanol.

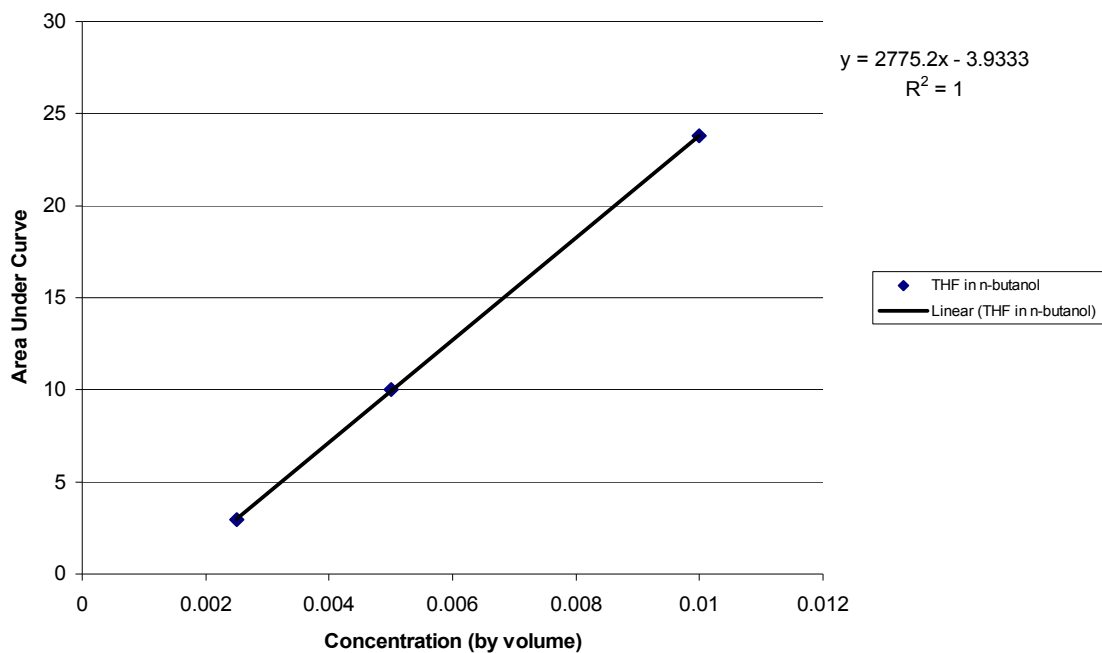


Figure 2.12 Headspace calibration curve of tetrahydrofuran in n-butanol.

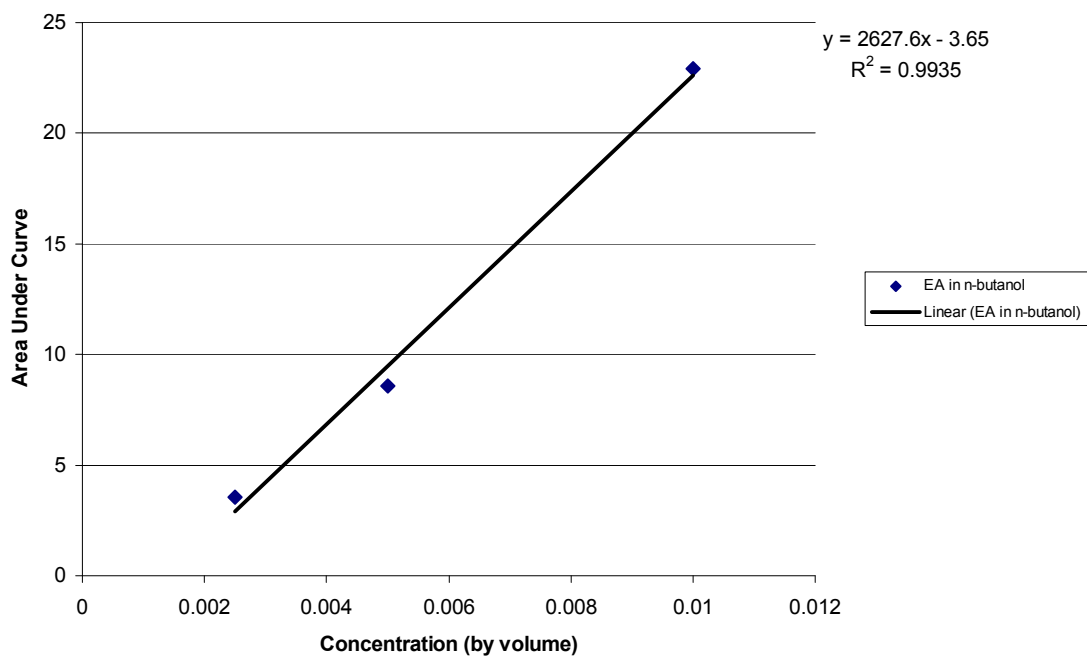


Figure 2.13 Headspace calibration curve of ethyl acetate in n-butanol.

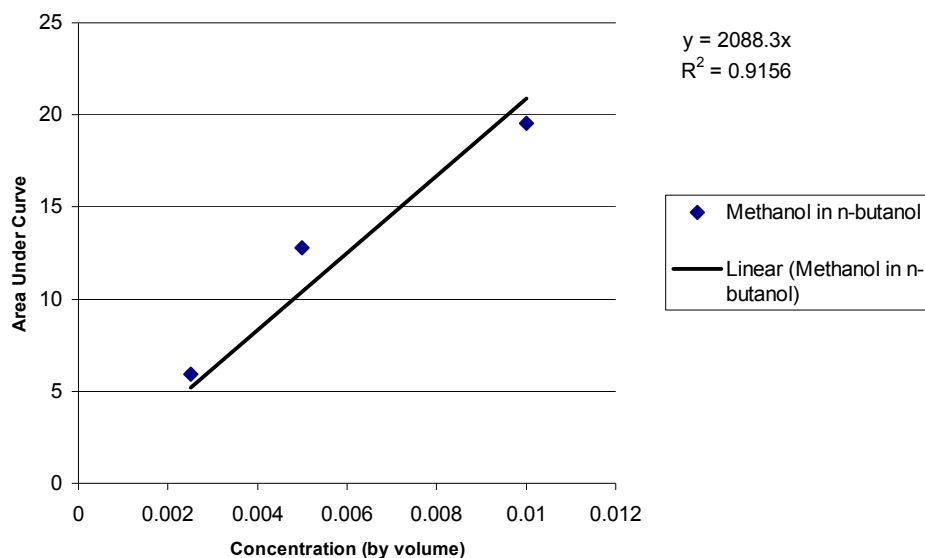


Figure 2.14 Headspace calibration curve of methanol in n-butanol.

2.8 Definitions of Flux and Separation Factor

Flux can be described as the capacity of fluid to traverse the membrane. Overall flux is inevitably important when designing and scaling up membrane-based processes for commercial or industrial applications. Since flux is dependent upon other factors such as membrane thickness, overall permeability coefficient, or Q_i , is seen as a more valuable performance parameter than flux. The following equation relates flux to overall permeability coefficient.

$$J_i = \frac{Q_i}{\delta} (x_i \gamma_i P_i^{\text{sat}} - y_i P_{\text{perm}}) \quad (2.1)$$

where J_i is the experimental flux of component i , Q_i is the permeability coefficient of the membrane, δ is the thickness of the membrane, x_i is the mole fraction of i in the feed, γ_i is

the activity coefficient of i , P_i^{sat} is the saturated vapor pressure of i at operating conditions, y_i is the mole fraction of i on the permeate side and P_{perm} is the vacuum pressure on the permeate side. Activity coefficients are generated through the use of the software package, ASPEN, whenever possible (see Appendix C). Flux of each component in the mixture is expressed in terms of $\text{g}/(\text{m}^2\text{-h})$. Data presented in the results section represent the average of at least three runs.

Separation factor, α_{ij} , is able to define the innate ability of a membrane to separate the different constituents, species i and j , of a mixture, the overall efficiency. It can be determined from:

$$\alpha_{ij} = \frac{y_{ip} / y_{if}}{y_{jp} / y_{jf}} \quad (2.2)$$

where y_{ip} and y_{jp} are the weight fractions of components i and j in the permeate and y_{if} and y_{jf} are the weight fractions of i and j in the feed. Water is typically chosen as the faster permeant in studies using the PDD-TFE membrane.

Equations 2.1 and 2.2 can be related to one another if certain conditions are met. If the product of the permeate pressure and the mole fraction of i on the permeate side are significantly smaller than that of the product of the activity coefficient, mole fraction of i on the feed side and vapor pressure, then this term becomes negligible.

$$J_i \cong \frac{Q_i}{\delta} (x_i \gamma_i P_i^{\text{sat}}) \quad (2.3)$$

Now, the expression of flux is simplified, containing only five variables. If a ratio of the flux for species i to the flux for species j is taken, this can estimate the amount of species i and j in the permeate as seen in equation 2.4.

$$\frac{J_i}{J_j} = \frac{Q_i / \sigma (\gamma_i x_i P_i^{\text{sat}})}{Q_j / \sigma (\gamma_j x_j P_j^{\text{sat}})} = \frac{y_i}{y_j} \quad (2.4)$$

Since this is true, this ratio can be substituted into another definition of separation factor. Now, for organic solvents, the densities can be assumed to be approximate. Therefore, both definitions of separation factor can be approximated to each other in equation 2.5.

$$\alpha^* \cong \frac{y_i}{y_j} \frac{x_j}{x_i} = \frac{Q_i}{Q_j} \frac{\gamma_{if}}{\gamma_{jf}} \frac{P_i^{\text{sat}}}{P_j^{\text{sat}}} \cong \alpha_{ij} \quad (2.5)$$

This relation is important because it emphasizes the most important parameters in the pervaporation process. The difference in vapor pressure, activity coefficients and overall permeability coefficient ultimately affect selectivity of the components in the mixture.

CHAPTER 3

RESULTS AND DISCUSSION OF THE PERVAPORATION PERFORMANCE OF PDD-TFE MEMBRANE FOR APROTIC SOLVENT-WATER SYSTEMS

The perfluoro-2,2,-dimethyl-1,1,3-dioxole-tetrafluoroethylene copolymer membrane of the CMS-3 variety is used to investigate dehydration of aprotic solvents. First, physical data on and molecular dimensions of aprotic solvents and water is presented such as vapor pressure and dimensional values. Furthermore, activity coefficients of these solvents in mixtures are also show calculated n in tabular form. This information is typically calculated using commercial software packages (Appendix C).

From a theoretical standpoint, dehydration of these solvents should be able to be completed with ease. Aprotic solvents such as N,N-dimethylformamide, N,N-dimethylacetamide and N,N-dimethylsulfoxide have considerably higher boiling points than water. Table 3.1 provides their boiling points whereas their vapor pressures at different temperatures are provided in Figure 3.1. Consequently, the vapor pressures of these aprotic solvents are significantly lower at any given temperature. The driving force for a pervaporation process is the difference between the effective partial pressures of the liquid component on the feed side and that on the permeate side. One would not expect aprotic solvents to be able to sorp and diffuse through the membrane very quickly compared to that of water if permeation were based on driving force alone. However, these particular aprotic solvents have shown to be very aggressive with a number of materials. Thus, dehydration by polymeric membranes, much less any other processes involving them, has proved to be a challenge in industrial applications.

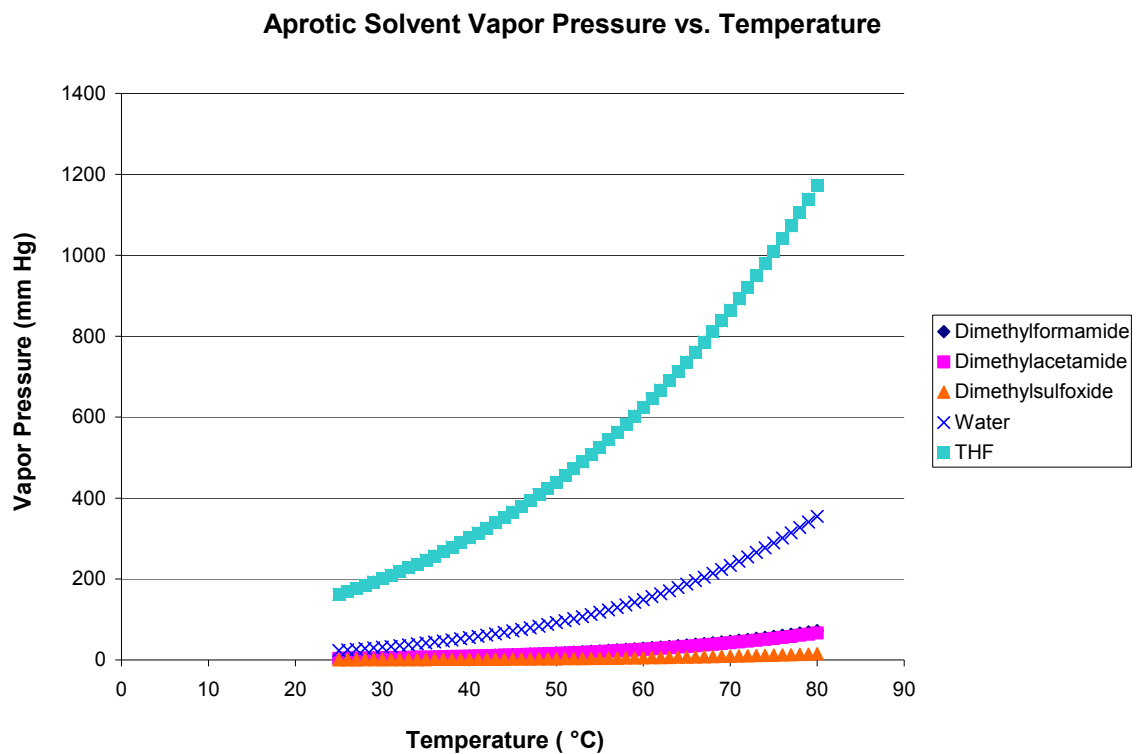
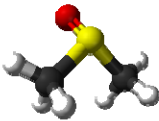
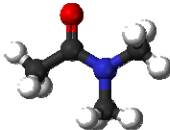
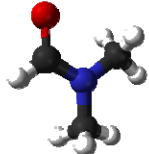
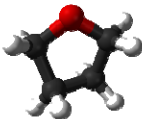



Figure 3.1 Vapor pressure of aprotic solvents and water versus temperature.

Table 3.1 Structural Dimensions and Physical Properties of Various Aprotic Solvents, and Water Used as a Comparison

Structure	Name	Bolling Pt. (deg C)	Vapor Pressure at 50°C (mm Hg)	Density (g/cm³)	Smallest Diameter* (Angstrom)	Largest Diameter* (Angstrom)	Area* (Angstrom²)	Volume* (Angstrom³)
	Dimethylsulfoxide	189	3.1	1.1004	3.575	4.542	102.4	77.8
	Dimethylacetamide	163	16.1	0.94	1.762	5.193	127.87	103.71
	Dimethylformamide	153	17.5	0.944	1.761	4.238	110.28	86.03
	Tetrahydrofuran	66	439.6	0.8892	3.306	4.191	105.06	86.33
	Water	100	92.5	1	0.967	1.561	36.43	19.39

*as estimated using WaveFunction Spartan program

Results from gas/vapor permeation data using similarly formulated membranes such as Teflon AF 1600, AF 2400, and Hyflon AD have yielded evidence that separation may be based on size exclusion as seen in Figure 3.2. In Figure 3.3, permeability coefficients of organic solvents, such as benzene, toluene, and benzyl alcohol, through Teflon AF 2400 decrease with increasing critical volume as well. For this reason, an effort is made to find a possible correlation between size and permeability for various solvents. Even if this membrane material separates solvent molecules of different sizes, there is a significant difference between the dimensions of the aprotic solvents and that of water.

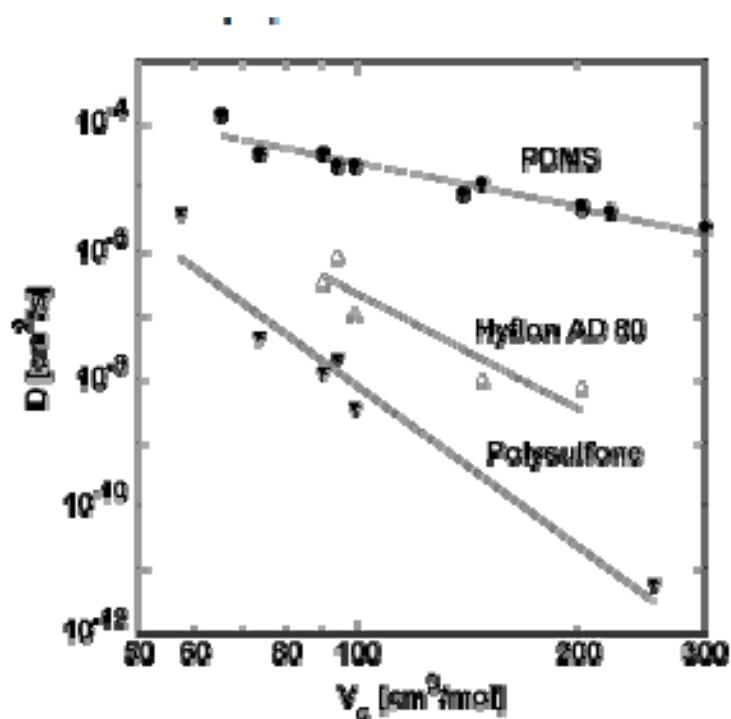


Figure 3.2 Reduction of diffusion coefficient with increasing critical volume of gases/vapors for Hyflon AD [19].

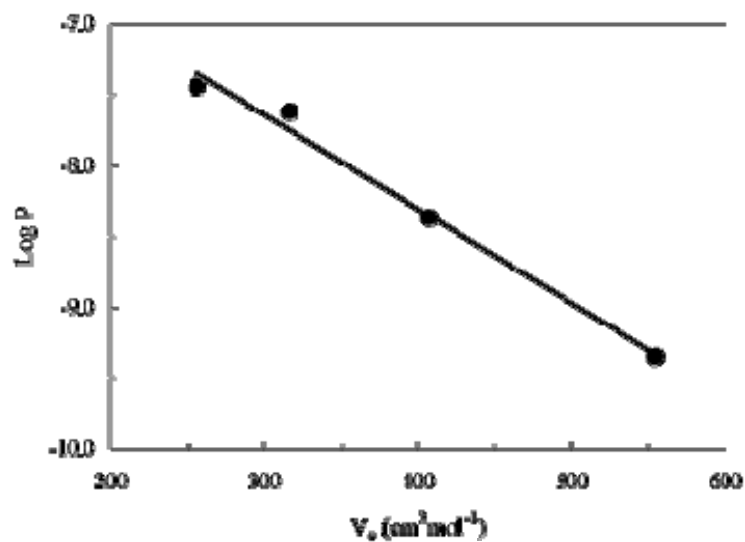


Figure 3.3 Size dependent permeability of organic solutes through Teflon AF films [20].

Another important factor that affects driving force across the membrane is the activity coefficient for mixed solvents. For pure component permeation, the activity coefficient is equal to unity. This is also true if ideality is assumed for mixtures as well, however, it is usually not the case for even some simple mixtures. To accommodate for this, approximations of activity coefficients are made using the NRTL from parameters obtained via ASPEN[®]. Tables 3.2, 3.3 and 3.4 are the results of these calculations at the corresponding compositions and temperatures.

Table 3.2 Activity Coefficients for N,N-Dimethylformamide and Water at Various Temperatures and Compositions

T (°C)	Composition		Activity Coefficient	
	DMF	Water	DMF	Water
30	90	10	0.957	1.126
50	90	10	0.953	1.087
60	90	10	0.951	1.069
30	95	5	0.974	1.176
50	95	5	0.973	1.125
60	95	5	0.972	1.103
30	99	1	0.994	1.224
50	99	1	0.994	1.161
60	99	1	0.994	1.133

Table 3.3 Activity Coefficients for N,N-Dimethylacetamide and Water at Various Temperatures and Compositions

T (°C)	Composition		Activity Coefficient	
	DMAc	Water	DMAc	Water
30	90	10	0.939	0.844
50	90	10	0.955	0.888
60	90	10	0.963	0.908
30	95	5	0.978	0.768
50	95	5	0.983	0.832
60	95	5	0.986	0.861
30	99	1	0.879	0.912
50	99	1	0.913	0.936
60	99	1	0.928	0.947

Table 3.4 Activity Coefficients for N,N-Dimethylsulfoxide and Water at Various Temperatures and Compositions

T (°C)	Composition		Activity Coefficient	
	DMSO	Water	DMSO	Water
30	90	10	0.836	0.143
50	90	10	0.856	0.213
60	90	10	0.865	0.251
30	95	5	0.930	0.090
50	95	5	0.940	0.143
60	95	5	0.945	0.174
30	99	1	0.989	0.056
50	99	1	0.991	0.096
60	99	1	0.992	0.119

3.1 Performance of PDD-TFE Membrane for Pure Aprotic Solvents

Pure component permeation tests for aprotic solvents are performed at 60°C. The vapor pressure for these high boiling solvents are considerably low compared to other organic solvents such as ethanol, and even n-butanol. At 60°C, the partial pressure difference across the membrane is, however, significant enough to allow for pure component permeation of the solvents.

Even at this operating temperature, very little permeate is found in the vacuum trap. A diluent solvent is introduced to capture the small amounts of solvent found on the permeate side. At first, water is used as a diluent solvent. This is chosen since water cannot be explicitly detected in the gas chromatograph. Therefore, peaks corresponding to aprotic solvents can be identified clearly compared to electronic noise or other impurities found in the sample. However, evaporative loss of water during storage and sampling has shown to affect the precision and accuracy of the results obtained from pure component permeation tests. To avoid these issues, an aprotic solvent is used to dilute the permeate sample. For example, in collecting a permeate sample containing N,N-dimethylsulfoxide or N,N-dimethylacetamide, N,N-dimethylformamide is used. For samples of N,N-dimethylformamide, N,N-dimethylsulfoxide is used as the diluent. By substituting water with solvents of higher boiling points, the relative stability of the samples is vastly increased and greater precision of concentration measurements could be obtained.

N,N-Dimethylacetamide flux through the membrane averages around 0.09 g/(m²-h). Pure N,N-dimethylformamide flux through the membrane is approximately 0.2 g/(m²-h). Though these results are fairly similar, the flux of N,N-dimethylformamide through

the membrane is more than two times greater than that of N,N-dimethylacetamide. This can be attributed to the DMF's larger vapor pressure at the same temperature as well as the smaller molecular dimensions of DMF.

3.2 Performance of PDD-TFE Membrane on Dehydration of Aprotic Solvents

From pure component permeation tests, it is observed that aprotic solvent flux through the membrane was fairly small. However, it is important to observe the flux behavior of these solvents as a function of temperature. Typically, an increase of flux with temperature is expected. This is in agreement with previous studies done by Smuleac et al. [21] and Polyakov et al. [22]. In Figure 3.4, variations of the fluxes of N,N-dimethylformamide, N,N-dimethylsulfoxide and N,N-dimethylacetamide with temperature are shown. Though flux of DMAc increases with increasing temperature, both DMF and DMSO experience an overall decrease in flux from 50°C to 60°C. Considering these behaviors along with the amount of permeate sample collected and errors in collection and measurement, flux of the aprotic solvents can at least be said to remain essentially constant in this temperature range.

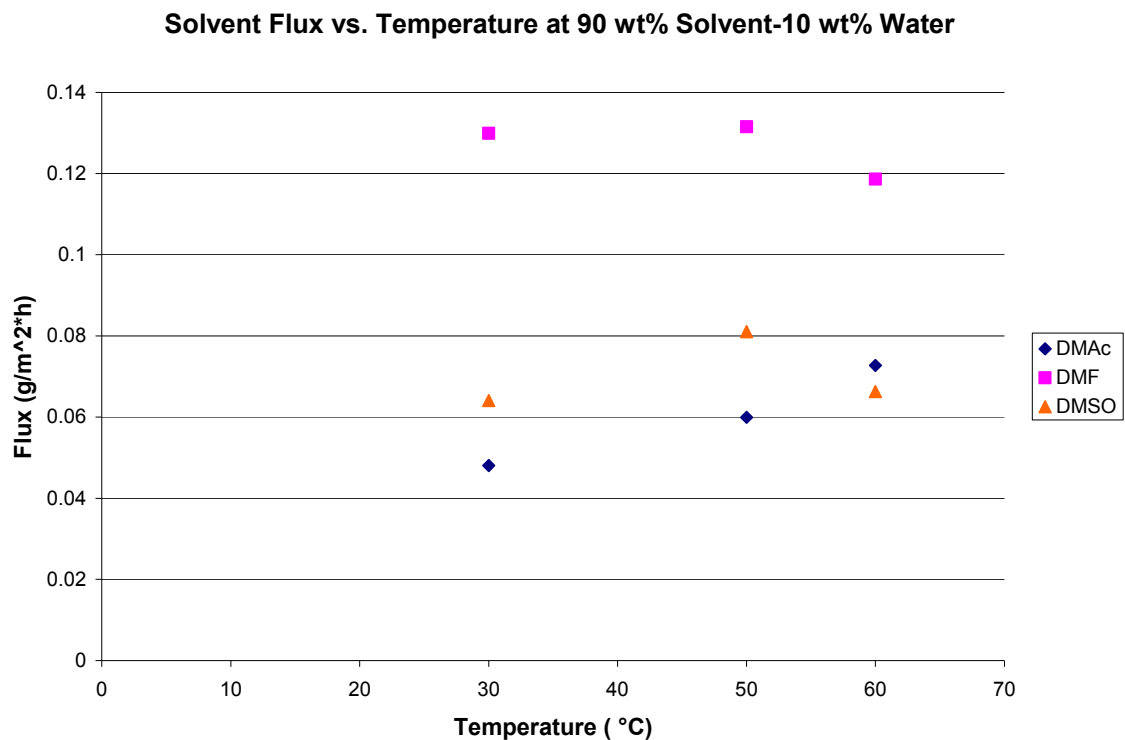


Figure 3.4 Comparison of aprotic solvent fluxes as a function of temperature for 90 wt% solvent and 10 wt% water solution.

Further analysis can be made regarding permeation of these solvents in mixture as they are made at the same temperature and feed composition. It has been hypothesized that this PDD-TFE, of the CMS-3 variety, separates mixtures based on size exclusion. If this were taken into account, one would expect larger flux values of solvents with smaller molecular dimensions. This is true for aprotic solvents if the longest molecular diameter is used in Table 3.1. The differences in diameters of these solvents are only fractions of an Angstrom.

As seen in Figure 3.4, all aprotic organic solvents demonstrate similar flux values of the same order. DMAC produces the least flux, having the largest molecular diameter among the solvents. DMSO possesses the second largest diameter and also has very little vapor pressure in the operating temperature range, and permeates through the membrane

in very little amounts. In comparison, DMF has a smaller size and higher vapor pressure that allows for almost three times as much flux as the other two solvents, approximately $0.12 \text{ g}/(\text{m}^2\text{-h})$ at a feed with 90 wt% solvent. Typically, results using a similarly formulated membrane, Teflon AF 2400, have shown the fluxes of chlorinated organic solvents increase with temperature [23]. Due to the small amounts of aprotic solvent found in the sample, average error is found to be 15%. Error for water flux measurements is 12% and found to be larger at higher temperatures. From the available data, organic solvent flux can be said to be at least constant with temperature.

Water fluxes in solution with DMAc and DMSO range from $6 - 9 \text{ g}/(\text{m}^2\text{-h})$ and $4.5 - 9.8 \text{ g}/(\text{m}^2\text{-h})$, respectively (Figures 3.5 and 3.6). In aqueous solutions of DMF, water flux can be as high as $77 \text{ g}/(\text{m}^2\text{-h})$ and decreases proportionally as the solvent concentration increases (Figure 3.7). In most cases, water flux through the membrane for all three systems experiences an overall increase from 30 to 60°C. Data at 50°C for DMAc-water systems can be considered outliers. Additionally, water flux in DMF-water systems had measured error up to 25% at 60°C. Previous work has shown water flux to increase with temperature using the PDD-TFE membrane in the dehydration of alcohol mixtures in pervaporation [21]. This increase in flux was linear when plotted on a semi-log scale.

This may be due to competitive sorption between the aprotic solvents and water on the feed side of the membrane. Aprotic solvents of DMSO and DMAc are more soluble in the membrane than that of DMF (as seen later in Table 4.2). These larger molecular solvents are sorbed with ease, however, diffusion is considerably more

difficult compared to that of water. Thus, DMSO and DMAc are able to block water in the free volume regions and decrease the overall flux through the membrane.

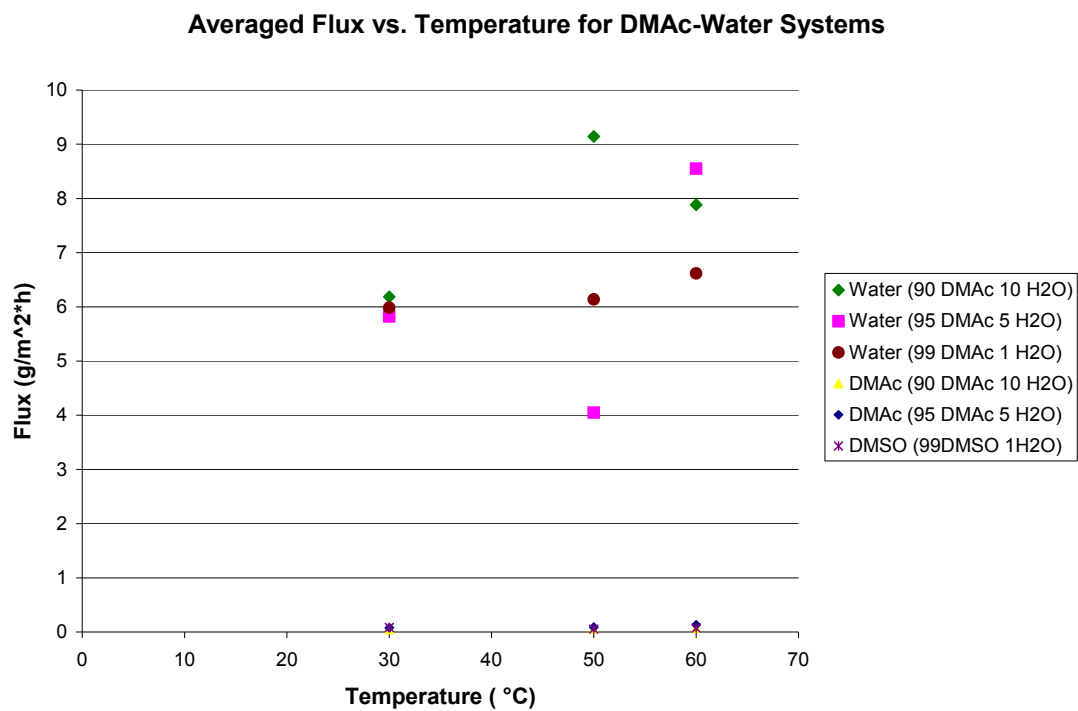


Figure 3.5 Solvent flux for N,N-dimethylacetamide and water with respect to temperature.

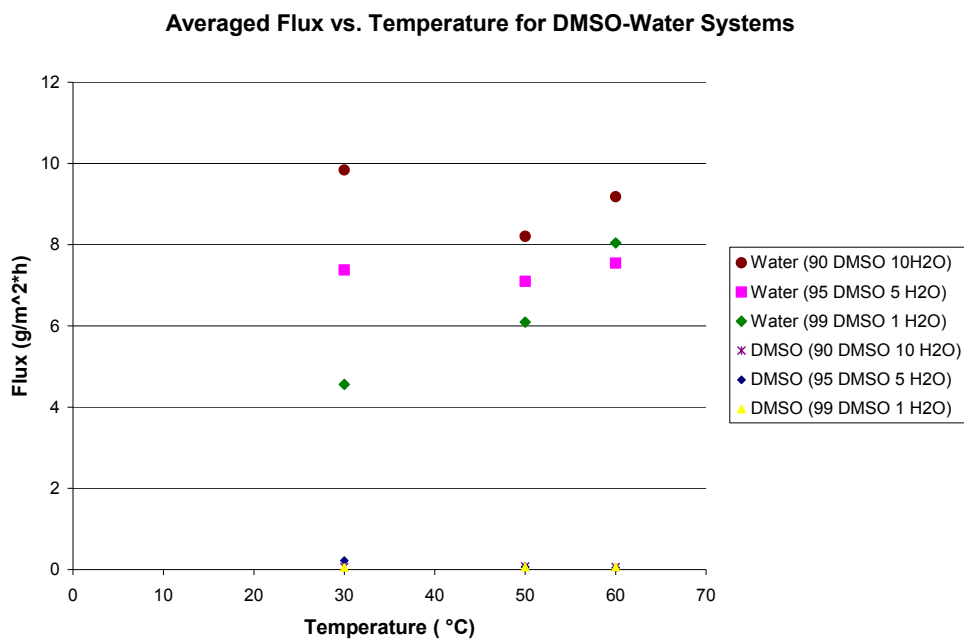


Figure 3.6 Solvent flux for N,N-dimethylsulfoxide and water with respect to temperature.

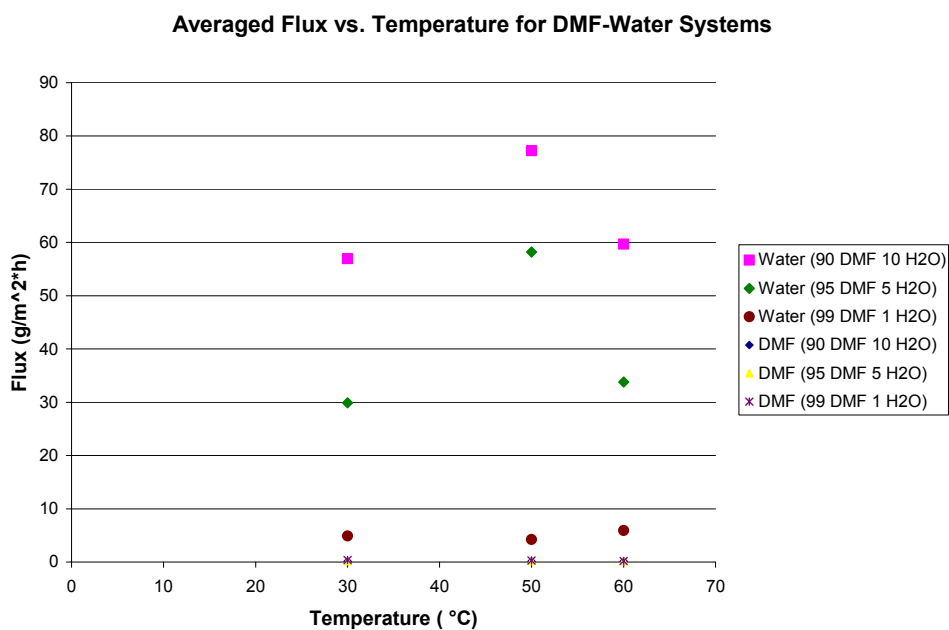


Figure 3.7 Solvent flux for N,N-dimethylformamide and water with respect to temperature.

Overall, very impressive separation factors are achieved by the PDD-TFE membrane, of the CMS-3 variety, on the order of 600 to 12,000 for systems of DMAc-water, DMSO-water and DMF water. It should be noted that opposite trends exist for DMAc-water and DMSO-water when compared to that of DMF-water. This is illustrated in Figures 3.8 and 3.9. Error can be quite high in terms of separation factor. However, separation factor is calculated from measurements of concentration in the permeate sample. Due to the small amount of aprotic solvent present in the permeate, there is already a considerable amount of error in analysis. The difference in behaviors of the aprotic systems can be attributed to the differences in flux and solvent sorption onto the membrane.

In DMAc-water and DMSO-water systems, there is an increase in separation factor as the aprotic solvent concentration increases. A decrease is typically expected in this situation, since the membrane is water selective. As water content in the feed decreases, there is less water available to permeate across the membrane and as a result, separation factor decreases as well. Yet, in the case of DMAc-water and DMSO-water systems, the observed trend is opposite of that. This is mainly an effect due to sorption of the DMAc and DMSO solvents onto the membrane. As previously mentioned, sorption of the solvents prevents significant amounts of water from permeating through the membrane due to their high solubility and scant diffusivity. At these concentrations of aprotic solvent, 90 wt% and greater, both aprotic solvent flux and water flux are approximately the same. As concentration of the DMAc or DMSO increases in the feed, there is observed increase in separation factor of water over aprotic solvent. A similar

result was obtained by Smuleac et al. in separating alcohol-water mixtures using this same PDD-TFE membrane via pervaporation [21].

Separation factors for DMF-water systems decrease as a function of feed concentration. The reduction is almost proportional to the decrease in the water concentration of the feed. If an emphasis is placed on the 50°C data for DMF-water systems in Figure 3.9, the separation factor decreases from about 12,000 at 10 wt% water in the feed to about 5,000 at 5 wt% water in the feed. From here, the separation factor decreases to 1,000 when the feed consists of 1 wt% water.

Separation Factor vs. Composition for DMAc-Water and DMSO-Water Systems

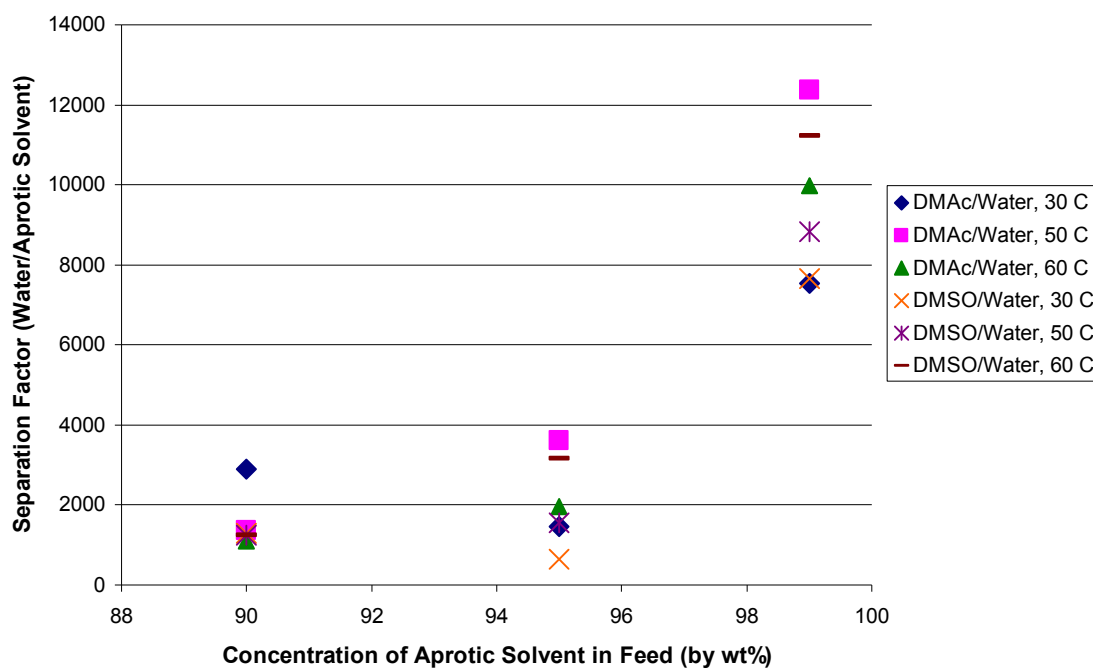


Figure 3.8 Separation factor of water over aprotic solvent (DMAc or DMSO) plotted against feed composition.

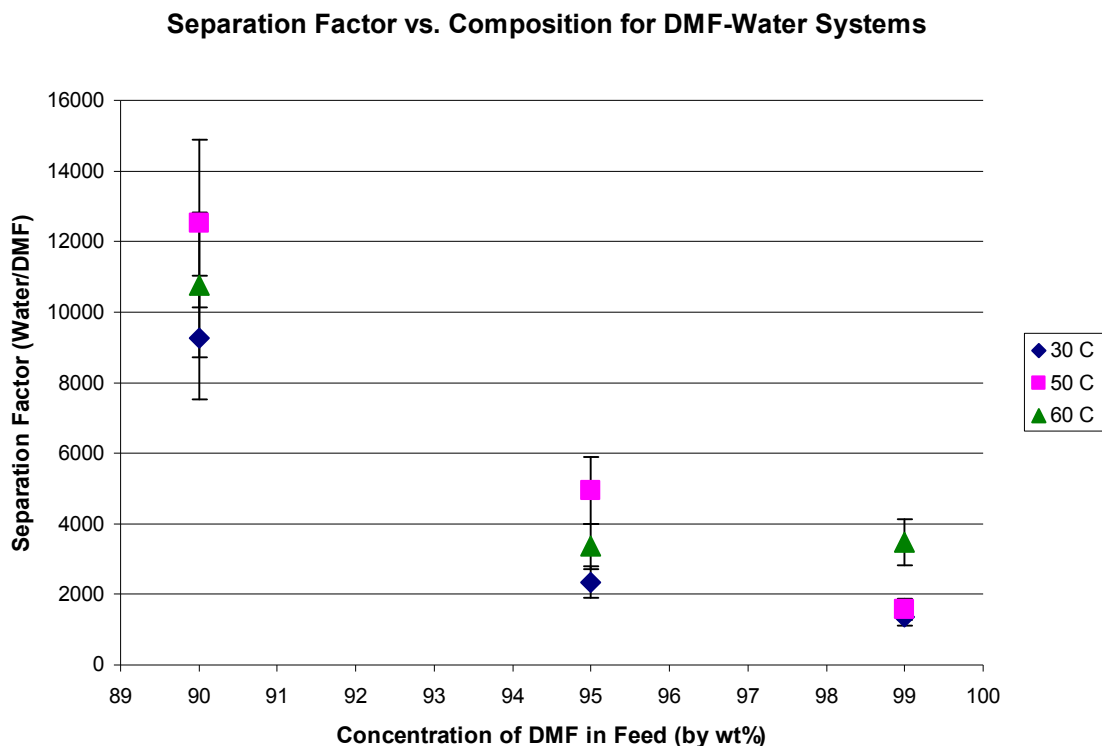


Figure 3.9 Separation factor of water over N,N-dimethylformamide plotted against feed composition.

It is useful to compare the water flux values in the NaA zeolite membrane against the values reported here. The highest water concentration in this study was 10 wt%. If one assumes a 1 μm thick composite PDD-TFE membrane, one can assume that the water flux (data from Figure 3.7 for 25 μm) at 10 wt% water concentration at 60°C for a DMF-water system is 1.5 $\text{kg}/(\text{m}^2\text{-h})$. This value compares very well with the measured water flux in commercial NaA zeolite membrane at a much higher water concentration of 70 wt% at 60°C [11]. It would be useful to compare also the water permeability coefficient for the membrane used here with that for zeolites. The zeolite data was estimated using 10% water – 90% solvent for flux while assuming the selectivity obtained at 70% water –

30% solvent. Estimations were made for K_w , water permeance, for both membranes [11].

It can be defined as:

$$K_w = \frac{Q_w}{\delta} \quad (3.1)$$

where Q_w is the overall permeability coefficient for water. Preliminary calculations indicate that the data of this membrane fall above and below the zeolite data depending on the temperature as seen in Figure 3.10. One can also compare the water flux of membranes of the present study with Hyb-Si silica membranes [24]. The commercialized silica membranes as mentioned in the introduction displayed a water flux of 1 – 3 kg/(m²-h) at 130°C for a 8 wt% water feed. Since the membranes of this study are 25 μm thick, one can expect the flux to be 25 x 77 g/(m²-h) i.e. 1.925 kg/(m²-h) based on flux data for water-DMF systems for 1 μm thick composite membrane.

It has been mentioned earlier that this membrane is exceptionally stable. A particular membrane sample was in fact used for many runs over many months with no change in performance. The manufacturer points out that the maximum amount of solvent sorption is less than 0.2 wt% [25].

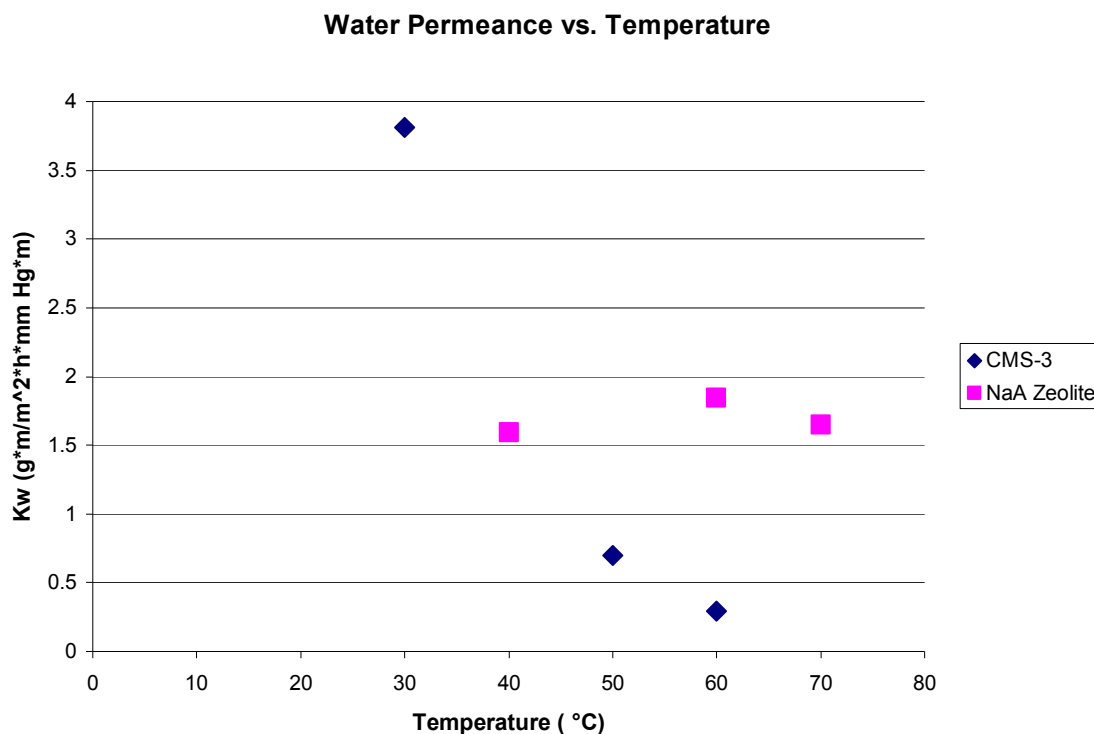


Figure 3.10 Calculations of permeance of PDD-TFE membrane compared to NaA zeolite data from Shah et al. for DMF-water systems [11].

Dehydration of a fourth aprotic solvent, tetrahydrofuran or THF also yields high separation factors as seen in Figure 3.11. THF is different from DMF, DMSO and DMAc physically. THF possesses a significantly higher vapor pressure at these temperatures due to its lower boiling point. In addition, it also has its own geometry and molecular dimensions. Separation factors for THF-water systems are significantly lower than that of the previous three aprotic solvent systems. These separation factors vary from approximately 190 to 500. This is due to the greater driving force for THF across the membrane. More THF is able to permeate through the membrane than the other aprotic solvents reducing the overall separation factor. This is more apparent if flux values of

THF and water are considered in Figure 3.12.

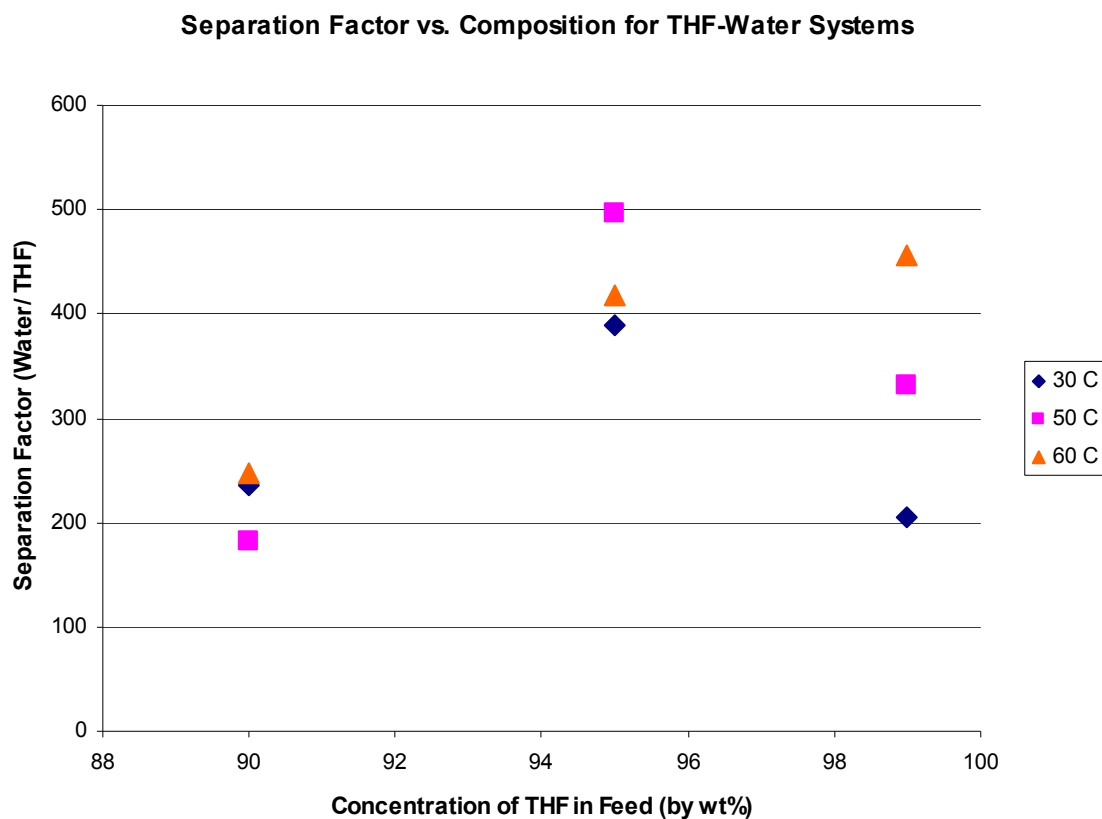


Figure 3.11 Separation factor of THF-water systems varying with feed concentration.

Water flux for THF-water systems are between 3 and 7 $\text{g}/(\text{m}^2\text{-h})$. This is approximately the same as in DMAc-water and DMSO-water systems. THF flux values hover around 0.2 and 0.3 $\text{g}/(\text{m}^2\text{-h})$.

Averaged Flux vs. Temperature for THF-Water Systems

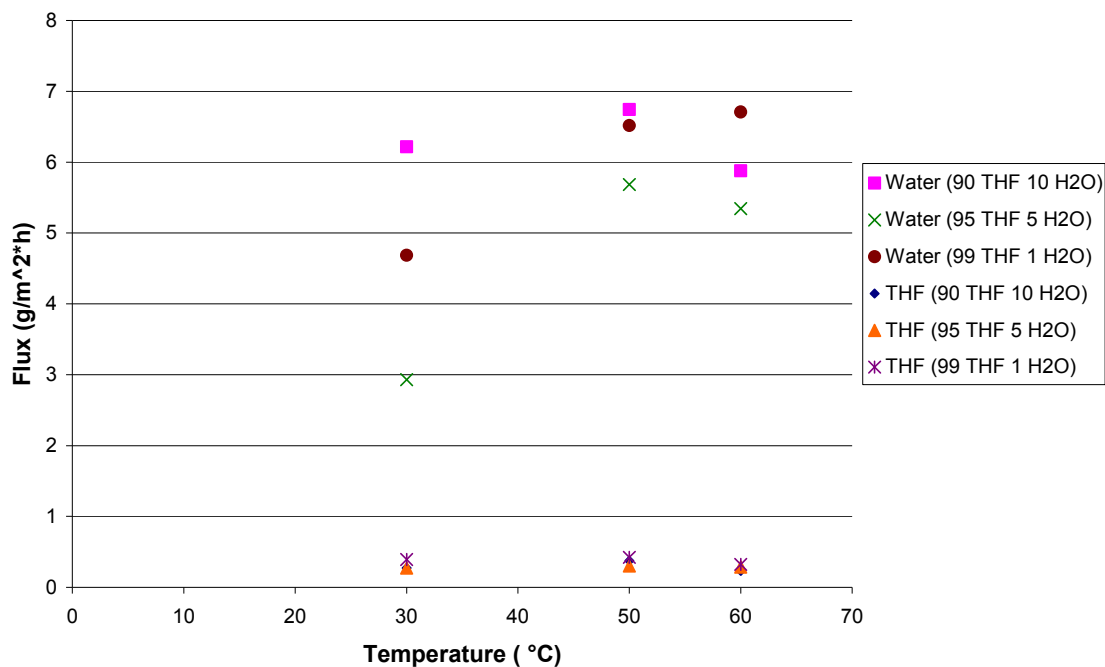


Figure 3.12 Flux values for THF-water systems as a function of temperature.

In analyzing the permeability coefficient of different species in solvent dehydration, it has been found that a negative trend exists with temperature. This result is not consistent with most other polymeric membranes. From a mathematical standpoint, this can be easily justified by the flux behavior with temperature. Permeability coefficient is calculated from flux measurements in which the flux value is finally multiplied by the membrane thickness, a constant, and the divided by the driving force of that species at a given temperature.

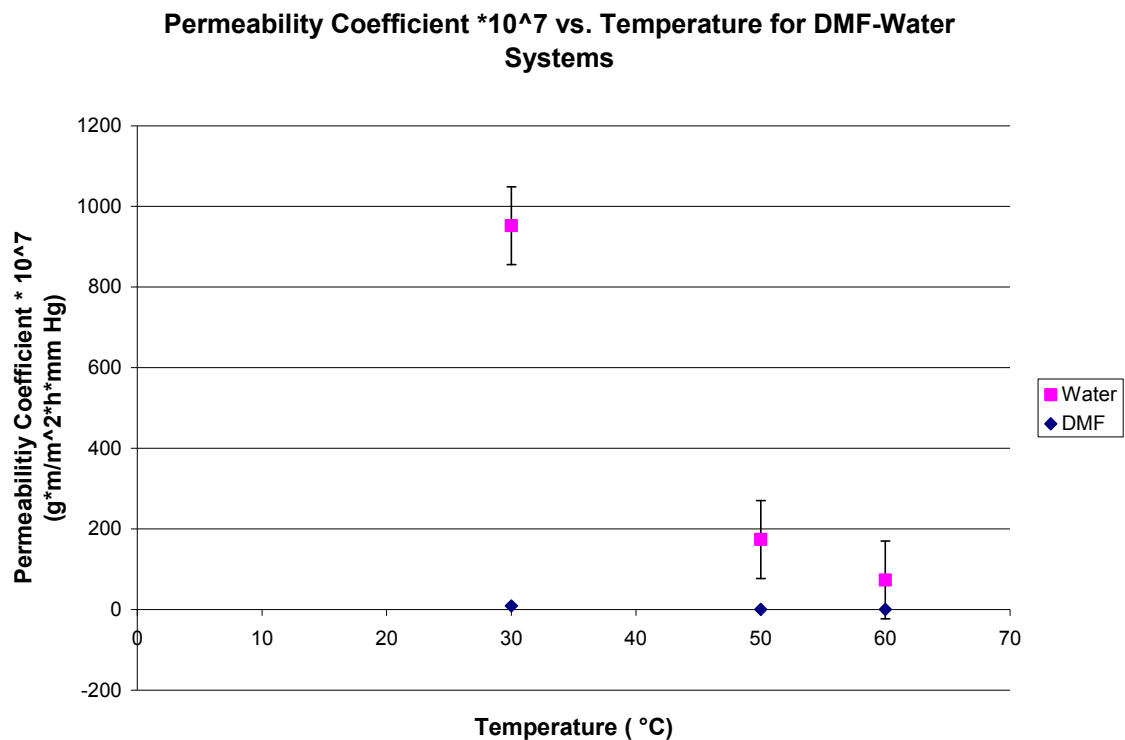


Figure 3.13 Permeability coefficient of water and DMF plotted against temperature for a 90 wt % DMF-10 wt% water feed.

Modest increases in flux with temperature are illustrated from Figures 3.5 to 3.7. Permeability coefficient of water decreases with temperature as seen in Figure 3.13. This is ultimately due to the fact that vapor pressure of water and various other species typically increase exponentially with temperature. If certain variables, such as activity coefficients, molar feed concentration and molar permeate concentration, are considered approximate, then it is apparent that as temperature increases the permeability coefficient would decrease. Similar values of flux are divided by exponentially increasing vapor pressures as temperature increases.

From another perspective, the behavior of the permeability coefficient could be dependent on a process phenomenon or principle. As temperature increases, and thus,

vapor pressure, the driving force across the membrane should increase as well. This larger differential in partial pressure typically results in the increase of solvent flux. The two major contributions for overall flux/selectivity of a membrane in pervaporation include solubility and diffusion. Figures 3.14 and 3.15 demonstrate how solubility and diffusion vary with temperature in a typical gas permeation process through a glassy polymer, polyethylene terephthalate or PET, respectively. These two phenomena behave oppositely as temperature increases. Diffusion increases many times as temperature increases as it is an activated process. On the other hand, solubility decreases with temperature. Overall permeability coefficient is the product of these two variables. In Figure 3.16, the increase in diffusion outweighs the decrease in solubility; the overall permeability coefficient usually increases with increasing temperature.

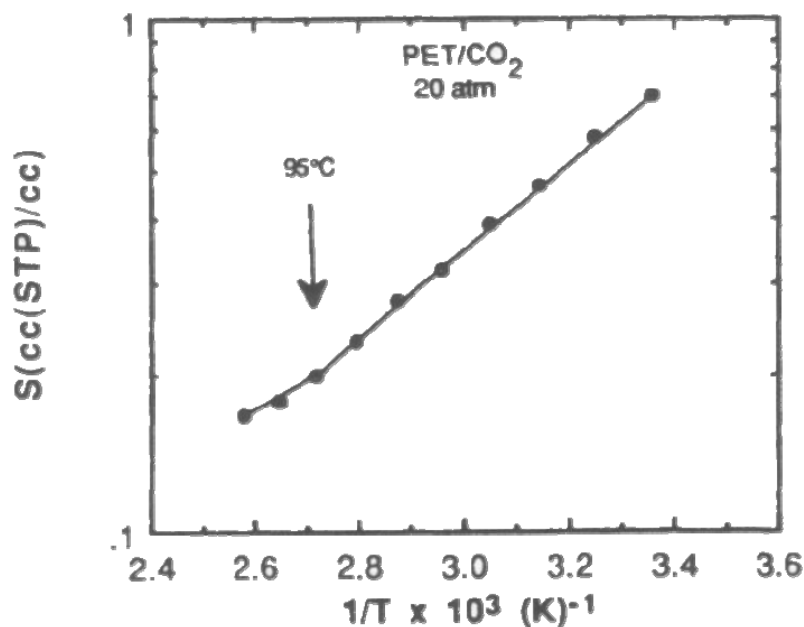


Figure 3.14 Typical behavior of solubility coefficient of CO₂ as a function of temperature [26].

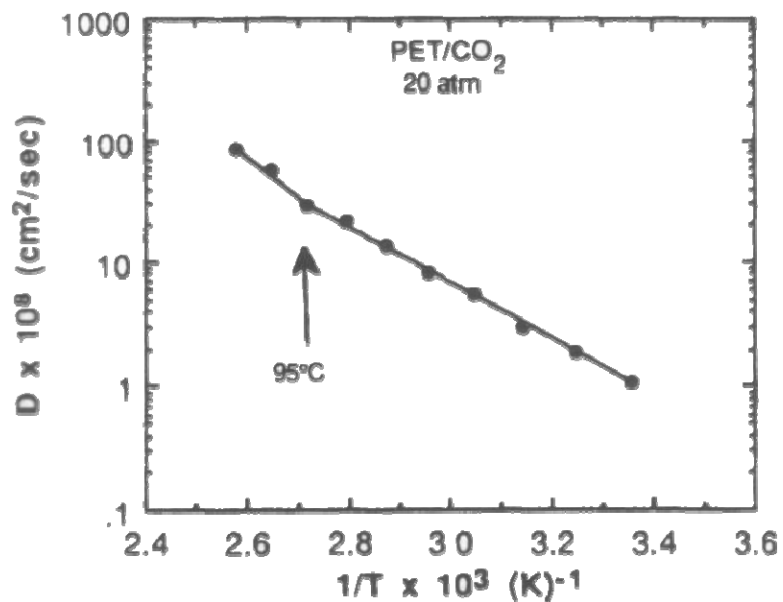


Figure 3.15 Typical behavior of diffusion coefficient as a function of temperature [26].

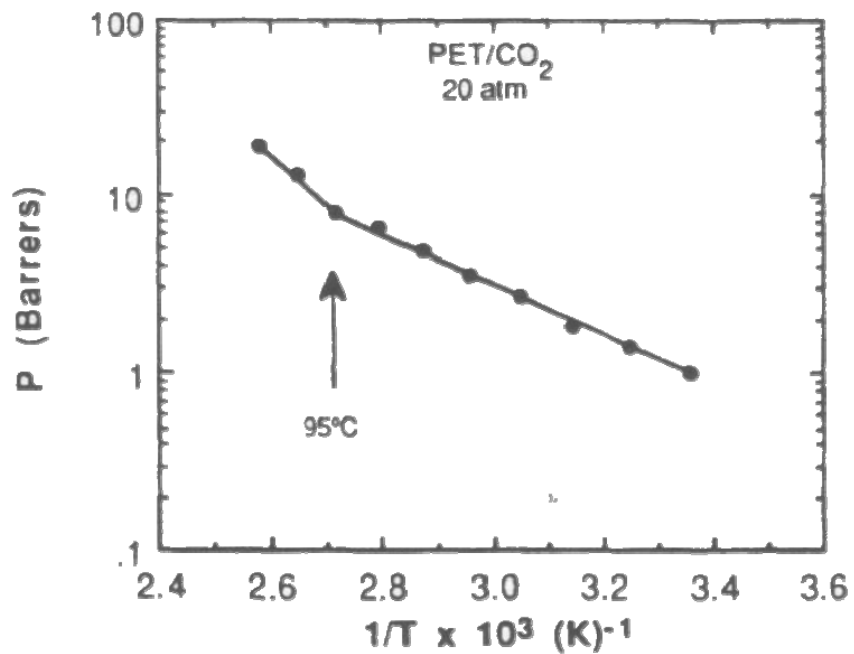


Figure 3.16 Typical behavior of overall permeability coefficient as a function of temperature [26].

However, in the case of aprotic dehydration using a PDD-TFE membrane, this does not occur. The overall permeability coefficient continues to decrease as a function of temperature. This may be attributed to sorption effects of the solvent into the membrane. For polar solvents, such as water, this is exceedingly difficult for a hydrophobic material such as PDD-TFE or CMS-3. Total sorption from the dual sorption model is due to Henry's Law sorption and Langmuir sorption as seen in Equation 3.2 (Appendix A) [27].

$$C_{im} = S_{im}P + \frac{C'_{Hi} b_i P}{[1 + b_i P]} \quad (3.2)$$

Here, C_{im} is the total concentration of species i in the membrane; S_{im} is the Henry's law sorption parameter, C'_{Hi} and b_i are the Langmuir sorption parameters and P is the total pressure. This overall behavior of solubility of a gas in a glassy polymer is illustrated in Figure 3.17 for methane solubility in a polystyrene membrane. Notably, solubility does not increase linearly with increasing pressure. Also, it is seen for Figure 3.18 that solubility parameter, C'_{Hi} , decreases with increasing temperature. This reduction in Langmuir sorption is likely to influence overall sorption of the solvent into the membrane and even affect the overall permeability coefficient with respect to temperature.

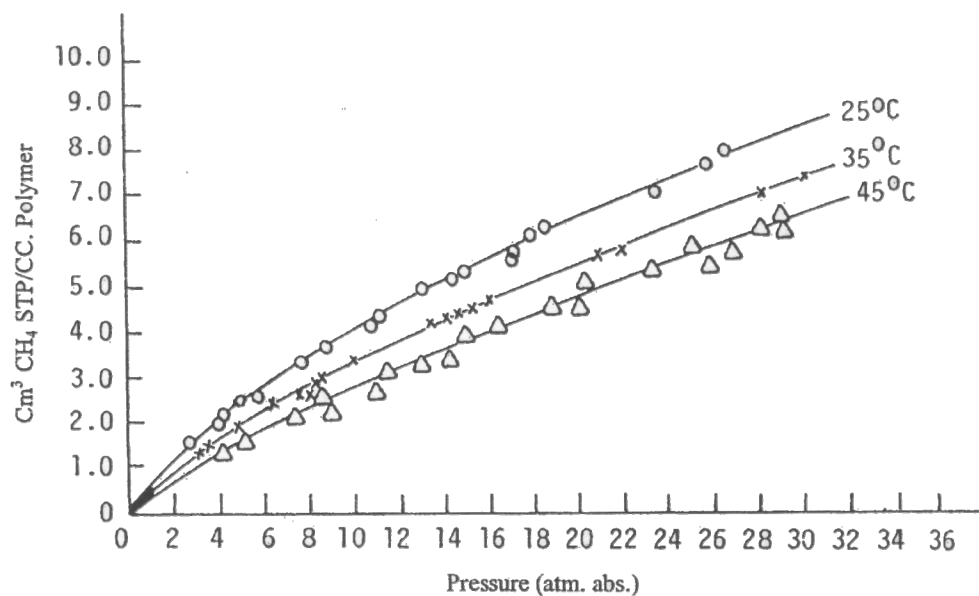


Figure 3.17 Methane solubility into a polymeric membrane as a function of temperature and pressure [28].

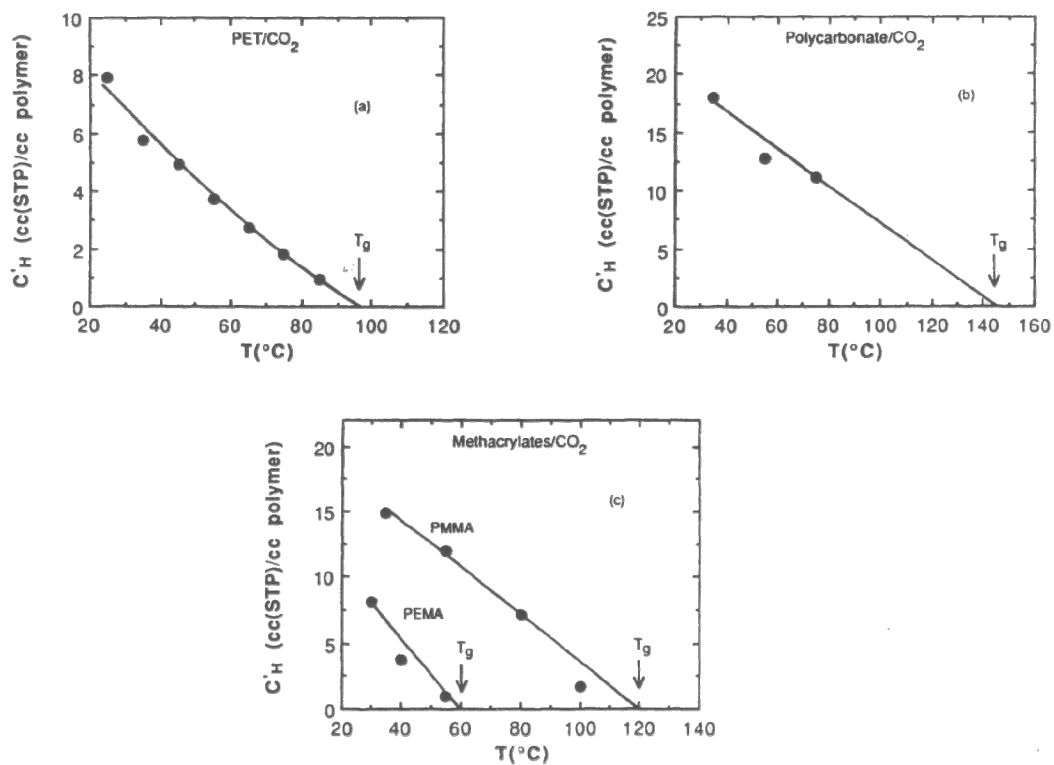


Figure 3.18 Langmuir sorption parameter as a function of increasing temperature [26].

Evidence from previous studies using Teflon AF 2400, a similar material to PDD-TFE of the CMS-3 variety, with vapor permeation has determined sorption parameters for a variety of gases. The following table has been developed from results obtained by Merkel et al. [27]. The rightmost columns have been calculated based upon conditions at 1 atm. At this pressure, Langmuir sorption typically contributes significantly more towards solubility of the gases and vapors than Henry's Law.

Table 3.5 Gas Sorption Parameters of Teflon AF 2400 by Merkel et al. [27]

Penetrant	S_{im} [cm ³ (STP) / (cm ³ atm)]	C'_{Hi} [cm ³ (STP) / (cm ³)]	b_i [1/ atm]	Henry's Law Contribution*	Langmuir Contribution*
O ₂	0.21	44	0.015	0.244	0.756
N ₂	0.11	38	0.015	0.164	0.836
CO ₂	1.60	26	0.070	0.485	0.515
CH ₄	0.35	25	0.036	0.287	0.713
C ₂ H ₆	1.50	16	0.220	0.342	0.658
C ₃ H ₈	4.20	13	0.830	0.416	0.584
CF ₄	0.45	29	0.082	0.170	0.830
C ₂ F ₆	1.60	18	0.590	0.193	0.807
C ₃ F ₈	6.40	19	2.200	0.329	0.671

If Langmuir sorption is the major contributor to overall sorption, then the effect of temperature on Langmuir sorption should greatly influence the solubility of the solvents into the membrane. This assumes that solubility is the limiting step in the pervaporation process and affects the overall permeability coefficient of each solvent through the PDD-TFE membrane.

CHAPTER 4

RESULTS AND DISCUSSION OF THE PERVAPORATION PERFORMANCE OF PDD-TFE MEMBRANE FOR ORGANIC-ORGANIC SYSTEMS

In light of the results obtained from the dehydration of aprotic solvent systems, the PDD-TFE of the CMS-3 variety has been found to have a considerable capacity to isolate water from these mixtures. Studies involving similar perfluorinated membranes have hypothesized that separation is based upon size exclusion on the molecular level. If this holds to be true, then water, compared to any other solvent, can easily pass through the membrane. However, a more in depth investigation must be completed in order to determine whether or not this hypothesis maintains merit for other organic solvent molecules of smaller dimensions.

Common organic solvents such as toluene, ethyl acetate, tetrahydrofuran, and methanol are used to determine the sieving property of the membrane at the level of dimensions of smaller organic solvents. Each solvent possesses slightly different molecular dimensions as well as shape and vapor pressure. Unlike in the previous chapter, the molecular dimensions of these solvents can be very similar. To illustrate the wide range of these solvents, the vapor pressures and dimensions can be seen in Figure 4.1 and Table 4.1. Only methanol seems to be significantly smaller than the others.

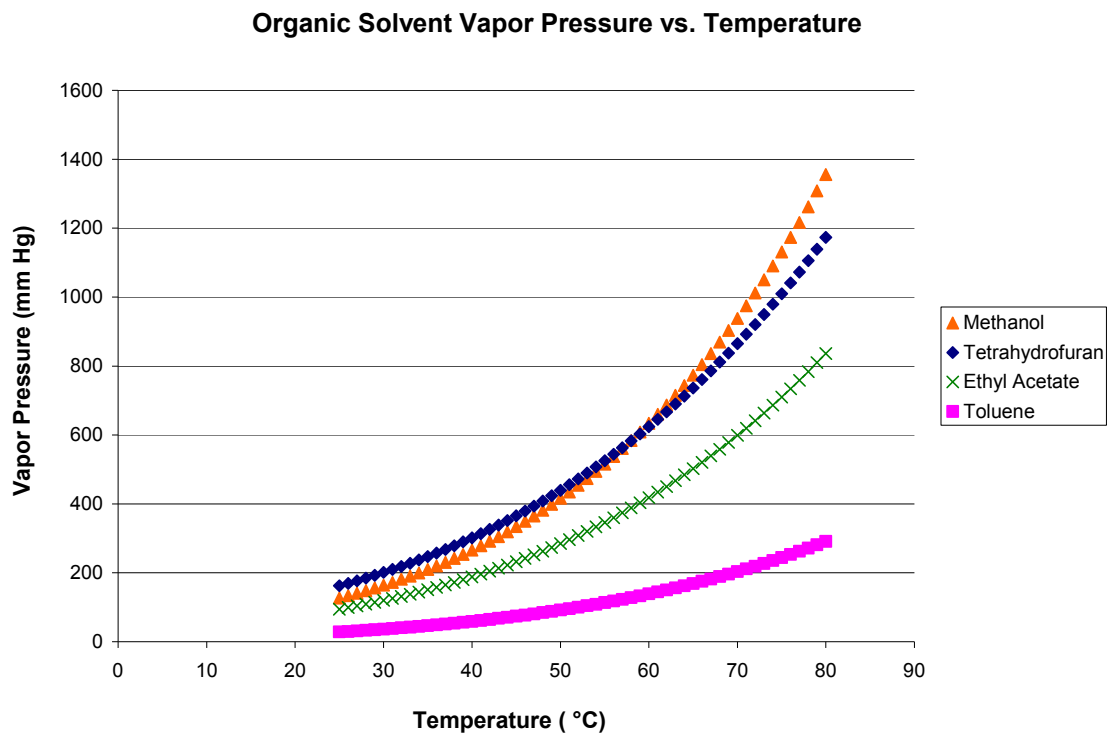


Figure 4.1 Vapor pressure of common organic solvents and water versus temperature.

Table 4.1 Various Properties and Structural Dimensions of a Few Organic Solvents

Structure	Name	Boiling Pt. (deg C)	Density (g/cm ³)	Smallest Diameter* (Angstrom)	Largest Diameter* (Angstrom)	Area* (Angstrom ²)	Volume* (Angstrom ³)
	Methanol	65	0.7918	1.757	2.844	61.23	40.75
	Ethyl Acetate	77.1	0.897	3.108	6.004	125.77	99.88
	Tetrahydrofuran	66	0.8892	3.306	4.191	105.06	86.33
	Toluene	110.8	0.8669	4.254	5.842	133.77	116.46

*as estimated using WaveFunction Spartan program

4.1 Performance of PDD-TFE Membrane on Pure Organic Solvents

4.1.1 Sorption of Pure Components onto PDD-TFE Membrane

As sorption is the initial step in the pervaporation process, it is useful to deliberate more on the information regarding competitive solubility gathered here to help understand the separation factor of one solvent over another. Preliminary measurements using pure components (Table 4.2) yield limited results in terms of differentiating one solvent from another except in the case of methanol. Solubility for most solvents is limited in this relatively inert, hydrophobic polymer; the weight gain by percent for the pure solvent did not exceed over 0.60%. More polar solvents such as methanol demonstrated significantly lower solubility in the PDD-TFE membrane than non-polar solvents. It has also been found that more polar solvents often had lower solubility in membranes of similar formulations [19]. This can apply to methanol, ethyl acetate and tetrahydrofuran when compared to that of toluene. Furthermore, methanol is a much smaller molecule. But the dimer of methanol will have dimensions around 5.69 Å. The range of average free volume dimensions in this membrane is between 5.9 to 6.3 Å [29]. Therefore, a dimer would have some difficulty in getting sorbed in the Langmuir sites. It should be emphasized that the Langmuir sites potentially play a dominant role in such a membrane. As a result, methanol solubility is very low in this membrane.

Table 4.2 Solubility of Pure Components by Weight at Room Temperature

Solvent	% Gain from Dry Weight
Ethyl Acetate	0.50
Tetrahydrofuran	0.55
Toluene	0.56
Methanol	0.29
DMF	0.20
DMAc	0.60
DMSO	0.55

4.1.2 Pervaporation Results of Pure Organic Solvents using PDD-TFE Membrane

Initial results from pure permeation tests with organic solvents have been obtained before pursuing separation studies. This would aid in generating estimates for performance values such as flux and its dependence on temperature.

Flux of methanol through the PDD-TFE membrane increases overall with temperature from 30 to 57°C. Flux values vary from 1.57 to 1.93 g/(m²-h) as seen in Figure 4.2. The increase in flux is modest. Methanol, being a smaller, yet more polar molecule, is expected to have considerably higher values than those observed. Water, a similar, but still smaller molecule in size, exhibits fairly high flux despite the membrane being a hydrophobic material. It has been shown by Jansen et al. that methanol, in fact, forms clusters of molecules in similar membrane materials such as Hyflon AD [30]. This study by Jansen et al. has confirmed that methanol is present as single molecules, dimers as well as even trimers [30]. Each variation demonstrates considerable different diffusion coefficients. Time lag experiments have shown that an average association factor of 1.8 for methanol molecules. On average, methanol molecules are present typically as dimers as they pass through the membrane. This increase in effective molecular size then impacts the methanol flux.

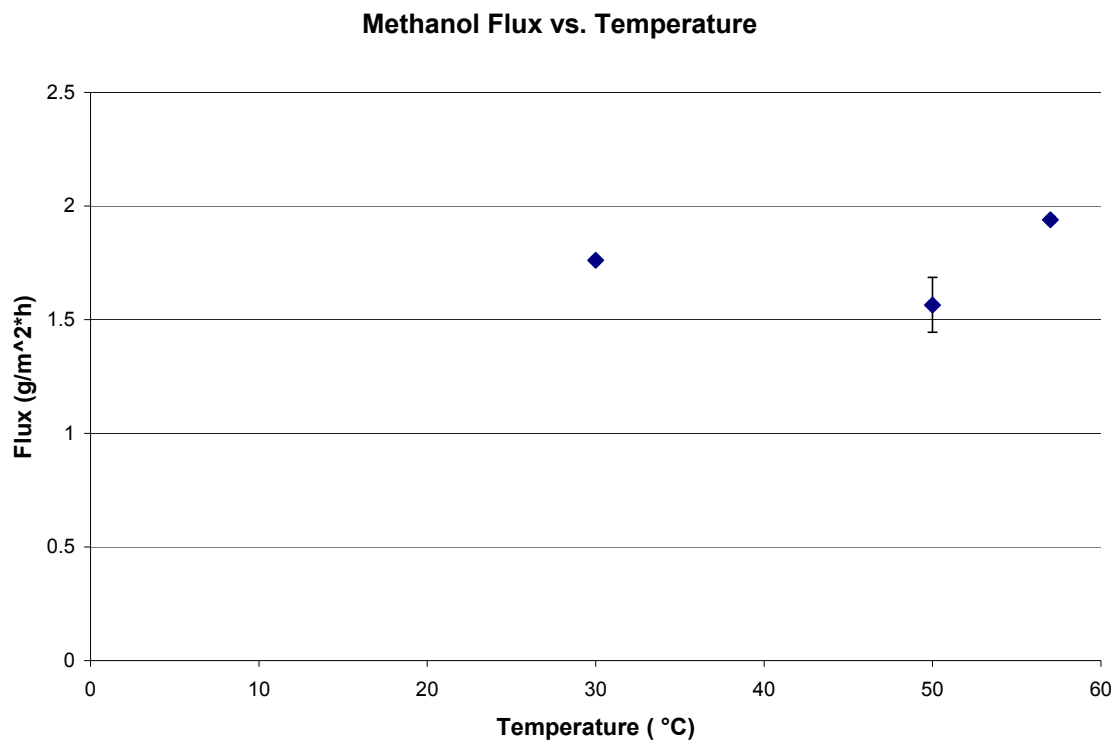


Figure 4.2 Flux of pure methanol through the PDD-TFE membrane as a function of temperature.

When the permeability coefficient is plotted against temperature, a negative temperature dependence can be observed for various pure solvents studied as seen in Figures 4.3, 4.5, 4.7 and 4.9. For methanol, the permeability coefficient decreases from $2.7 \cdot 10^{-7}$ g-m/(m²-h-mm Hg) to $9.0 \cdot 10^{-8}$ g-m/(m²-h-mm Hg). These results are similar to that obtained by Pinnau and Toy [18] for gas permeation using a related amorphous copolymer membrane, Teflon AF 2400. Their study has focused on determining the permeability coefficients for hydrogen, nitrogen, helium, oxygen, carbon dioxide, ethane, propane and chlorodifluoromethane.

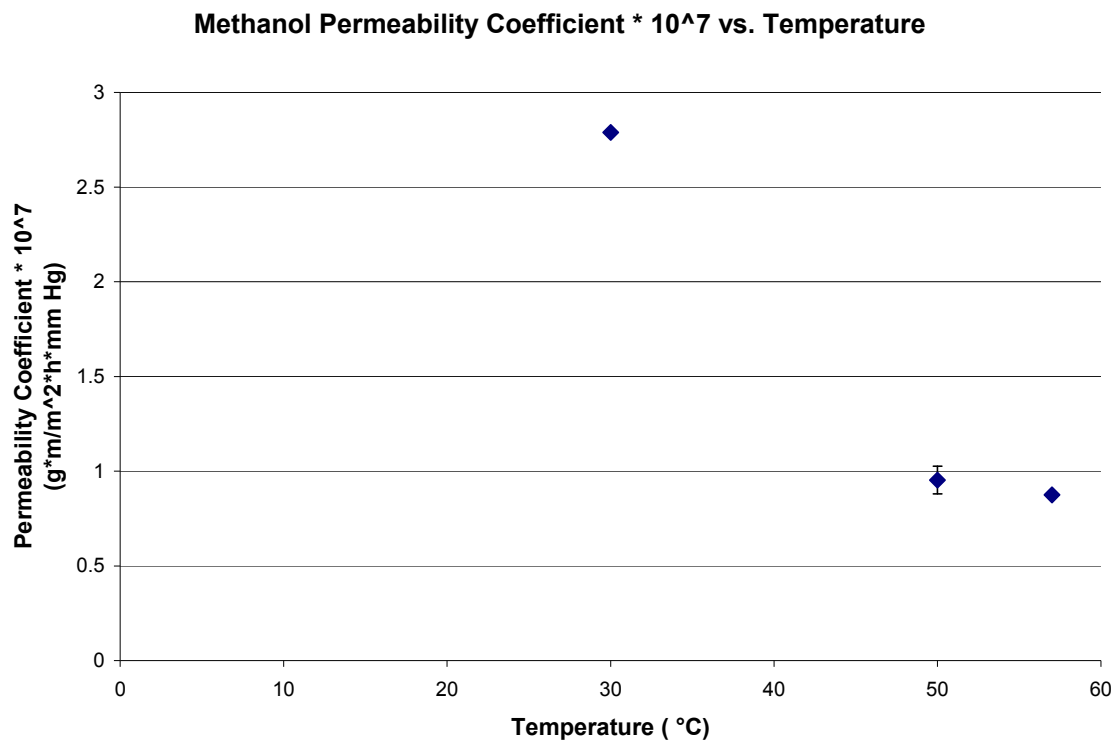


Figure 4.3 Overall permeability coefficient of methanol as a function of temperature.

Ethyl acetate is a long chain-like, polar molecule. Its size and shape are considerably different than the other common solvents investigated in this study. Both its size and polarity appears to have an effect on its flux through the perfluoropolymer membrane. In Figure 4.4, the flux of ethyl acetate decreases with increasing temperature. At temperatures above 50°C, ethyl acetate flux is similar to that of methanol. However, below 50°C, it has values of about 2.0 g/(m²-h) at 30°C and 3.3 g/(m²-h) at 25°C. This can be justified by comparing the solubility of ethyl acetate to that of methanol. If ethyl acetate has greater solubility in the PDD-TFE matrix, then its permeability coefficient is larger and is able to permeate through the membrane at a higher rate other properties being constant. Figure 4.5 illustrates the behavior of the permeability coefficient of ethyl

acetate as a function of temperature. It also follows the exponentially decreasing behavior with increasing temperature as observed for methanol.

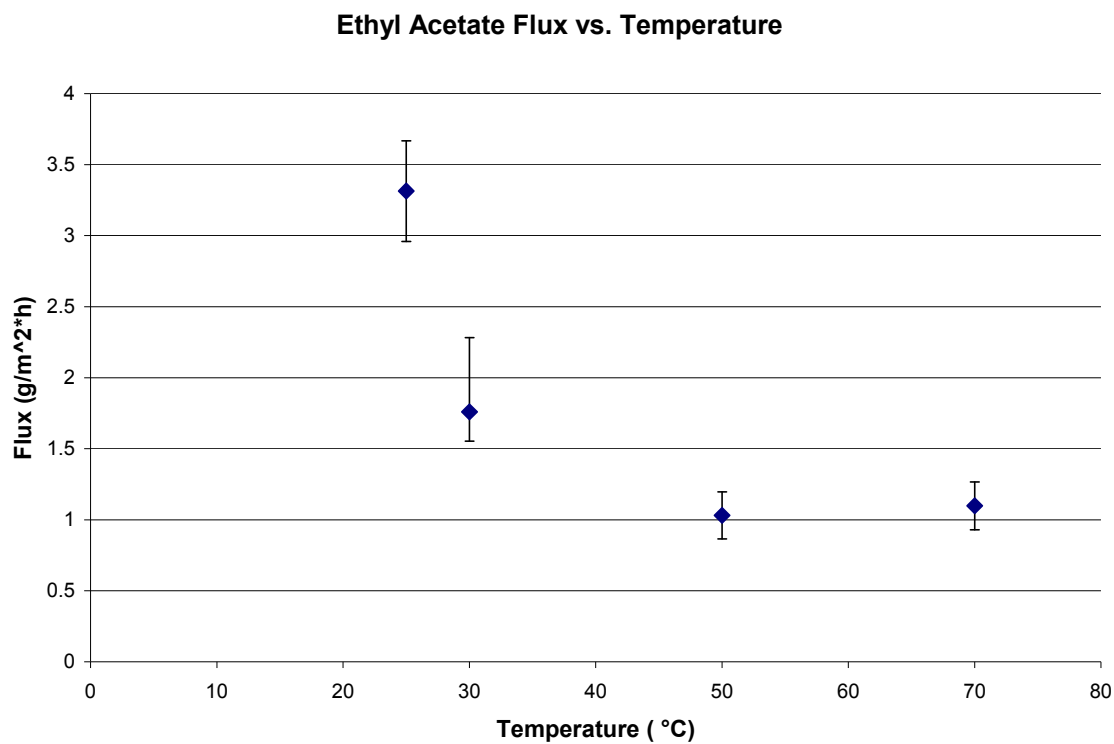


Figure 4.4 Flux of pure ethyl acetate through the PDD-TFE membrane as a function of temperature.

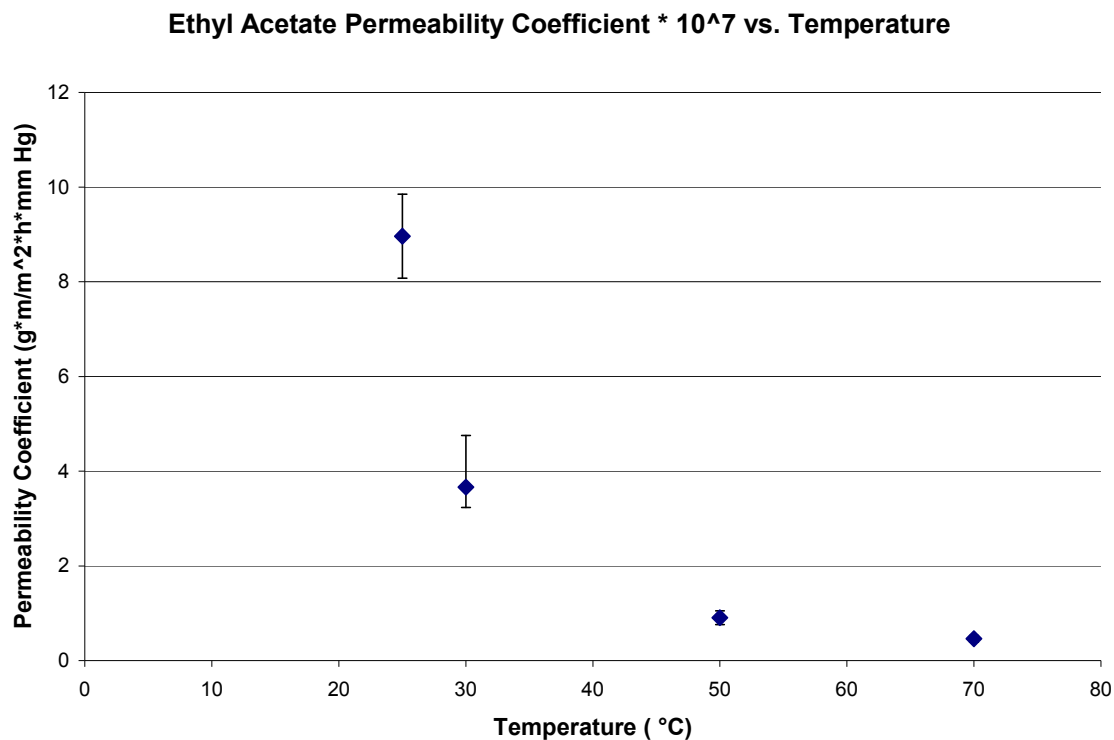


Figure 4.5 Overall permeability coefficient of ethyl acetate as a function of temperature.

Tetrahydrofuran (THF) can be described as a radially symmetrical molecule possessing some polarity. Its boiling point is on par with that of methanol and therefore, the driving force for the solvent to permeate through the membrane should be approximately similar. However, its molecular dimensions are significantly larger than methanol and its flux should reflect it if PDD-TFE retains its molecular sieve-like property. The observed flux for THF, Figure 4.6, varies from 0.15 to 0.35 g/(m²-h) as the temperature increases from 30 to 60°C. This agrees with the expectation, still, the magnitude for THF appears to be much lower than that of ethyl acetate which is much larger than THF in terms of molecular diameter. The depression of flux is probably caused by the same phenomenon present in pure methanol permeation.

Da Silva et al. [31] have determined that THF may be present in the form of dimers both in the gas and liquid phase. This can effectively alter the molecular diameter of THF permeating through the membrane from 4.191 to 8.382 Å. If this molecular dimension is used and compared to that of ethyl acetate, THF becomes the largest solvent molecule based on the longest molecular diameter. This would explain why THF flux through the membrane is significantly lower than that of both methanol and ethyl acetate. The permeability coefficient for THF is one order of magnitude lower than the solvents previously investigated. The trend decreases with increasing temperature from 1.9 g-m/(m²-h-mm Hg) at 30°C to 1.45 g-m/(m²-h-mm Hg) at 60°C in Figure 4.7.

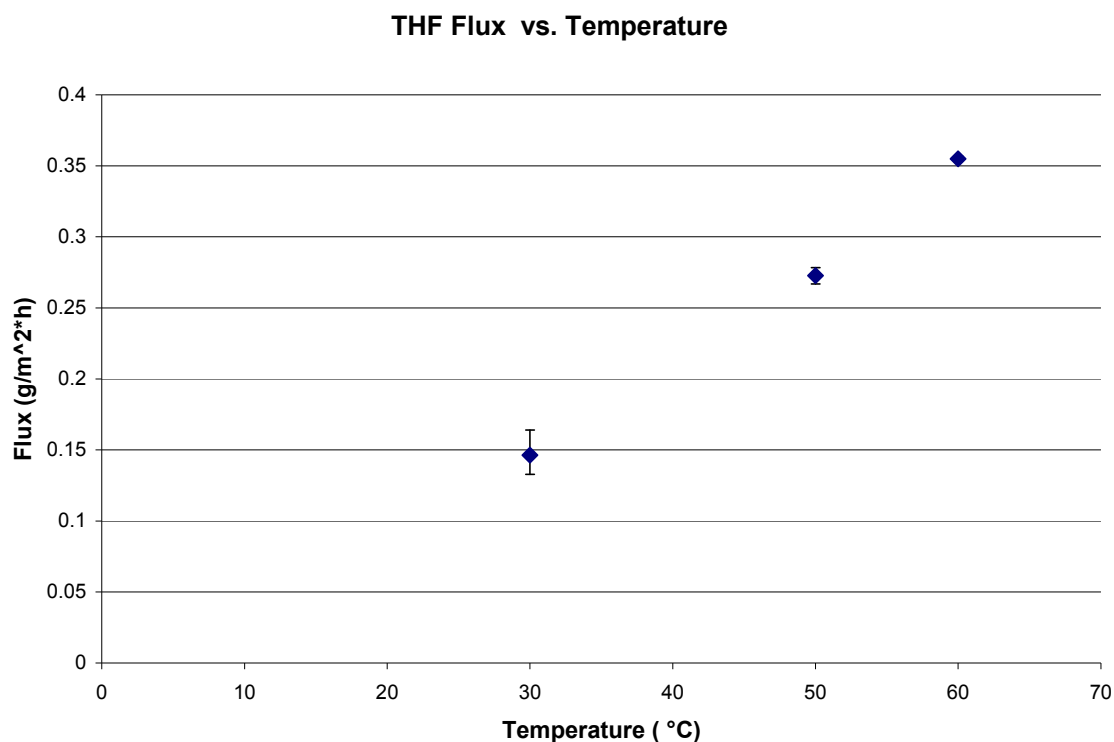


Figure 4.6 Flux of pure tetrahydrofuran through the PDD-TFE membrane as a function of temperature.

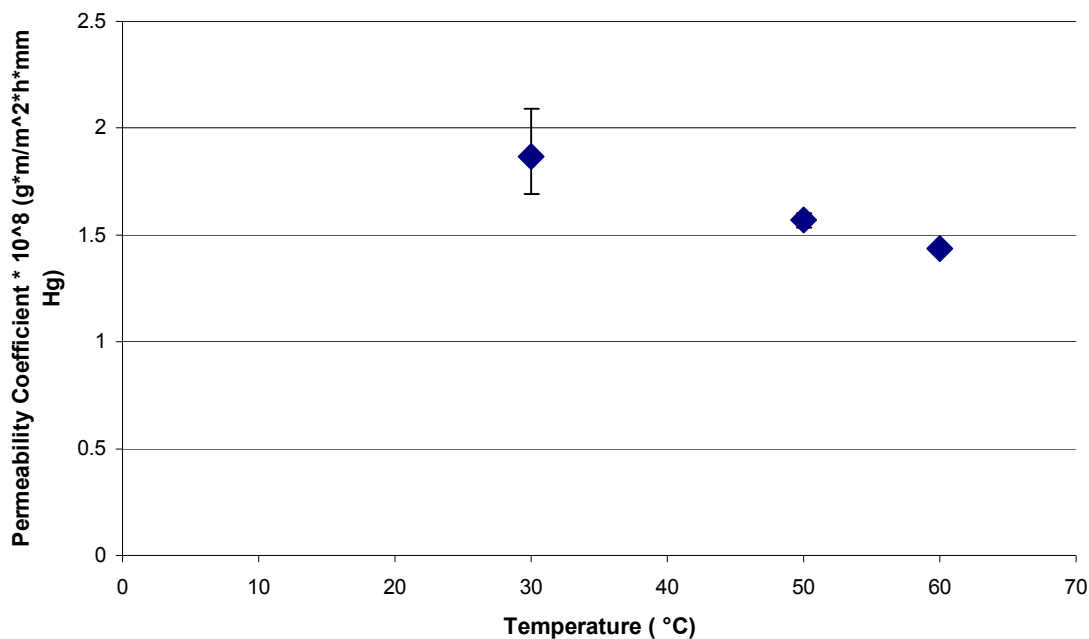
THF Permeability Coefficient * 10⁸ vs. Temperature

Figure 4.7 Overall permeability coefficient of tetrahydrofuran as a function of temperature.

Compared to the previously mentioned solvents, toluene can be considered much different due to its non-polar nature and size. Though it has significantly larger dimensions, toluene may also be able to sorp through the membrane more so than the other organic solvents and could potentially compete with them in this way when separating organic-organic solvent mixtures. In pure component permeation tests, toluene flux through the membrane increases steadily from 0.38 g/(m²-h) at 30°C to approximately 0.49 g/(m²-h) at 63°C as seen in Figure 4.8. Consequently, the overall permeability coefficient over this temperature range varies from 3.1×10^{-7} g-m/(m²-h-mm Hg) to 8.0×10^{-8} g-m/(m²-h-mm Hg), as illustrated in Figure 4.9. If these values are compared to the permeability coefficient values of pure methanol, they lie in approximately the same range.

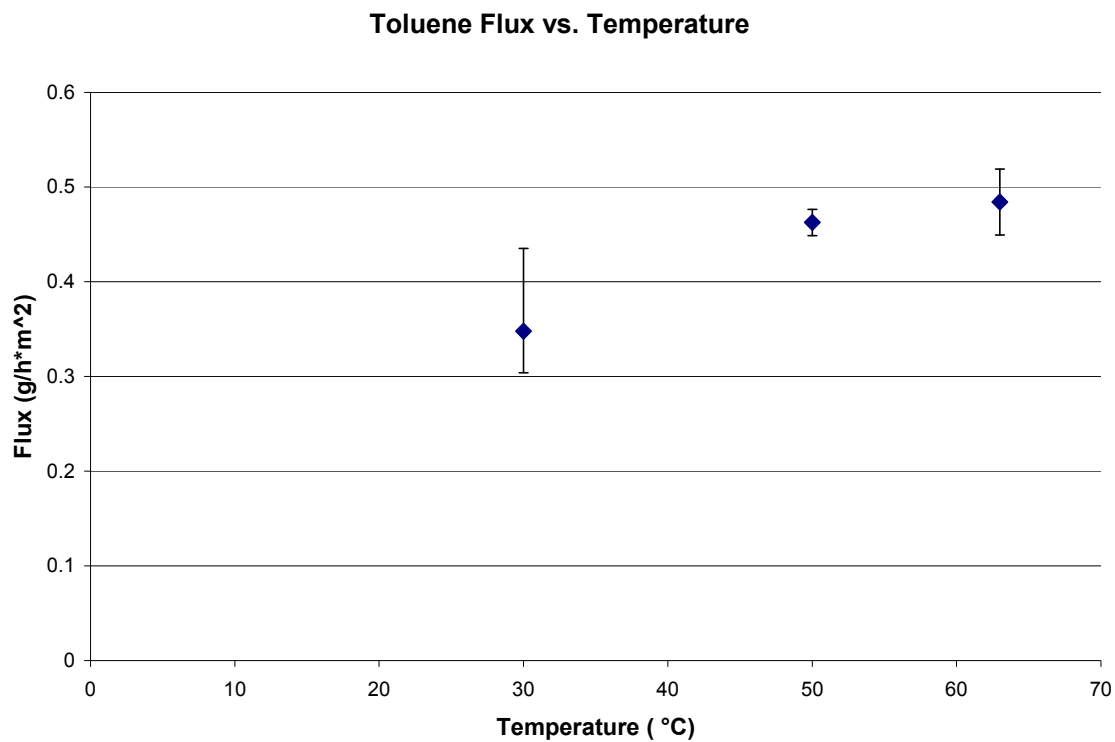


Figure 4.8 Flux of pure toluene through the PDD-TFE membrane as a function of temperature.

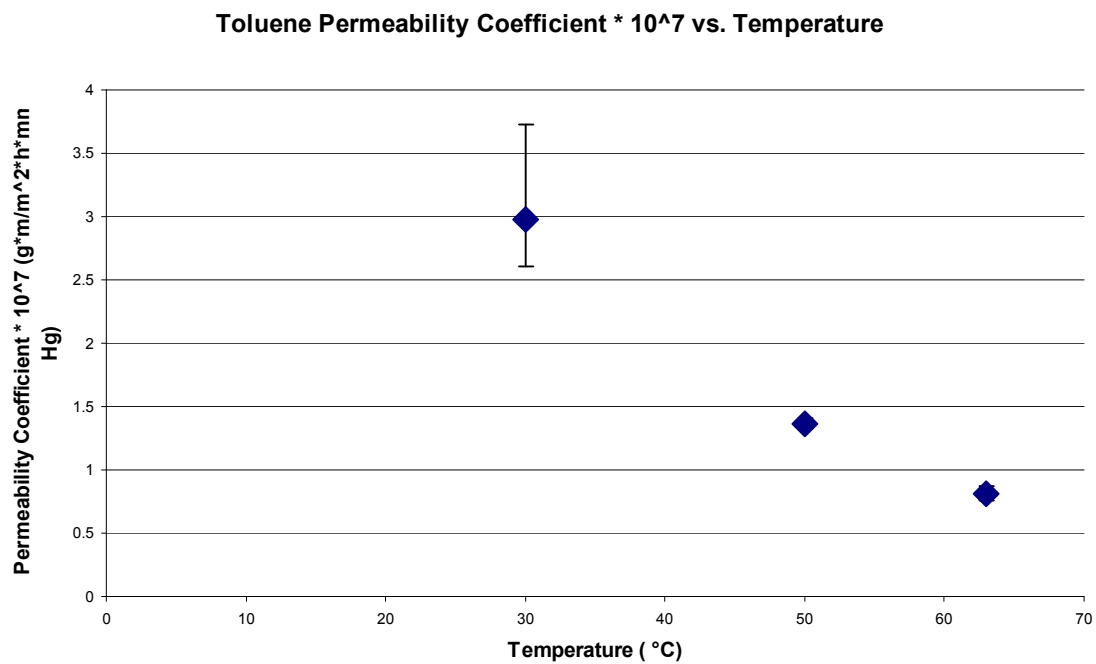


Figure 4.9 Overall permeability coefficient of toluene as a function of temperature.

Figure 4.10 demonstrates the pure solvent flux of the four organic solvents of interest over the explored temperature range. Here, it can be observed that typically smaller molecules with higher vapor pressures are able to permeate through the PDD-TFE membrane at higher rates than those having effectively large dimensions, such as THF due to likely dimerization, or lower vapor pressures.

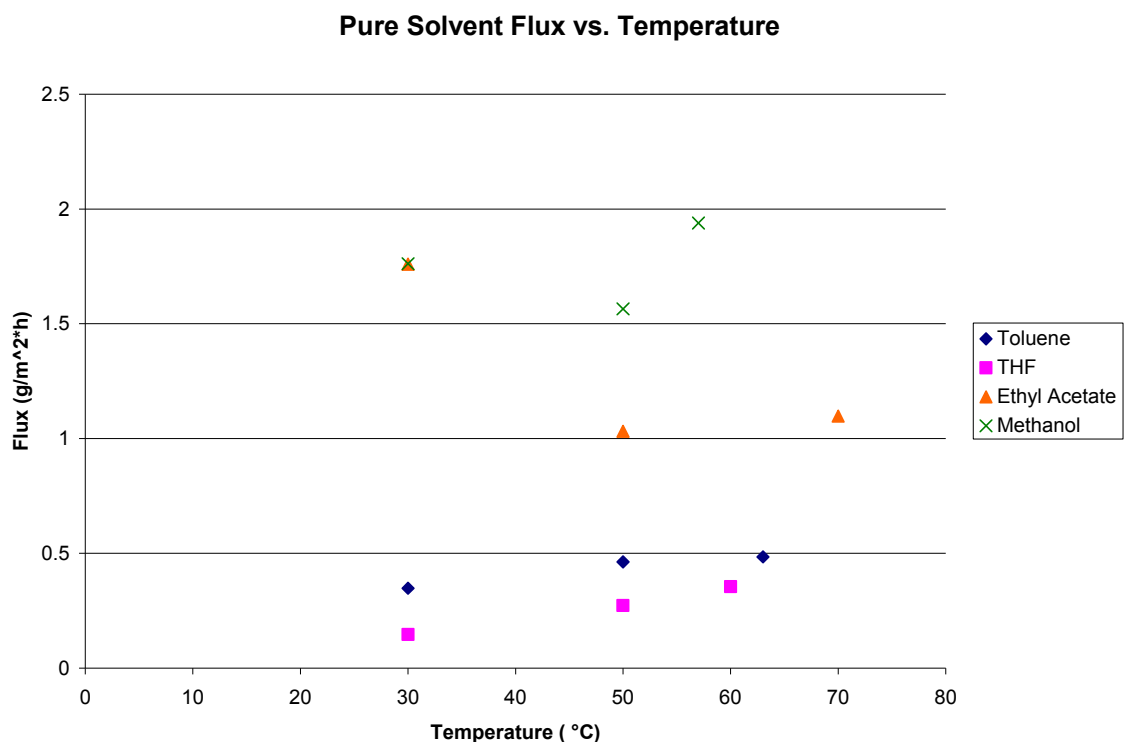


Figure 4.10 Increasing flux observed with temperature for pure organic solvents between 30 to 70°C.

Figure 4.11 illustrates the overall permeability coefficients of the common organic solvents corresponding to the flux values at each temperature. This emphasizes the prevalent decrease in permeability coefficient with temperature regardless of solvent used with the exception of tetrahydrofuran. The values plotted are numerically approximate for three of the organic solvents.

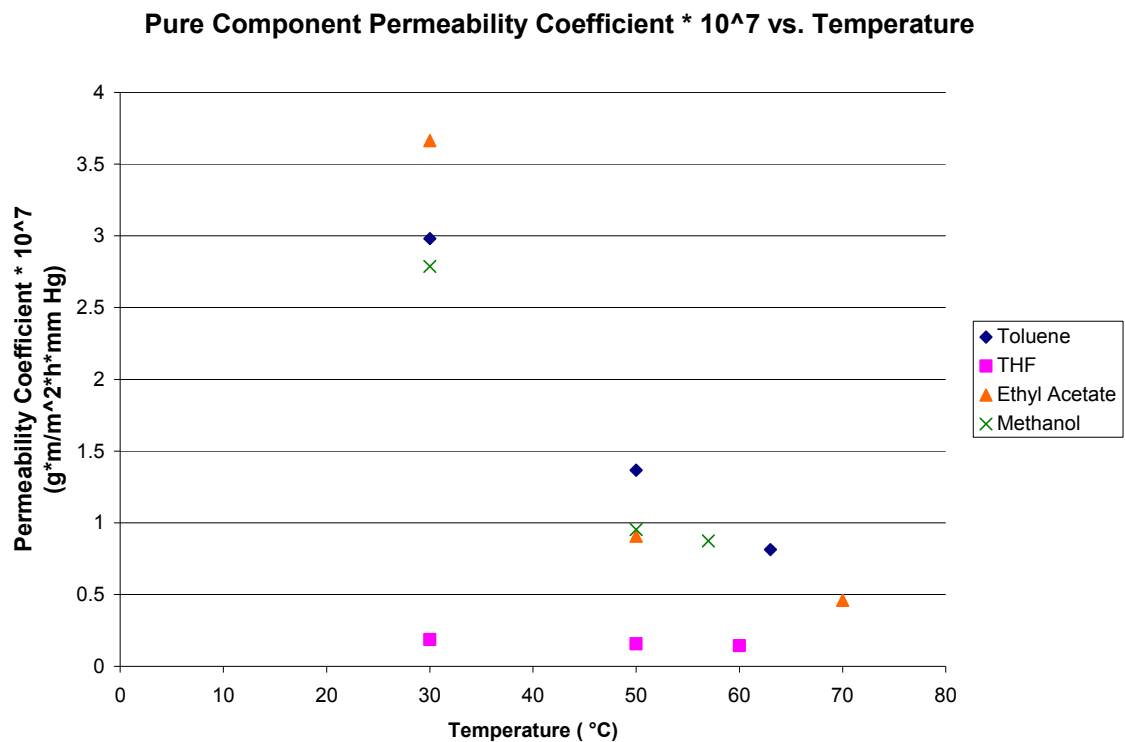


Figure 4.11 Decreasing permeability coefficient with temperature for pure solvent components through a PDD-TFE membrane.

The hypothesis of Smuleac et al. [21] that the PDD-TFE membrane acts as a size exclusive molecular sieve cannot be tested unless permeability coefficient is plotted against some molecular dimension. In Figure 4.12, this is done with the molecular dimension chosen as the longest molecular diameter. Here, it can be seen that there is some correlation between the molecular size of the solvent and a solvent's ability to permeate through the membrane. At first glance, the curve would be incomplete without adjusting the dimensions of dimers of methanol and tetrahydrofuran. This was done by multiplying their longest molecular diameter by a factor of two from Table 4.1. Though the accuracy of the actual dimer dimensions may be somewhat different from a molecular

modeling standpoint, this calculation helps estimate and facilitate understanding solvent permeation through this membrane.

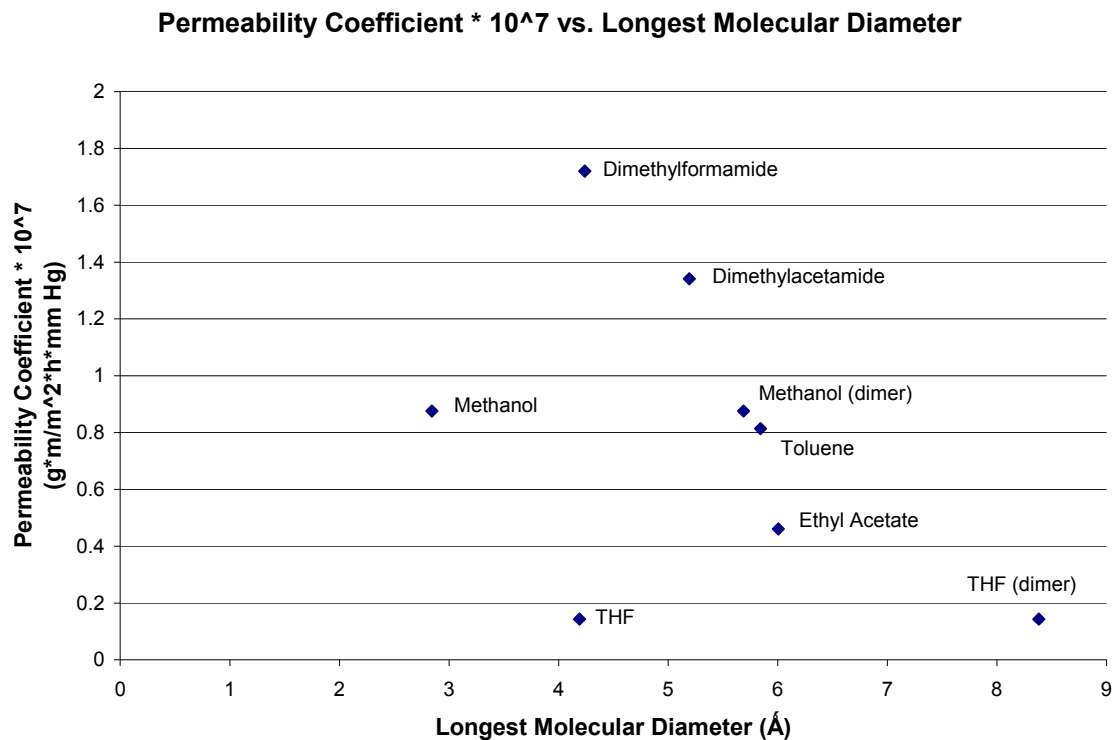


Figure 4.12 Permeability coefficients as a function of a single dimension, longest molecular diameter.

However, if the units of permeability coefficient are converted using gram moles instead of grams, the result would be Figure 4.13. It is clear that the permeability coefficient of a smaller molecule methanol would increase significantly and a more distinct curve is generated from this plot. Still, this does not adjust the permeability coefficient values of tetrahydrofuran which seem to deviate from the other points.

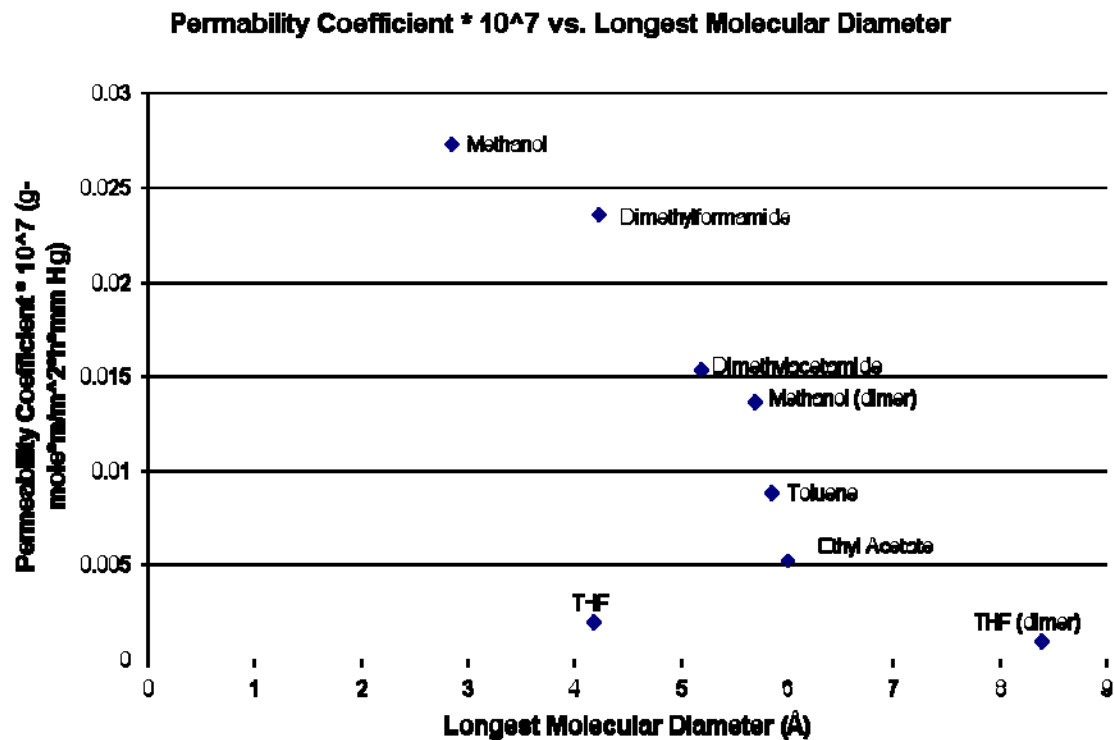


Figure 4.13 Permeability coefficients for pure solvents calculated on a per gram mole basis as a function of the longest molecular diameter.

There is an Arrhenius type relationship between the permeability coefficient and the activation energy of permeation. It is given by the following equation:

$$Q_i = Q_{i0} \exp(-E_p / RT) \quad (4.1)$$

When plotted, the slope is used to determine the required activation energy for each organic solvent. This is illustrated in Figure 4.14. The values of activation energy for ethyl acetate, toluene, tetrahydrofuran and methanol are as follows: -54.0 kJ/mol, -34.8 kJ/mol, -73.4 kJ/mol, and -37.6 kJ/mol respectively. These negative values have been reported for gas/vapor permeation through Teflon AF 2400, another amorphous polytetrafluoroethylene copolymer material [18].

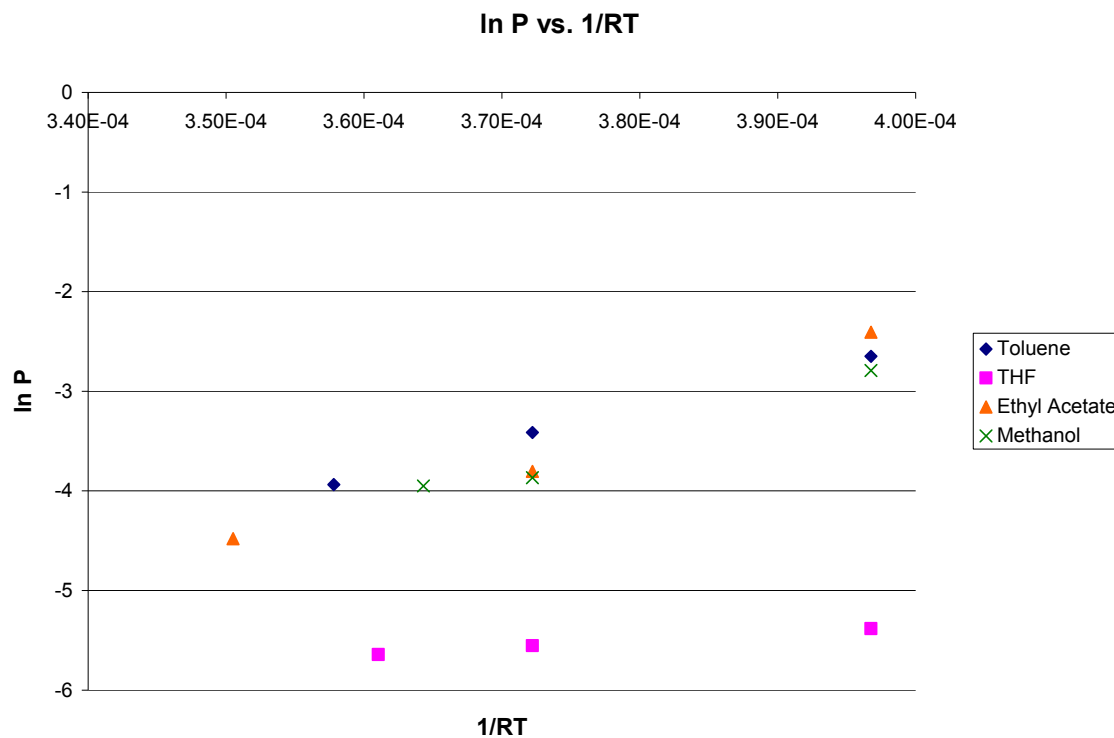


Figure 4.14 A plot of the natural log of the permeability coefficient to determine the permeation energy of pure solvents e.g., toluene, THF, ethyl acetate and methanol.

4.2 Performance of PDD-TFE Membrane to Separate Organic-Organic Systems

4.2.1 Sorption of Organic-Organic Mixtures onto PDD-TFE Membrane

A more useful approach would be to compare competitive sorption when both solvents are present. These results are summarized in Table 4.3. Headspace analysis via gas chromatography allows for the determination of the concentration of each solvent sorbed into the membrane, not the total amount sorbed. In this fashion, the distribution of solvents present in the membrane can be found. Using mixtures comprised of 50 wt%-50 wt% organic solvents, it was discovered that toluene is typically more soluble than THF, methanol and ethyl acetate. In mixtures of THF and toluene, toluene made up

approximately 57.3% of the total liquid sorbed. A similar amount was found between ethyl acetate and toluene, toluene comprising 55% of the liquid sorbed. Preliminary results from pure component sorption tests are reflected in competitive sorption for methanol. Only 0.29% by weight was sorbed in pure component solubility measurements. Here in mixture studies, methanol consists of only 0.5% of the total amount of liquid sorbed in the presence of toluene; toluene virtually occupied all free volume regions in this membrane in preference to methanol. This will affect the separation factor for methanol over toluene which otherwise should have been much larger as will be seen soon.

Table 4.3 Solubility of Mixtures by Composition

Mixture (A-B)	Sorption of A (%)	Sorption of B (%)
Methanol-Toluene	0.5	99.5
Ethyl Acetate-Toluene	45	55
Tetrahydrofuran-Toluene	42.7	57.3

4.2.2 Pervaporation Results Separating Organic-Organic Systems using PDD-TFE Membrane

By varying both temperature and composition of each mixture, flux and selectivity may change. As different solvent molecules permeate through the membrane, there is considerable competition for Langmuir sorption sites. In this way, rates of sorption and diffusion cannot be reliably predicted from pure component permeation results. As a real process, diffusion is a coupled process during pervaporation. Permeation of a faster molecule may speed up the permeation of a slower one and vice versa. In addition, solvent interaction can also play a role in affecting the thermodynamics of the system. To

account for these interactions, the activity coefficients of each system at each temperature and composition is calculated through the NRTL method using parameters determined in the software package ASPEN ©. These results can be found in Table 4.4.

In the toluene-ethyl acetate system, Figure 4.15 shows that the flux behavior with temperature and composition appears to be governed by the dominant component in the mixture. At a 50-50 weight percent mixture, toluene flux is reduced from 5.0 to 2.4 $\text{g}/(\text{m}^2\text{-h})$ as the temperature was increased from 30 to 60°C; the flux of ethyl acetate behaves similarly. However, when toluene makes up 75 weight percent with ethyl acetate completing the balance, toluene flux illustrates the more expected positive temperature dependence, increasing from 3.3 to 5.0 $\text{g}/(\text{m}^2\text{-h})$. It should be noted that at any given composition of toluene and ethyl acetate, the flux of either species is higher than their pure component permeation. This may be due to coupling.

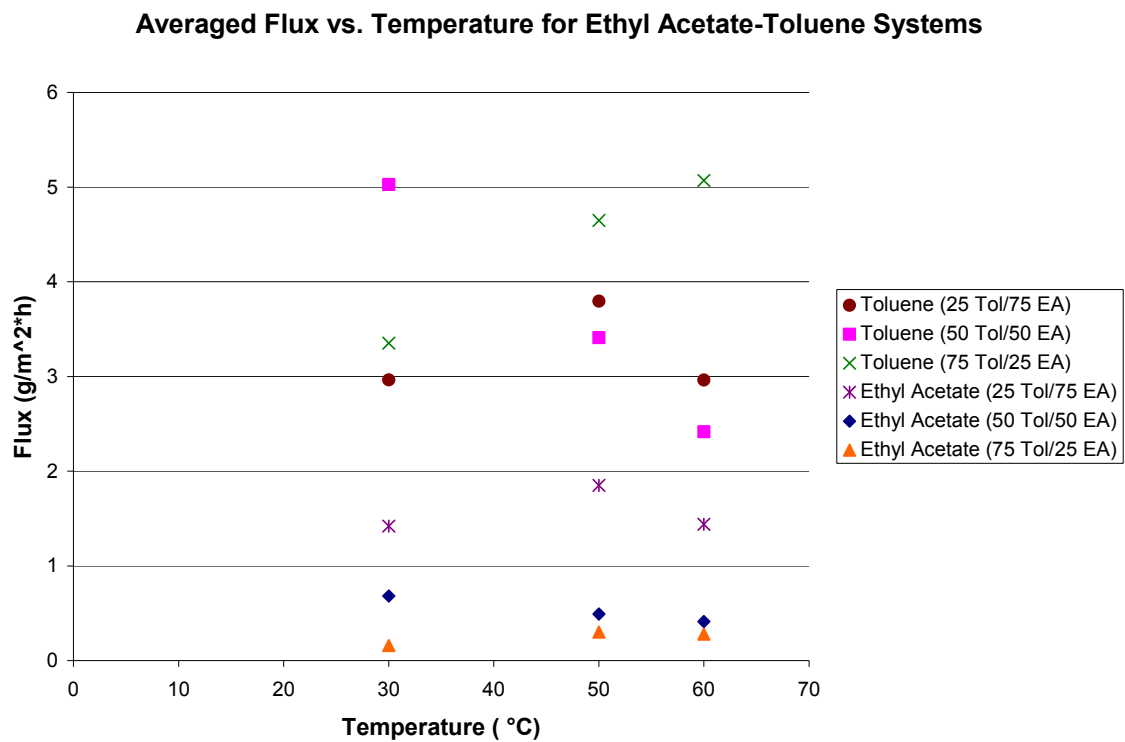


Figure 4.15 Flux behavior of toluene and ethyl acetate at varying compositions with respect to temperature.

Table 4.4 Organic Solvent Activity Coefficients at Varying Compositions and Temperatures for Three Different Organic-Aqueous Systems

	Methanol-Toluene (A-B)						Ethyl Acetate-Toluene (A-B)						THF-Toluene (A-B)					
	30°C		50°C		60°C		30°C		50°C		60°C		30°C		50°C		60°C	
A-B	γ_A	γ_B	γ_A	γ_B	γ_A	γ_B	γ_A	γ_B	γ_A	γ_B	γ_A	γ_B	γ_A	γ_B	γ_A	γ_B	γ_A	γ_B
25%-75%	1.66	1.75	1.62	1.70	1.61	1.68	1.47	1.00	1.35	1.01	1.29	1.01	0.70	0.94	0.79	0.96	0.83	0.97
50%-50%	1.20	2.88	1.19	2.76	1.18	2.71	1.21	1.06	1.16	1.07	1.13	1.07	0.83	0.85	0.89	0.89	0.91	0.91
75% 25%	1.07	4.15	1.06	3.93	1.06	3.83	1.05	1.26	1.04	1.23	1.03	1.21	0.93	0.72	0.96	0.80	0.97	0.83

The PDD-TFE membrane seems to be selective for toluene over ethyl acetate, despite the much higher boiling point of toluene and the differences in their molecular dimensions. Figure 4.16 illustrates the separation factor remaining relatively constant at 6 over all compositions of this binary system and temperatures. This might be in part due to ethyl acetate's long chain-like structure versus toluene's more globular shape (Table 4.1). The longest diameter of ethyl acetate is approximately 6 Å whereas for toluene, it is slightly smaller at 5.8 Å. The average free volume dimensions of these membrane materials have been reported to be approximately 5.9 – 6.3 Å [29]. Though the molecular dimensions of these two solvents are slightly different, the differences in hydrophobic interactions with the membrane material may allow one solvent to occupy preferentially the free volume regions and therefore pass through significantly easier than the other. Competitive sorption results of this mixture show that toluene has a significantly higher solubility than ethyl acetate (Table 4.3). Permeability coefficient for both ethyl acetate and toluene follow a negative temperature dependence as seen previously with pure permeation tests as well as dehydration of aprotic solvents. This trend can be seen in Figure 4.17.

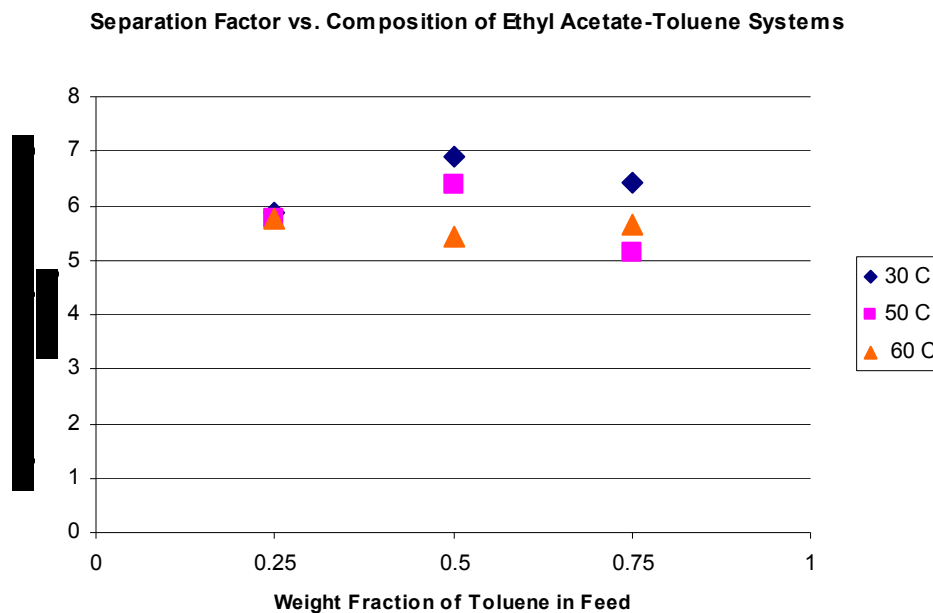


Figure 4.16 Separation factor of the PDD-TFE membrane as a function of feed composition for systems of ethyl acetate and toluene at varying temperatures.

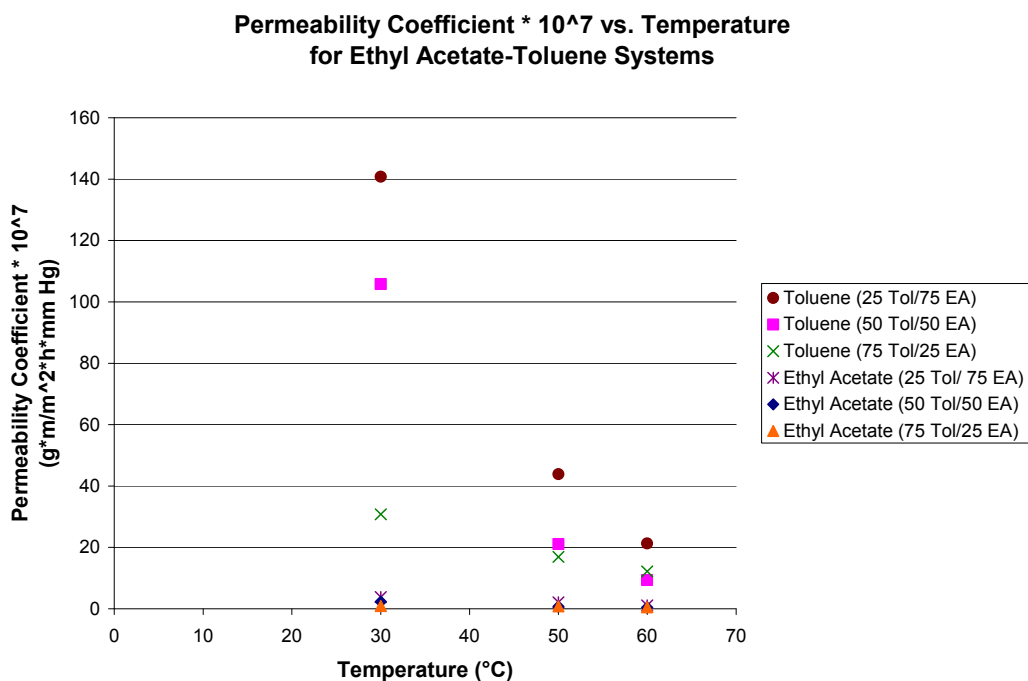


Figure 4.17 Decreasing permeability coefficient with temperature for ethyl acetate-toluene systems through a PDD-TFE membrane.

Results from separating methanol-toluene mixtures reflect pure component permeation more so than in the toluene-ethyl acetate system. Figure 4.18 shows that the separation factor for methanol over toluene increases from 2.8 to 7.7 as toluene concentration in the feed increases. This is likely to be due to the increase in the activity coefficient of methanol in mixtures with higher toluene concentration (Table 4.4).

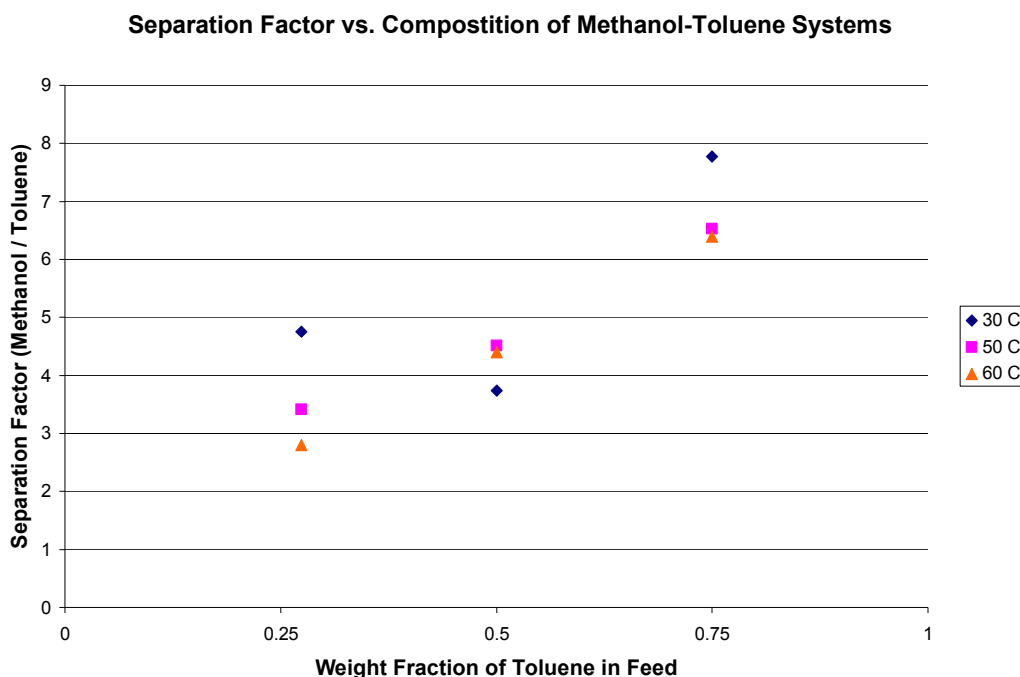


Figure 4.18 Separation factor of the PDD-TFE membrane as a function of feed composition for systems of methanol and toluene at varying temperatures.

The overall performance of the membrane can be attributed to a sieving behavior with caveats. Methanol is a significantly smaller molecule compared to toluene in all dimensions, radius, area and volume. Methanol has a much higher vapor pressure than toluene. Thus, it should pass through the membrane much more easily than toluene. It is also speculated that the flux and the separation factor of methanol would have been much

higher if there were no self-association of methanol molecules; further, methanol being highly polar and potentially present as a dimer undergoes very poor sorption in the free volume holes in the membrane compared to toluene (Table 4.3). The flux values of individual species in toluene-methanol mixtures are shown in Figure 4.19. Methanol permeates through the membrane at a much higher rate at all temperatures and compositions, ranging from 0.9 to 2.3 g/(m²-h). Toluene flux values are between 0.08 and 0.63 g/(m²-h). Overall permeability coefficients for this system are shown in Figure 4.20.

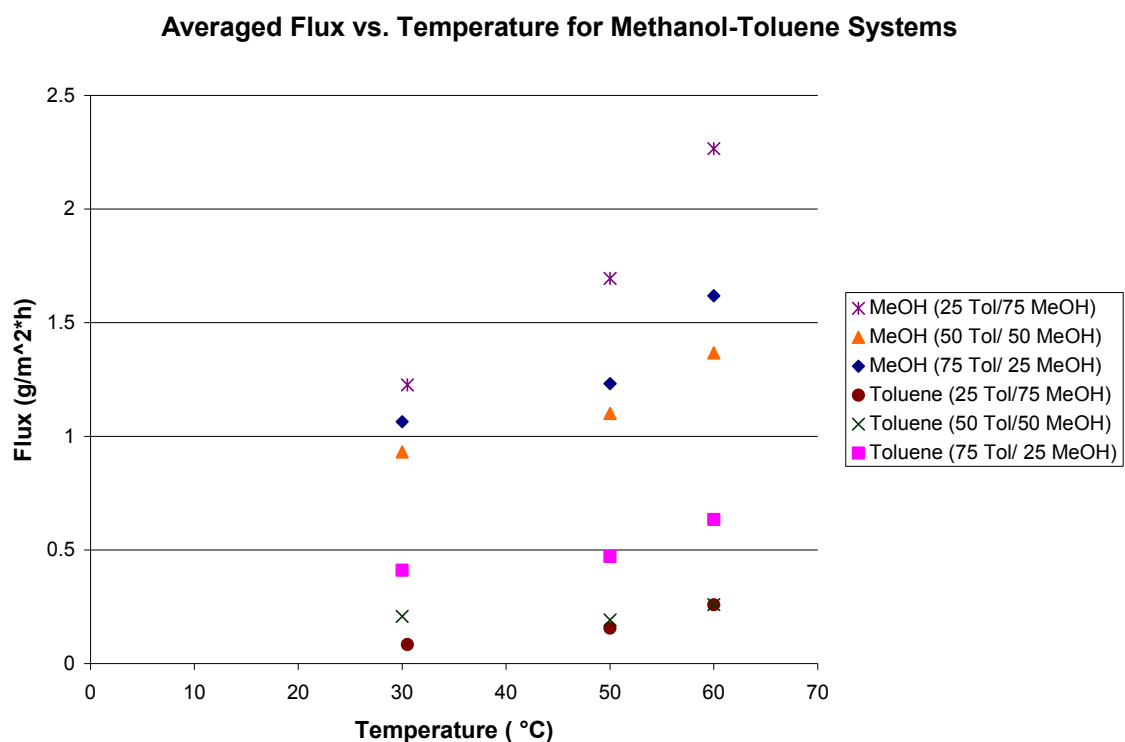


Figure 4.19 Flux behavior of toluene and methanol at varying compositions with respect to temperature.

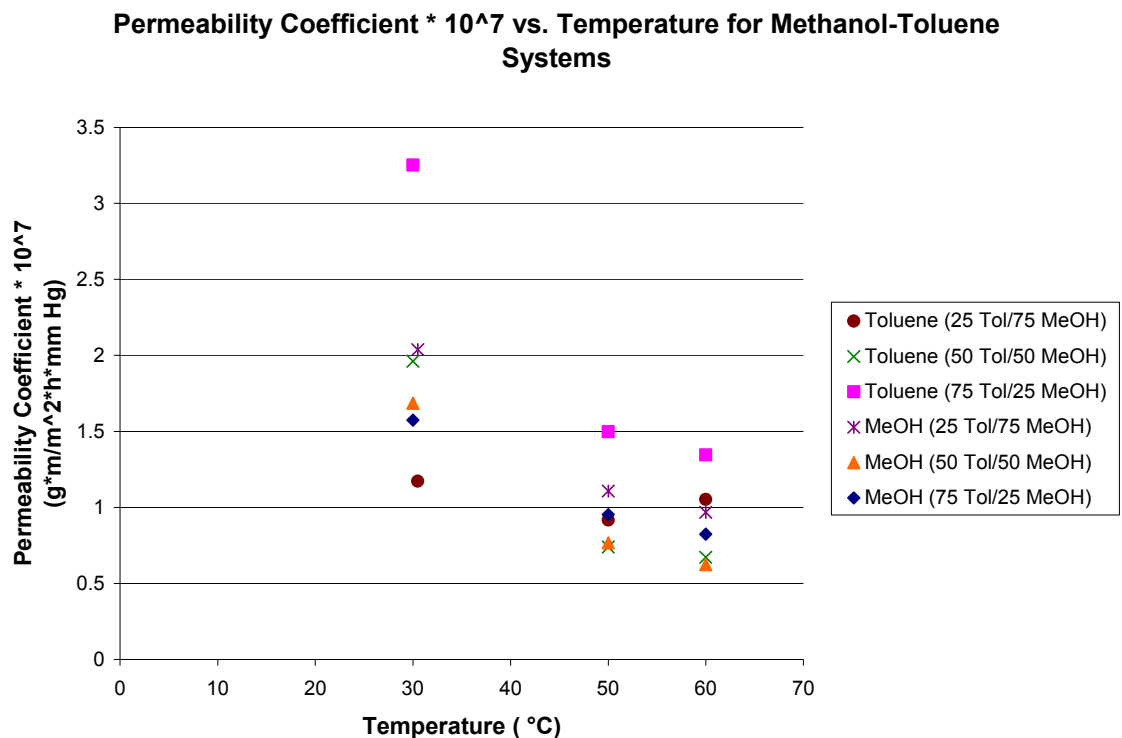


Figure 4.20 Decreasing permeability coefficient with temperature for methanol-toluene systems through a PDD-TFE membrane.

Similar observations are made when separating mixtures of toluene and tetrahydrofuran (Figures 4.21, 4.22, 4.23). Both solvents have molecular dimensions that are similar in shape and value. However, tetrahydrofuran is smaller by a couple of Angstroms in some cases. At lower temperatures, 30°C, the membrane achieves separation factors of only 1.2 to 1.5 for tetrahydrofuran over toluene over all composition ranges. Note, however that THF is much lower boiling, has a much higher vapor pressure; one would therefore expect high selectivity for THF over toluene. However, it has a significantly lower sorption than toluene in a mixture presumably due to its polar nature (Table 4.3). In addition, the more polar THF undergoes association (Figure 4.12) which will reduce its sorption, diffusion and therefore permeation.

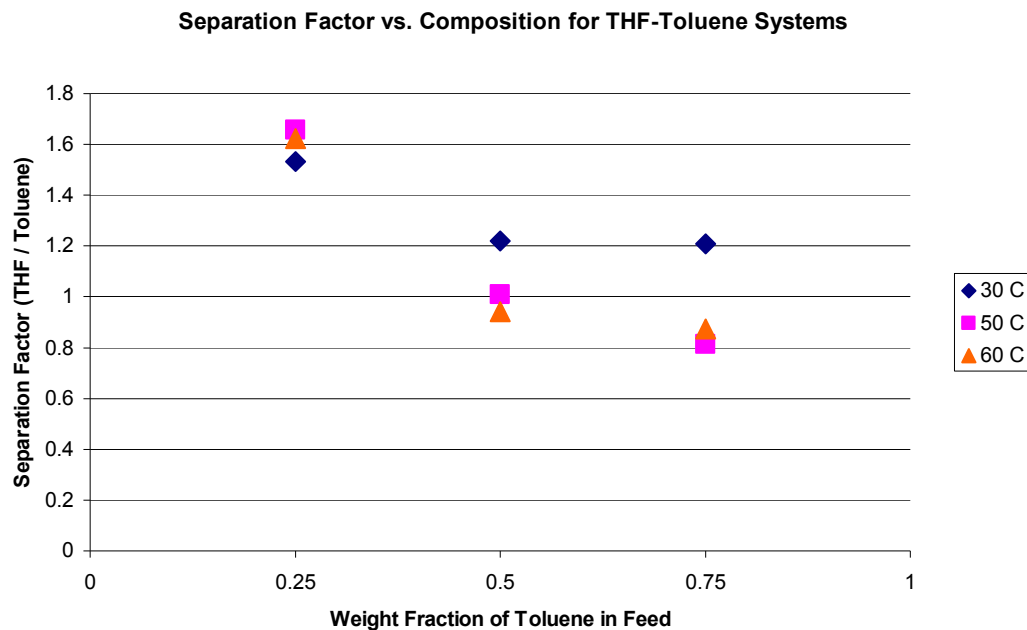


Figure 4.21 Separation factor of the PDD-TFE membrane as a function of feed composition for systems of tetrahydrofuran and toluene at varying temperatures.

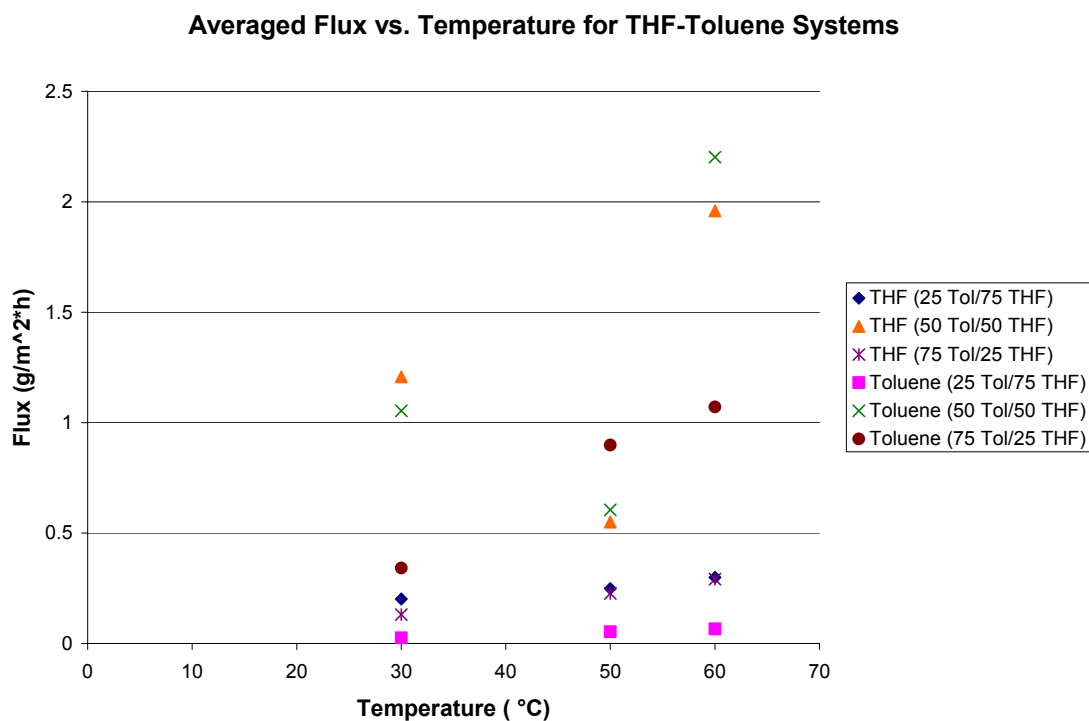


Figure 4.22 Flux behavior of toluene and THF at varying compositions with respect to temperature.

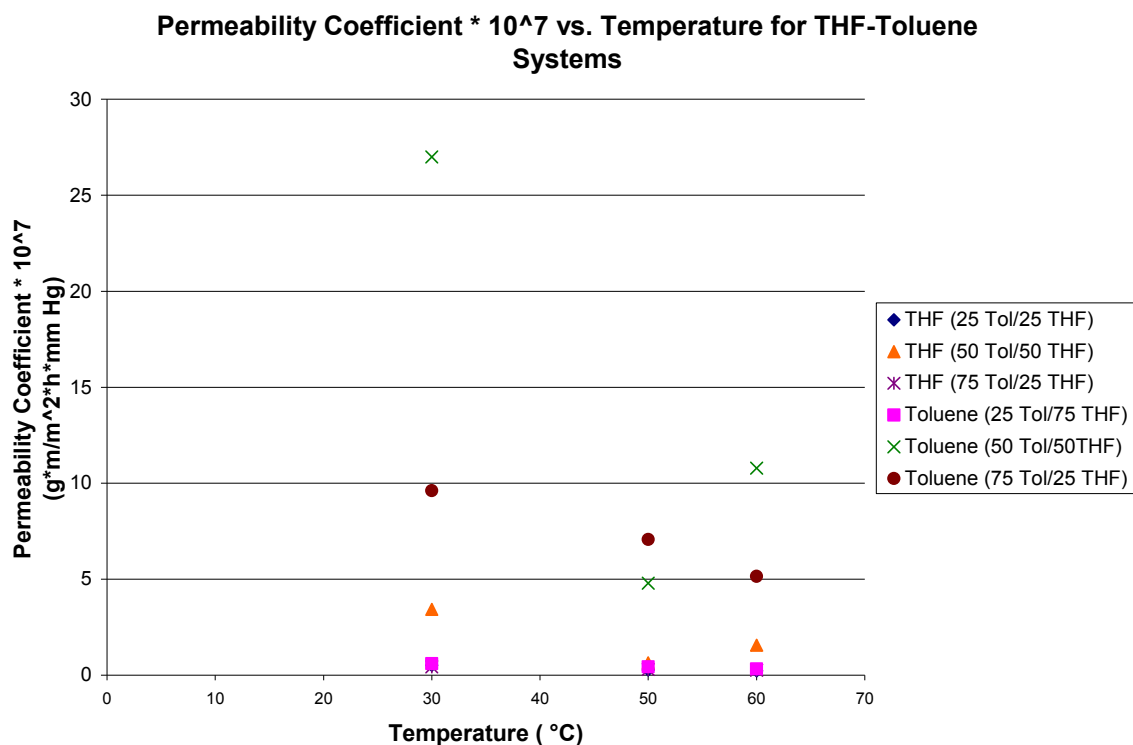


Figure 4.23 Decreasing permeability coefficient with temperature for THF-toluene systems through a PDD-TFE membrane.

Permeability coefficients for all solvents, pure or in mixture, decrease as a function of temperature (see Figures 4.3, 4.5, 4.7, 4.9, 4.17, 4.20, and 4.23). As previously mentioned in Chapter 3, this is an unexpected result as the overall permeability coefficients for solvents through polymers typically increase with increasing temperature. Still, the overall permeability coefficient is a product two parameters, the diffusion coefficient and the solubility coefficient. Diffusion coefficient increases significantly with temperature, while the solubility coefficient behaves in the opposite manner. For this reason, the solubility coefficient may give further information about

solvent permeation through the amorphous glassy perfluoropolymer membranes of the type being studied.

From a previous study of permeation of various gases through a Teflon AF 2400 membrane by Merkel et al. [27], several sorption parameters were determined for a variety of gases for both Henry's Law and Langmuir sorption. An initial analysis using this data had shown (Table 3.2) that Langmuir sorption contributes much more (around 60 – 75%) towards total sorption than the sorption attributed to Henry's Law. It should also be noted that the Langmuir sorption parameter also decreases strongly with increasing temperature. It is speculated that Langmuir sorption influences overall sorption of the various organic solvents onto the PDD-TFE membrane.

CHAPTER 5

ALTERNATIVE USES OF PDD-TFE MEMBRANE IN DEHYDRATION

Performance of PDD-TFE is significantly higher in removing solvents with particularly smaller molecular dimensions from feed solutions. The results from Chapter 3 and Chapter 4 demonstrate the membrane's ability to separate solvents based on size exclusion. However, the larger the disparity between the solvents' dimensions, the greater the separation factor is between these solvents. Specifically, water permeates through the membrane at a much higher rate than any pure organic solvent or organic solvent in mixture. Utilizing this membrane material for dehydration of organic solvents would produce insight into additional applications outside of the pharmaceutical industry.

5.1 Dehydration of Volatile Organic Compounds

Recovery of volatile organic compounds (VOCs) such as acetone, ethanol, and n-butanol are highly desired as sustainable sources of energy. However, production of these VOCs via fermentation is in a solution with large quantities of water. One specific example is obtaining fermentation broth through the growth of *C. acetobutylicum* (ATCC 824) bacteria culture in what is called the ABE (acetone-butanol-ethanol) fermentation. A typical fermentation broth consists of 1.5 – 2.5% n-butanol, 0.5 – 0.8% ethanol and 0.4 – 1% acetone by weight and the balance is water. Dehydration of such a solution would greatly increase the cost of separating these VOCs. The presence of water in fermentation broth also creates an azeotrope with ethanol. This azeotrope places traditional separation techniques like distillation at a disadvantage.

Thongsukmak and Sirkar [15] have developed a pervaporation membrane using a liquid membrane of trioctylamine immobilized on a porous hollow fiber support having a nanoporous fluorosilicone coating. This liquid membrane provides significant selectivity values for organic solvents useful as a fuel source while returning water back to the fermentation broth. This membrane produces a vacuum pervaporation-based permeate that is composed of approximately 10 wt% water, a considerable reduction from 95.7 wt% in the original fermentation broth. If complete dehydration of this permeate is achieved, then another subsequent separation process can be applied for effective purification of VOCs.

Figures 5.1 and 5.2 show of the dehydration of a processed fermentation broth. The feed solution consists of 10.8% water, 56.2% n-butanol, 5.3% ethanol and 27.7% acetone by weight [15]. This investigation has been carried out at two temperatures, 30°C and 50°C. As seen in the separation for aprotic solvent-water systems in Chapter 3, water permeates significantly faster through the membrane when compared to organic solvents. In Figure 5.1, it can be seen that as temperature increases, the flux increases as well. Water flux through the membrane increases from 27.1 g/(m²-h) to 33.1 g/(m²-h). The fluxes of acetone and ethanol remain somewhat constant, 0.415 g/(m²-h) and 0.00013 g/(m²-h) at 30°C, and 0.396 g/(m²-h) and 0.000136 g/(m²-h) at 50°C respectively. The flux for n-butanol increases from 0.0266 g/(m²-h) to 0.0637 g/(m²-h). This value may seem high in comparison to the other solvents with smaller molecular dimensions and higher vapor pressure such as acetone and ethanol. However, n-butanol is significantly less polar than any other solvent in the system and is present at considerably higher concentrations in the feed.

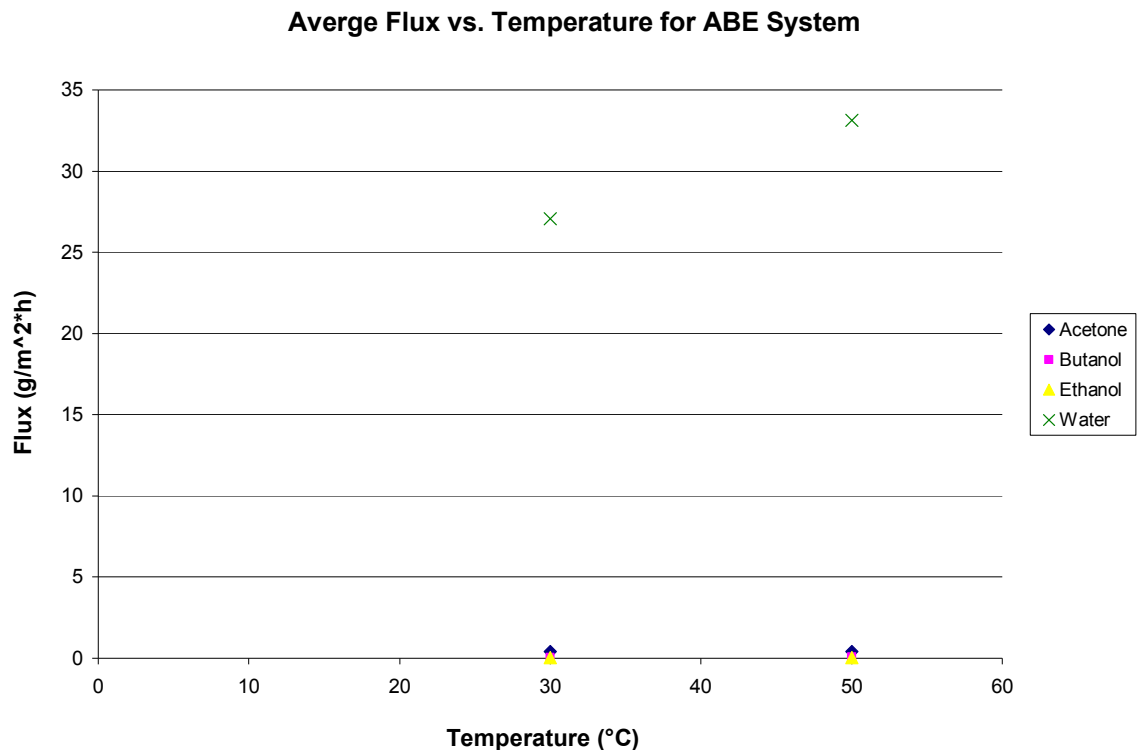






Figure 5.1 Flux of acetone, n-butanol, ethanol and water through a PDD-TFE membrane as a function of temperature.

The PDD-TFE copolymer membrane is typically more selective for water compared to other solvents with larger molecular dimensions as seen in Figures 3.8, 3.9 and 3.11. This correlation has been determined earlier through pure component permeation tests for six organic solvents, Figures 4.13. If the molecular dimensions of these compounds are analyzed against each other, a chart such as Table 5.1 can be produced. Here it can be seen that water still possesses smaller molecular dimensions than the VOCs under considerations. The separation factor for water over an organic solvent or a VOC is shown in Figure 5.2. Separation factor for water over n-butanol is the largest at approximately 7,180 at 30°C. Additionally, the separation factor for water over

ethanol is slightly higher than that over acetone, 900 versus 235, respectively. This is consistent with previously compiled data. The PDD-TFE membrane is somewhat size exclusive and it can be seen that separation factors for larger molecules like n-butanol are significant over smaller ones such as acetone. Given such high separation factors for water over organic solvents, the permeate produced from this process consists of 1.2 wt% acetone, 0.08 wt% n-butanol, 0.06 wt% ethanol and the balance is water.

Table 5.1 Molecular Dimensions of ABE Solvents and Water

Structure	Name Mol. Wt.	Boiling Pt. (° C)	Density (g/cm ³)	Smallest Diameter* (Å)	Largest Diameter* (Å)	Area* (Å ²)	Volume* (Å ³)
	Acetone 58.08	56	0.79	1.753	4.264	95.2	72.12
	n-butanol 74.12	118	0.81	1.749	6.665	121.77	95.68
	Ethanol 46.07	78.4	0.789	1.759	3.667	81.92	59.24
	Water 18.02	100	1	0.967	1.561	36.43	19.39

*as estimated using WaveFunction Spartan program

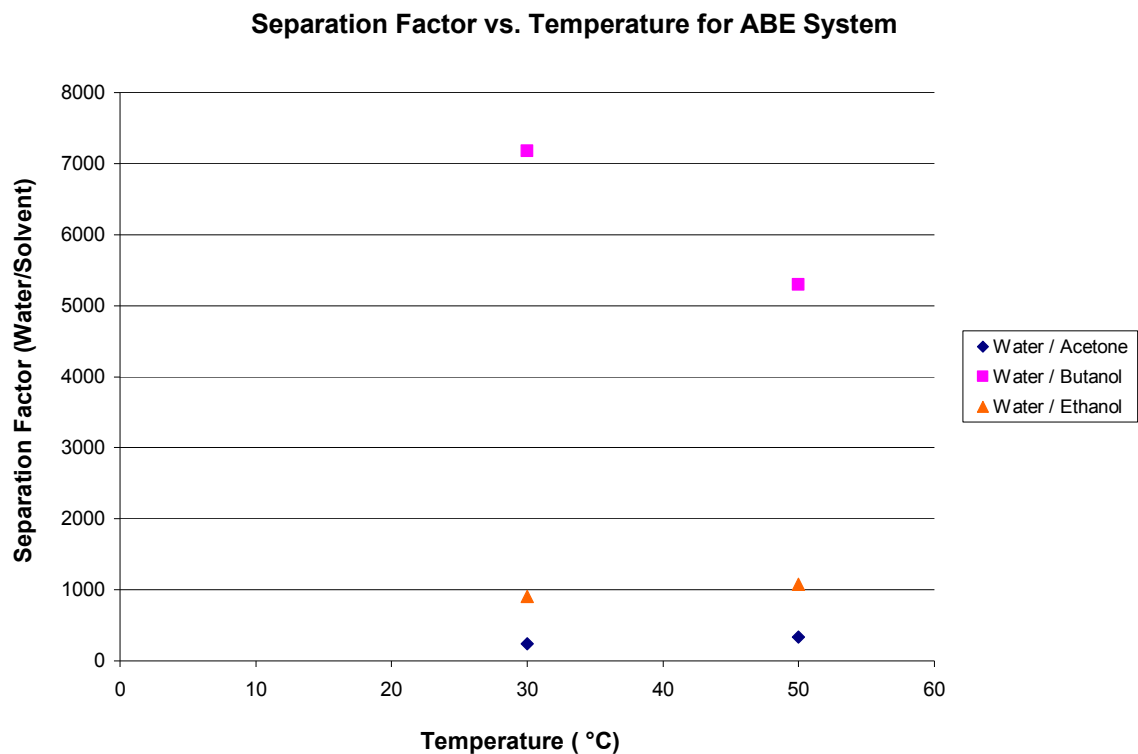


Figure 5.2 Separation factor of the PDD-TFE membrane of water over VOCs as a function of temperature.

This result is significantly different than those found by Smuleac et al. [21].

Dehydration of aqueous solutions of ethanol has achieved selectivity values as high as 318 using a feed stock of 1.2 wt% water and 98.8 wt% ethanol. However, at higher concentrations of ethanol, selectivity of the membrane reduces to approximately to 33 [21]. To reiterate, the feed used in this thesis contains 5.3 wt% of ethanol and 10.8 wt% water. In this situation, there is much more water present in the feed than ethanol. Therefore, water can readily permeate across the PDD-TFE membrane at higher rates than ethanol. At the same time, the presence of n-butanol and acetone introduces more

sources of solvent-solvent interaction and solvent-membrane interaction. This can further affect the amount of effective ethanol available at the membrane interface.

Solubility of each solvent into PDD-TFE has not been measured for pure component. Both acetone and ethanol are significantly more polar than n-butanol. Competitive sorption as well as molecular dimensions would strongly affect the selectivity of the membrane for one solvent over the other. Given the sorption values of other solvents, acetone and ethanol would not increase the dry weight of PDD-TFE by more than 0.6%.

5.2 Dehydration of Ethylene Glycol

Ethylene glycol has been widely used as a coolant or a non-volatile antifreeze. In addition, it is present as a precursor in manufacturing polyesters. More importantly, ethylene glycol is synthesized via the hydrolysis of ethylene oxide in the presence of water. The products of the reaction are then dried through a series of evaporators and then undergo a further distillation process in order to recover purified ethylene glycol [32]. Distillation, for the removal of water, may not be economical due to the significant boiling point of water if compared to its molecular weight. Effective and cost efficient removal of water from this polar solvent is highly desired. PDD-TFE membrane in a pervaporation process has, so far, been proved to be effective for dehydration purposes.

Results using this PDD-TFE membrane material have exhibited some success. The separation factor for water over ethylene glycol ranges from 2,400 to 12,800 depending on the concentration of water present in the feed as seen in Figure 5.3 Much higher separation factors have been speculated for this system in view of the results of

aprotic solvent dehydration. Ethylene glycol is similar to that of DMSO, DMF, and DMAc in many respects when compared to water. These solvents are significantly larger than water in terms of molecular dimensions. In addition, ethylene glycol possesses a rather high boiling point of 197.3°C, greater than those of the previous aprotic solvents studied.

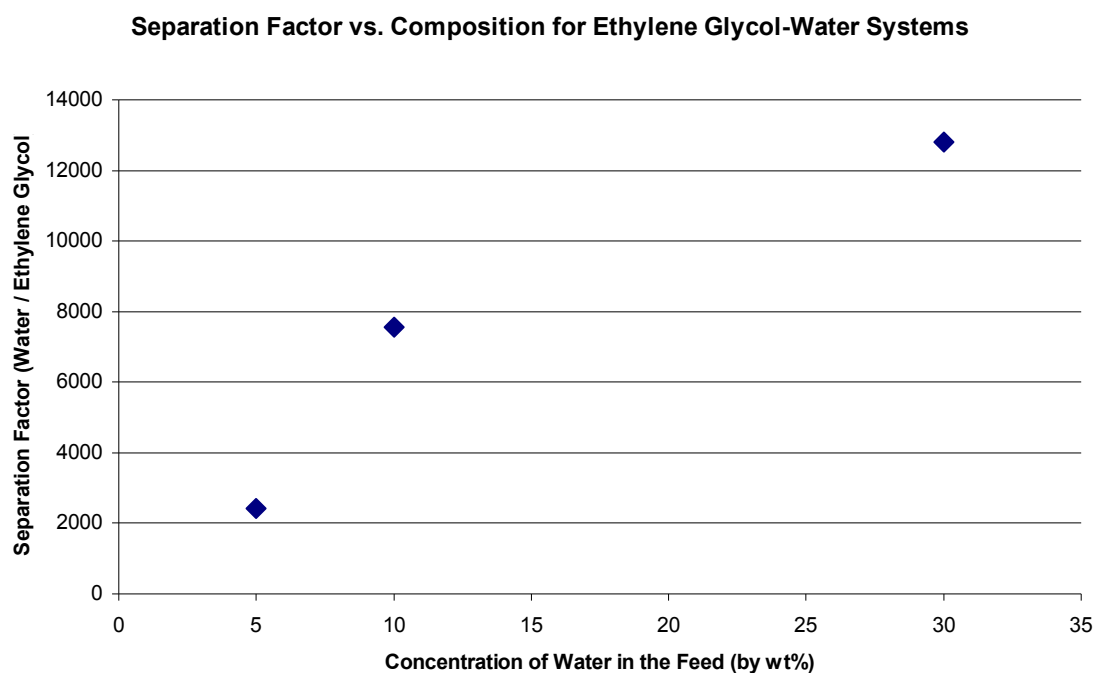


Figure 5.3 Separation factor of a PDD-TFE membrane for ethylene glycol-water systems.

Ethylene glycol flux through the membrane also is dependent on the feed composition. Though it is not apparent in Figure 5.4, the flux for ethylene glycol decreases from 0.015 g/(m²-h) to 0.0008 g/(m²-h) as the concentration of water in the feed increases from 5 wt% to 30 wt%. Water flux ranges from 13.6 to 24.1 g/(m²-h) from these results.

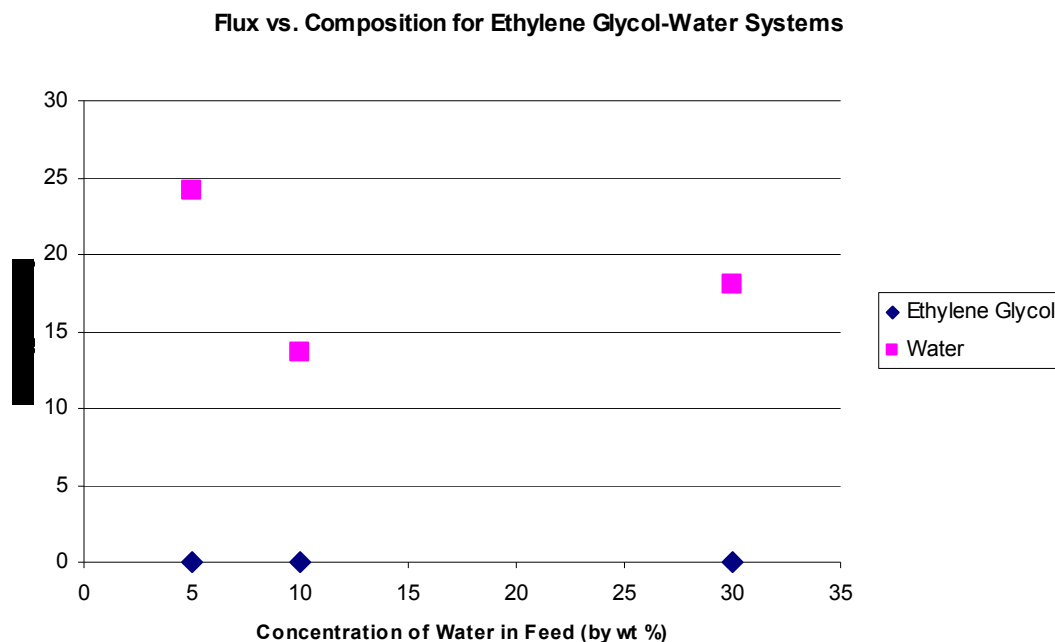


Figure 5.4 Flux across a PDD-TFE membrane for ethylene glycol-water system.

These results are higher than those found by composite membranes containing carbon nanotubes [33] and NaA zeolite membrane materials also used in pervaporation [34]. Composite membranes composed of polyvinylamine (PVAm) and poly(vinyl alcohol) incorporating carbon nanotubes are placed onto a microporous substrate of polysulfone. Using a 1-99 wt% water-ethylene glycol feed at 70°C, a composite membrane containing 2 wt% carbon nanotubes has been found to achieve a separation factor of 1,160 and a permeation flux of 146 g/(m²-h) [33]. ON a per micron basis, overall separation factor and flux using a PDD-TFE membrane are significantly larger. A recent study using a NaA zeolite membrane in a pilot scale operation has been able to achieve separation factors greater than 5,000 and permeation flux of 4.04 kg/(m²-h) using a feed containing 20 wt% water [34]. The PDD-TFE membrane offers higher performance in terms of separation factor.

CHAPTER 6

GENERAL CONCLUSIONS AND RECOMMENDATIONS FOR THE FUTURE

A poly-2,2-dimethyl-1,1,3-dioxole-tetrafluoroethylene (PDD-TFE) copolymer membrane of the CMS-3 variety has demonstrated success in separating gases such as oxygen and nitrogen [16 – 17]. PDD-TFE membranes have unique characteristics, particularly, that of possessing a high fractional free volume. Furthermore, the sizes of these free volume regions are large on average, between 5.9 – 6.3 Å [29]. This potentially allows for the separation of liquid organic solvent molecules to be removed via size exclusion. Due to tetrafluoroethylene being incorporated into the material, the membrane also exhibits extremely high solvent resistance and a high T_g . As a polymer membrane material, this enables it to be used widely across a number of applications industrially from inert gases to aggressive liquid solvents. The motivation behind this research is to apply a known membrane used in gas separation and to determine its performance in pervaporation to separate liquid solvent mixtures. To fully explore the capabilities of the membrane, systems of solvents containing solvents of various characteristics have been selected.

Aprotic solvents, such as N,N-dimethylformamide, N,N-dimethylacetamide, and N,N-dimethylsulfoxide, possess rather large molecular dimensions as well as high boiling points. Separation factors between 600 to 12,000 have been achieved by dehydrating aprotic solvent-water feeds containing 1 to 10 wt% water. This is due in part of the PDD-TFE copolymer membrane's ability to separate by size exclusion compounded by the limited driving force of high boiling solvents in the pervaporation process. Water, in comparison to these aprotic solvents, has significantly smaller molecular dimensions as

well as a lower boiling point which allow it to permeate through the membrane more selectively and at a faster rate. Water fluxes in solution with DMAc and DMSO range from $6 - 9 \text{ g}/(\text{m}^2\text{-h})$ and $4.5 - 9.8 \text{ g}/(\text{m}^2\text{-h})$, respectively (Figures 3.5 and 3.6). In aqueous solutions of DMF, water flux can be as high as $77 \text{ g}/(\text{m}^2\text{-h})$ and decreases proportionally as the solvent concentration increases (Figure 3.7). The overall performance of the PDD-TFE membrane can be comparable to that of NaA zeolite membranes on a per micron basis. This provides a polymeric membrane alternative which is typically much more economical in commercial scale processes.

The size selective nature of the PDD-TFE copolymer membrane is of great interest. If a relationship can be observed between molecular dimensions and permeability coefficient, then a molecular transport profile can be generated for this membrane. In order to tease out the sensitivity and the limits of the membrane, separation of common organic solvents has been completed which includes methanol, tetrahydrofuran, toluene and ethyl acetate. These solvents possess a wide range of molecular dimensions, geometries, volatilities, and polarities. Separation of these organic solvents has been less successful than the dehydration of the aprotic solvents. A separation factor of approximately 6 has been achieved for ethyl acetate-toluene systems across all compositions. Separating mixtures of methanol and toluene have produced a maximum separation factor of 7.7. Finally, very little if any separation occurs when separating tetrahydrofuran-toluene systems. Flux values for organic solvents are considerably less than water flux found in the dehydration of aprotic solvents. Though performance using these organic solvents has been limiting, pure component permeation results have been able to yield a correlation between molecular dimension and overall

permeability coefficient. Such a result will potentially allow this membrane to be useful for other separations.

Permeability coefficient of any solvent with PDD-TFE decreases with increasing temperature. This behavior is not expected for typical glassy polymers in which diffusion coefficients increase dramatically compared to the decrease of solubility coefficients with increasing temperature. It has been observed that from gas permeation results by Merkel et al. [27], that solvent solubility into the membrane is influenced particularly by Langmuir sorption.

The PDD-TFE copolymer membrane possesses potential specifically in dehydration which can be used in removing water from fermentation broth as well as mixtures with ethylene glycol. The maximum separation factor achieved for ethylene glycol-water systems is approximately 12,800 with a water fluxes of 24.1 g/(m²-h). This result is similar to those observed during dehydrating N,N-dimethylformamide. The removal of water from a pervaporation-based permeate produced by Thongsukmak and Sirkar [15] has yielded promising results. From a feed of 5.3 wt% ethanol, 10.8 wt% water, 27.7 wt% acetone and 56.2 wt% n-butanol, the highest separation factor achieved for water over each organic solvent is 900, 235 and 7,180. The water flux that has been observed is between 27 and 33 g/(m²-h).

Further prospects for the usage of PDD-TFE as a pervaporation membrane may lie in separating mixtures of alcohols such as ethanol and n-butanol for energy usage. Though distillation of the two can produce high yields, a pervaporation process may prove to be more economical. An estimate from previous results gives a separation factor of ethanol over n-butanol of approximately 8. However, the feed contains a significant

amount of water as well as acetone, more than one third of the composition by weight. Binary separation of ethanol and n-butanol may give rise to larger separation factors and flux values. Potential other uses for PDD-TFE as a membrane are directly related to that of dehydration in both liquid and gas phase. As water is an invaluable resource with increasing scarcity, the purification of water is ever growing in importance. PDD-TFE may also be useful in removing potable water from highly contaminated water sources, occurring both naturally, or in industry.

APPENDIX A

ESTIMATION OF SOLUBILITY PARAMETERS OF SOLVENTS INTO TRADITIONAL GLASSY POLYMERS

Dual mode sorption (DMS) has been a useful method in determining how solutes are able to penetrate through amorphous polymeric materials. The principle behind solute sorption in a polymer has been spearheaded by Cohen and Turnbull [33] in which they profess that any molecular transport that occurs in a liquid may cause a redistribution of free volume in that liquid. The relevancy of this founding concept has been expanded upon in the polymer field. Though the free volume in glassy polymers can be as much as approximately 30% for perfluorinated copolymers such as PDD-TFE, typical glassy polymers possess a fractional free volume of about 13%. Even at 13% or lower, the fractional free volume in a polymer system is still significant to affect both sorption and diffusion of a fluid through that material.

In dual mode sorption, molecules either are sorbed by the membrane through ordinary dissolution mechanism or in void regions of frozen polymer often referred to as “holes.” Sorption occurs in these cases by a linear Henry’s Law relation and Langmuir-type expression, respectively [34]:

$$C = C_D + C_H = k_D P + \frac{C'_H b P}{1 + b P} \quad (\text{A.1})$$

where C is the molar concentration of the solute in the polymer, C_D and C_H are the amounts of solute contributed by Henry’s Law and Langmuir sorption respectively, k_D is the Henry’s Law constant, P is pressure, C'_H is the Langmuir sorption capacity, b is the Langmuir affinity constant.

It should be noted that “holes” are not restricted to areas of solely sorption. A fraction, F , of the “holes” present in the polymer also contributes to diffusion through the membrane. To account for this, the molar concentration can be expressed as $C = C_D + FC_H$. Diffusion in these regions can be described as Fickian in nature as described by the following relation [34].

$$N = -D_D \frac{dC}{dz} \quad (\text{A.2})$$

where N is the molar flux, D_D represents the diffusion coefficient, C is the molar concentration and z is in the direction of the membrane thickness. The allowance of diffusion to occur in these frozen polymer regions accounts for the effect of pressure on diffusion during time-lag measurements. This was done for Teflon AF 2400 for solutes such as methanol [30]. The time measured before constant permeation can be observed is known as time-lag. If “holes” were completely immobile, then pressure would not affect diffusion, only sorption.

If the expression for molar concentration is differentiated using Equation A.3, molar flux can be seen as (Dual Transport):

$$N = -D_D \frac{dC_D}{dz} - FD_D \frac{dC_H}{dz} \quad (\text{A.3})$$

From this relationship, it is more apparent that contributions to diffusion also correspond to Henry’s Law and Langmuir sorption into the membrane material. Dual mode sorption is successful in modeling experimental data since it allows for some fraction of regions

surrounded by frozen polymer to act both as sites of sorption as well as pathways for diffusion.

However, the dual mode sorption model is empirical in nature. This is in contrast with other popular theoretical methods of determining sorption coefficients such as the Flory-Huggins relationship. The Flory-Huggins equation has been used to estimate solubility of a particular solute into a polymer. This can be done by calculating the activity of a desired solute in the polymer system given by the following relation [35].

$$\ln a_1 = \frac{\Delta\mu_1}{RT} = \ln \varphi_1 + \left(1 - \frac{1}{r}\right)\varphi_2 + \chi\varphi_2^2 \quad (\text{A.4})$$

where $\Delta\mu_1$ is the chemical potential of dissolution for the solute, φ_1 and φ_2 are volume fractions of the solute and polymer in the stationary phase, r is the degree of polymerization and χ is the Flory-Huggins interaction parameter. This calculation also requires some rigor in estimating the parameters needed to determine the activity of the solute in the polymer system, particularly the Flory-Huggins interaction parameter. It has been shown by Belov et al. [35] that this parameter can be determined at infinite dilution using Equation A.4.

$$\chi^\infty = \ln \frac{RT}{V_g P_1^0 M_1} - \frac{P_1^0}{RT} (B_{11} - V_1) - \left(1 - \frac{1}{r}\right) \quad (\text{A.4})$$

Experimental support has been given by Patterson et al. [36]. The above equation has been verified to be applicable to elastic flexible polymers with relatively weak interactions. However, this is not the case for a glassy polymer such as PDD-TFE. To emphasize the difference between the behavior of rubbery and glassy polymers, Belov et

al. [37] have succinctly summarized studies on sorption of Teflon AF 1600 and Teflon AF 2400 in both their rubbery and glassy state. It can be seen in the retention diagrams of $C_{13} - C_{17}$ n-alkanes in Figure A.1 that there is a substantial change in behavior once the glass transition temperature, T_g , is exceeded.

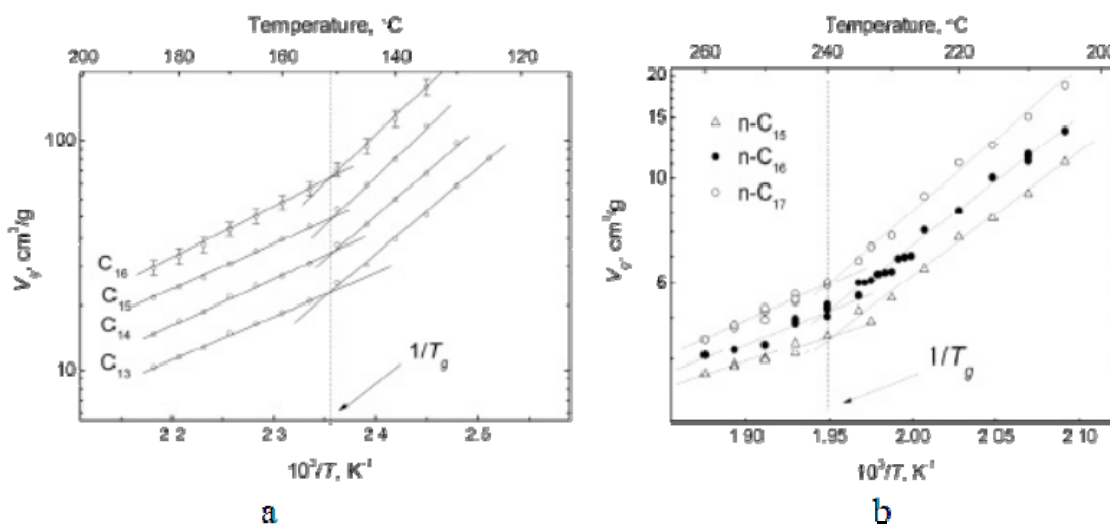


Figure A.1 Retention diagrams for n-alkanes in (a) AF1600 and (b) AF2400.

Sorption correspondingly is affected when the temperature is above or below T_g . Teflon AF 1600 and AF 2400 in the rubbery state can be characterized by positive excess partial molar enthalpies. These findings reflect the unfavorable interactions between large chain hydrocarbons and perfluorinated polymers. Below the T_g as a glassy polymer, Teflon AF 1600 and AF 2400, these once positive excess partial molar enthalpies become negative. It has been commented that cohesive energy of the glassy polymer may have a considerable influence on the total excess partial molar enthalpy. As a result of these negative molar enthalpies, solubility coefficients of Teflon AF 1600 and AF 2400 are two orders of magnitudes larger than their rubbery counterparts.

A recently published work by Sarti and De Angelis aims to expand the limitations of the Flory-Huggins relationship for glassy polymers [38]. In general, the calculation of

any liquid solute in a glassy polymer differs from a rubbery one. When a glassy polymer is heated beyond its glass transition temperature, it reaches a state of equilibrium which can be predicted by a number of models. These models may include the lattice fluid theory (LF), statistical associating fluid theory (SAFT) and perturbed hard sphere chain theory (PHSC). However, for glassy polymers, they are less than desirable as accurate models due their non-equilibrium state below the glass transition temperature.

To account for glassy non-equilibrium state of the polymer, two popular equations of states arise from this lack in accurate thermodynamics modeling, non-equilibrium thermodynamics of glassy polymers (NET-GP) and non-equilibrium lattice fluid theory (NELF). The former has been said to be successful at predicting solubility isotherms for gases and vapors in pure glasses or in glassy polymer blends. The latter has been used to estimate solubility of single gases in glassy polymeric blends and in composite membranes as well as mixed gases in glassy polymers.

Sarti and De Angelis [38] have focused on estimating solubility of liquid solutes in glassy polymers in particular, a more suitable tool for a pervaporation process. This study utilizes a NET-GP approach and NELF in conjunction with a number of other assumptions to model the interactions between the non-equilibrium state of the polymer and the solute molecules. The investigation had succeeded in estimating solubility of water in polycarbonate when swelling is a non-issue. Still, this model may not be suitable for PDD-TFE, a copolymer that possesses a significant amount of free volume as it is dependent on K_{ij} , a binary interaction parameter. The binary interaction parameter as it is defined only accounts for behavior of the liquid solute inside of the rubbery version of

the polymer. It might not be able to accurately estimate solubility of the same solute into the glassy polymer which can be two orders of magnitude times larger than that in the rubbery state.

Thermodynamic models such as the Flory-Huggins relationship can accurately predict solubility of solutes into rubbery polymers. However, for glassy polymers, the non-equilibrium state of the frozen polymer regions must be accounted for when calculating these parameters. Additional models such as NET-GP and NELF have provided some insight into estimating these forces at the membrane interface. Despite recent success in thermodynamics, the current models cannot be applied to copolymer materials such as PDD-TFE.

APPENDIX B
EXPERIMENTAL DATA

The following tables include both operating conditions and the data obtained under those conditions. Each experiment is typically run for approximately 7 hours using a membrane sample with an effective area of about 11.39 cm².

B.1 Experiments on Dehydrating Aprotic Solvents with Small Amounts of Water

Table B.1 Experimental Data for DMAc (99 wt%) – Water (1 wt%) Systems

Temperature (°C)	30	50	60
Feed Concentration (wt%)			
Water	1	1	1
N,N-Dimethylacetamide	99	99	99
Permeate Concentration (wt%)			
Water	98.7	99.2	99.0
N,N-Dimethylacetamide	1.3	0.8	1.0
Mass Flux (g/(m ² -h))			
Water	5.983	6.139	6.618
N,N-Dimethylacetamide	0.085	0.055	0.070
Separation Factor (Water-DMAc)	7537	12373	9985

Table B.2 Experimental Data for DMAc (95 wt%) – Water (5 wt%) Systems

Temperature (°C)	30	50	60
Feed Concentration (wt%)			
Water	5	5	5
N,N-Dimethylacetamide	95	95	95
Permeate Concentration (wt%)			
Water	98.7	99.4	98.3
N,N-Dimethylacetamide	1.3	0.6	2.5
Mass Flux (g/(m ² -h))			
Water	5.825	4.046	8.549
N,N-Dimethylacetamide	0.080	0.091	0.133
Separation Factor (Water-DMAc)	1470	3607	1953

Table B.3 Experimental Data for DMAc (90 wt%) – Water (10 wt %) Systems

Temperature (°C)	30	50	60
Feed Concentration (wt%)			
Water	10	10	10
N,N-Dimethylacetamide	90	90	90
Permeate Concentration (wt%)			
Water	99.7	99.3	99.1
N,N-Dimethylacetamide	0.3	0.7	0.9
Mass Flux (g/(m ² -h))			
Water	6.186	9.145	7.886
N,N-Dimethylacetamide	0.048	0.060	0.073
Separation Factor (Water-DMAc)	2891	1353	1107

Table B.4 Experimental Data for DMF (10 wt%) – Water (90 wt%) Systems

Temperature (°C)	30	50	60
Feed Concentration (wt%)			
Water	10	10	10
N,N-Dimethylformamide	90	90	90
Permeate Concentration (wt%)			
Water	99.8	99.8	99.8
N,N-Dimethylformamide	0.2	0.2	0.2
Mass Flux (g/(m ² -h))			
Water	56.941	77.239	59.689
N,N-Dimethylformamide	0.130	0.132	0.119
Separation Factor (Water-DMF)	9276	12514	10766

Table B.5 Experimental Data for DMF (95 wt%) – Water (5 wt%) Systems

Temperature (°C)	30	50	60
Feed Concentration (wt%)			
Water	5	5	5
N,N-Dimethylformamide	95	95	95
Permeate Concentration (wt%)			
Water	99.8	99.5	99.3
N,N-Dimethylformamide	0.2	0.5	0.7
Mass Flux (g/(m ² -h))			
Water	29.878	58.223	33.799
N,N-Dimethylformamide	0.155	0.208	0.184
Separation Factor (Water-DMF)	2344	4943	3359

Table B.6 Experimental Data for DMF (99 wt%) – Water (1 wt%) Systems

Temperature (°C)	30	50	60
Feed Concentration (wt%)			
Water	1	1	1
N,N-Dimethylformamide	99	99	99
Permeate Concentration (wt%)			
Water	92.5	93.7	97.0
N,N-Dimethylformamide	7.5	6.3	3.0
Mass Flux (g/(m ² -h))			
Water	4.881	4.217	5.912
N,N-Dimethylformamide	0.394	0.301	0.181
Separation Factor (Water-DMF)	1372	1583	3478

Table B.7 Experimental Data for DMSO (90 wt%) – Water (10 wt%) Systems

Temperature (°C)	30	50	60
Feed Concentration (wt%)			
Water	10	10	10
N,N-Dimethylsulfoxide	90	90	90
Permeate Concentration (wt%)			
Water	99.3	98.9	99.3
N,N-Dimethylsulfoxide	0.7	1.1	0.7
Mass Flux (g/(m ² -h))			
Water	9.838	8.207	9.185
N,N-Dimethylsulfoxide	0.064	0.081	0.066
Separation Factor (Water-DMSO)	1281	1234	1251

Table B.8 Experimental Data for DMSO (95 wt%) – water (5 wt%) Systems

Temperature (°C)	30	50	60
Feed Concentration (wt%)			
Water	5	5	5
N,N-Dimethylsulfoxide	95	95	95
Permeate Concentration (wt%)			
Water	97.0	98.3	99.4
N,N-Dimethylsulfoxide	3.0	1.7	0.6
Mass Flux (g/(m ² -h))			
Water	7.380	7.099	7.548
N,N-Dimethylsulfoxide	0.225	0.066	0.043
Separation Factor (Water-DMSO)	654	1555	3152

Table B.9 Experimental Data for DMSO (99 wt%) – Water (1 wt%) Systems

Temperature (°C)	30	50	60
Feed Concentration (wt%)			
Water	1	1	1
N,N-Dimethylsulfoxide	99	99	99
Permeate Concentration (wt%)			
Water	98.7	98.8	99.1
N,N-Dimethylsulfoxide	1.3	1.2	0.9
Mass Flux (g/(m ² -h))			
Water	4.561	6.094	8.046
N,N-Dimethylsulfoxide	0.056	0.066	0.065
Separation Factor (Water-DMSO)	7664	8834	11226

B.2. Experiments Separating Organic-Organic Mixtures

Table B.10 Experimental Data for Methanol (25 wt%) – Toluene (75 wt%) Systems

Temperature (°C)	30	50	60
Feed Concentration(wt%)			
Methanol	25	25	25
Toluene	75	75	75
Permeate Concentration (wt%)			
Methanol	72.2	68.5	68.1
Toluene	27.8	31.5	31.9
Mass Flux (g/(m ² -h))			
Methanol	1.064	1.232	1.619
Toluene	0.431	0.472	0.634
Separation Factor (Methanol-Toluene)	7.8	6.6	6.4

Table B.11 Experimental Data for Methanol (50 wt%) – Toluene (50 wt%) Systems

Temperature (°C)	30	50	60
Feed Concentration(wt%)			
Methanol	50	50	50
Toluene	50	50	50
Permeate Concentration (wt%)			
Methanol	78.9	81.5	81.5
Toluene	21.1	18.5	18.5
Mass Flux (g/(m ² -h))			
Methanol	0.931	1.100	1.368
Toluene	0.208	0.209	0.259
Separation Factor (Methanol-Toluene)	3.7	4.4	4.4

Table B.12 Experimental Data for Methanol (75 wt%) – Toluene (25 wt%) Systems

Temperature (°C)	30	50	60
Feed Concentration(wt%)			
Methanol	75	75	75
Toluene	25	25	25
Permeate Concentration (wt%)			
Methanol	92.6	90.1	88.1
Toluene	7.4	9.9	11.9
Mass Flux (g/(m ² -h))			
Methanol	1.227	1.694	2.266
Toluene	0.084	0.156	0.259
Separation Factor (Methanol-Toluene)	4.8	3.4	2.8

Table B.13 Experimental Data for THF (25 wt%) – Toluene (75 wt%) Systems

Temperature (°C)	30	50	60
Feed Concentration(wt%)			
THF	25	25	25
Toluene	75	75	75
Permeate Concentration (wt%)			
THF	29.0	21.3	22.5
Toluene	71.0	78.7	77.5
Mass Flux (g/(m ² -h))			
THF	0.131	0.226	0.291
Toluene	0.342	0.898	1.071
Separation Factor (THF-Toluene)	1.2	0.8	0.9

Table B.14 Experimental Data for THF (50 wt%) – Toluene (50 wt%) Systems

Temperature (°C)	30	50	60
Feed Concentration(wt%)			
THF	50	50	50
Toluene	50	50	50
Permeate Concentration (wt%)			
THF	54.9	49.8	48.5
Toluene	45.1	50.2	51.5
Mass Flux (g/(m ² -h))			
THF	1.208	0.550	1.959
Toluene	1.054	0.605	2.203
Separation Factor (THF-Toluene)	1.2	1.0	0.9

Table B.15 Experimental Data for THF (75 wt %) – Toluene (25 wt%) Systems

Temperature (°C)	30	50	60
Feed Concentration(wt%)			
THF	75	75	75
Toluene	25	25	25
Permeate Concentration (wt%)			
THF	89.4	83.2	83.0
Toluene	10.6	16.8	17.0
Mass Flux (g/(m ² -h))			
THF	0.202	0.249	0.300
Toluene	0.026	0.053	0.066
Separation Factor (THF-Toluene)	2.9	1.7	1.6

Table B.16 Experimental Data for Ethyl Acetate (25 wt%) – Toluene (75 wt%) Systems

Temperature (°C)	30	50	60
Feed Concentration(wt%)			
Ethyl Acetate	25	25	25
Toluene	75	75	75
Permeate Concentration (wt%)			
Ethyl Acetate	4.9	6.0	5.6
Toluene	95.1	94.0	94.4
Mass Flux (g/(m ² -h))			
Ethyl Acetate	0.160	0.339	0.281
Toluene	3.353	5.739	5.069
Separation Factor (Toluene-Ethyl Acetate)	6.5	5.3	5.7

Table B.17 Experimental Data for Ethyl Acetate (50 wt%) – Toluene (50 wt%) Systems

Temperature (°C)	30	50	60
Feed Concentration(wt%)			
Ethyl Acetate	50	50	50
Toluene	50	50	50
Permeate Concentration (wt%)			
Ethyl Acetate	12.6	13.5	15.6
Toluene	87.4	86.5	84.4
Mass Flux (g/(m ² -h))			
Ethyl Acetate	0.681	0.493	0.412
Toluene	5.027	3.410	2.418
Separation Factor (Toluene-Ethyl Acetate)	6.9	6.4	5.5

Table B.18 Experimental Data for Ethyl Acetate (75 wt%) – Toluene (25 wt%) Systems

Temperature (°C)	30	50	60
Feed Concentration(wt%)			
Ethyl Acetate	75	75	75
Toluene	25	25	25
Permeate Concentration (wt%)			
Ethyl Acetate	32.9	34.3	34.2
Toluene	67.1	65.7	65.8
Mass Flux (g/(m ² -h))			
Ethyl Acetate	1.574	1.851	1.441
Toluene	3.470	3.794	2.964
Separation Factor (Toluene-Ethyl Acetate)	6.1	5.7	5.8

B.3 Separating Volatile Organic Compounds from Water for Biofuels

Table B.19 Experimental Data for a Synthetic ABE Feed Containing Water

Temperature (°C)	30	50
Feed Concentration(wt%)		
Acetone	27.68	27.68
Butanol	56.19	56.19
Ethanol	5.28	5.28
Water	10.84	10.84
Permeate Concentration (wt%)		
Acetone	1.12	0.01
Butanol	0.08	0.13
Ethanol	0.06	0.05
Water	98.75	99.06
Mass Flux (g/(m ² -h))		
Acetone	0.415	0.396
Butanol	0.027	0.064
Ethanol	0.021	0.024
Water	27.066	33.112
Separation Factor		
Water over Acetone	235	337
Water over Butanol	7182	5299
Water over Ethanol	904	1075

APPENDIX C
SAMPLE CALCULATIONS

The following section includes calculations required to determine parameters such as activity coefficients, separation factor, flux and overall permeability coefficient. These are necessary in order to measure the general performance of a pervaporation process.

C.1 Estimating Activity Coefficients from NTRL Using Parameters in ASPEN

Example: Use the NTRL relation to determine the activity coefficients of a 72.6 wt%-27.4 wt% mixture of methanol and toluene at 30°C using the provided equations from ASPEN.

$$\ln \gamma_i = \frac{\sum_j x_j \tau_{ji} G_{ji}}{\sum_k x_k G_{ki}} + \sum_j \frac{x_j G_{ij}}{\sum_k x_k G_{kj}} \cdot \left(\tau_{ij} - \frac{\sum_m x_m \tau_{mj} G_{mj}}{\sum_k x_k G_{kj}} \right) \quad (\text{C.1})$$

$$G_{ij} = \exp(-\alpha_{ij} \tau_{ij}) \quad (\text{C.2})$$

$$\tau_{ij} = a_{ij} + \frac{b_{ij}}{T} + e_{ij} \cdot \ln(T) + f_{ij} \cdot T \quad (\text{C.3})$$

$$\alpha_{ij} = c_{ij} + d_{ij} \cdot (T - 273.15) \quad (\text{C.4})$$

If methanol is defined as species i, and toluene as species j, the following mixture specific parameters available from ASPEN are as follows:

Table C.1 Activity Coefficients for a 72.6 – 26.4 wt% Methanol-Toluene Mixture

	Methanol, i		Toluene, j
a_{ij}	0	a_{ji}	0
b_{ij}	640.5	b_{ji}	821.9
c_{ij}	0.3	c_{ji}	0.3
d_{ij}	0	d_{ji}	0
e_{ij}	0	e_{ji}	0
f_{ij}	0	f_{ji}	0

For methanol:

$$x_i = (72.6/32.04)/((72.6/32.04)+(27.4/92.14)) = 0.884$$

$$\alpha_{ij} = 0.3 + 0*(303.15 - 273.15) = 0.3$$

$$\tau_{ij} = 0.3 + (640.5 / 545.67) + 0*\ln(545.67) + 0*(545.67) = 1.474$$

$$G_{ij} = \exp((- 0.3)*(1.474)) = 0.703$$

For toluene:

$$x_j = (27.4/92.14)/((72.6/32.04)+(27.4/92.14)) = 0.116$$

$$\alpha_{ji} = 0.3 + 0*(303.15 - 273.15) = 0.3$$

$$\tau_{ji} = 0.3 + (821.9 / 545.67) + 0*\ln(545.67) + 0*(545.67) = 1.50$$

$$G_{ji} = \exp((- 0.3)*(1.50)) = 0.637$$

The parameters involving interactions of methanol with toluene (i-j) and toluene with methanol (j-i) are both required to determine the activity coefficient of both species i and j in Equation C.1. By reducing Equation C.1 to a system involving only two species, the final results can be found:

$$\gamma_i = 1.07 \text{ (for methanol)}$$

$$\gamma_j = 4.15 \text{ (for toluene)}$$

C.2 Separation Factor and Flux

Example: Determine flux of tetrahydrofuran for a PDD-TFE membrane using a 75 wt% - 25 wt% feed of tetrahydrofuran and toluene at 30°C and the separation factor of tetrahydrofuran over toluene at the same conditions.

Experimental flux is typically defined as the total weight of solvent that permeates through the membrane area, A_m , over a period time, t , in hours. This is given in the following relation.

$$J_{\text{exp}} = \frac{V_i \cdot \rho_i}{A_m t} \quad (\text{C.5})$$

The volume of permeate present in the sample is determined by gas chromatography by use of a calibration curve. Analysis by gas chromatography results in a measurement of area under a curve of a peak that correlates to a particular solvent.

For tetrahydrofuran, i:

$$\rho_i = 0.8892 \text{ g/m}^3$$

$$A_m = 0.001139 \text{ m}^2$$

$$t = 7 \text{ hours}$$

$$\text{Area under the curve} = 104.9 \mu\text{V}^2$$

$$V_i = C_i * V_T$$

$$V_T = 0.85 \text{ mL}$$

where V_i is the volume of species i in the permeate sample, C_i is the volumetric concentration of species i , and V_T is the total volume of the permeate sample.

From the calibration curve:

$$104.9 = (43582)C_i + 29.012$$

$$C_i = 0.0017 \text{ mL THF / mL}$$

$$V_i = 0.001445 \text{ mL}$$

Therefore, the experimental flux for tetrahydrofuran under these conditions is:

$$J_{\text{exp}} = (0.001445 * 0.8892) / (0.001139 * 7) = 0.0209 \text{ g/(m}^2\text{-h)}$$

To determine the separation factor between tetrahydrofuran and toluene, the weight, W_i , present in permeate of each solvent must be found. This can be calculated using V_i , C_i , V_T and ρ_i . Then the weight fraction in the permeate, y_i , is determined by dividing the weight of solvent i by the total weight of the solvent in the sample, W_T . This is done on an average basis of five runs by gas chromatography.

$$W_i = (C_i * V_T) * \rho_i = V_i * \rho_i$$

$$W_T = W_i + W_j$$

$$y_i = W_i / W_T$$

On average:

$$V_i = 0.00143 \text{ mL}$$

$$V_j = 0.000177 \text{ mL}$$

For tetrahydrofuran, i , and toluene, j :

$$\rho_i = 0.8892 \text{ g/mL}$$

$$\rho_j = 0.8669 \text{ g/mL}$$

$$W_i = (0.00143 * 0.8892) = 0.001272 \text{ grams}$$

$$W_j = (0.000177 * 0.8669) = 0.000153 \text{ grams}$$

$$W_T = (0.001272 + 0.000153) = 0.001425 \text{ grams}$$

$$y_{ip} = (0.001272 / 0.001425) = 0.894$$

$$y_{jp} = (0.000153 / 0.001425) = 0.106$$

For separation factor, α_{ij} :

$$\alpha_{ij} = \frac{y_{ip} / y_{if}}{y_{jp} / y_{jf}} \quad (2.2)$$

$$\alpha_{ij} = (0.894 / 0.75) / (0.106 / 0.25) = 2.88.$$

C.3 Estimate the Overall Permeability Coefficient from Experimental Flux

Example: Estimate the overall permeability coefficient for methanol in a 50 wt% – 50 wt% methanol-toluene mixture through a PDD-TFE membrane at 50 °C.

$$J_i = \frac{Q_i}{\delta} (x_i \gamma_i P_i^{\text{sat}} - y_i P_{\text{perm}}) \quad (2.1)$$

From operating conditions and/or literature values:

$$\delta = 0.000025 \text{ m}$$

$$\gamma_i = 1.188$$

$$P_i^{\text{sat}} = 416.6 \text{ mm Hg}$$

$$y_i = 0.927$$

$$P_{\text{perm}} = 9 \text{ mm Hg}$$

From experimental values:

$$x_i = 0.792$$

$$J_i = 1.10 \text{ g}/(\text{m}^2\text{-h})$$

The above relation, Equation 2.1, can be re-arranged for a more direct calculation for overall permeability coefficient.

$$Q_i = \frac{J_i \cdot \delta}{(x_i \gamma_i P_i^{sat} - y_i P_{perm})} \quad (\text{C.6})$$

$$Q_i = (1.10 * 0.00025) / ((0.792 * 1.188 * 416.6) - (0.967 * 9))$$

$$Q_i = 7.667 * 10^{-8} \text{ (g-m) / (m}^2\text{-h-mm Hg)}$$

REFERENCES

1. Tsapatsis, M., Toward High-Throughput Zeolite Membranes, *Science* 334 (2011) 767-768.
2. Fleming, H.L., Slater, C.S., in *Membrane Handbook*, ed. Ho and Sirkar, Norwell, Massachusetts: Kluwer Academic Publishers (1992) 105-159.
3. Panek, D., Konieczny, K., Pervaporation of toluene and toluene/acetone/ethyl acetate aqueous mixtures through dense composite polydimethylsiloxane membranes, *Desalination* 200 (2006) 367-373.
4. Villaluenga, J.P.G., Khayet, M., Godino, P., Seoane, B., Mengual, J.I., Pervaporation of Toluene/Alcohol Mixtures through a Coextruded Linear Low-Density Polyethylene Membrane, *Ind. Eng. Chem. Res.* 42 (2003) 386-391.
5. Lue, S.J., Ou, J.S., Kuo, C.H., Chen, H.Y., Yang, T., Pervaporative separation of azeotropic methanol/toluene mixtures in polyurethane-poly(dimethylsiloxane) (PU-PDMS) blend membranes: Correlation with sorption and diffusion behaviors in a binary solution system, *J. Membr. Sci.* 347 (2010) 108-115.
6. Zhou, M., Persin, M., Sarrazin, J., Methanol removal from organic mixtures by pervaporation using polypyrrole membranes, *J. Membr. Sci.* 117 (1996) 303-309.
7. Ray, S., Ray, S.K., Separation of organic mixtures by pervaporation using crosslinked and filled rubber membranes, *J. Membr. Sci.* 285 (2006) 108-119.
8. Mandal, S., Pangarkar, V.G., Separation of methanol-benzene and methanol-toluene mixtures by pervaporation: effects of thermodynamics and structural phenomenon, *J. Membr. Sci.* 201 (2002) 175-190.
9. Aminabhavi, T.M., Naik, H. G., Pervaporation separation of water/dimethylformamide mixtures using poly(vinyl alcohol)-g-polyacrylamide copolymeric membranes, *J. Appl. Poly. Sci.* 83 (2002) 273.
10. Devi, D.A., Smitha, B., Sridhar, S., Aminabhavi, A.M., Pervaporation separation of dimethylformamide/water mixtures through poly(vinyl alcohol)/poly(acrylic acid) blend membranes, *Sep. and Purif. Technol.* 51 (2006) 104.
11. Shah, D.; Kissick, K., Ghorpade, A., Hannah, R., Bhattacharyya, D., Pervaporation of alcohol-water and dimethylformamide-water mixtures using hydrophilic zeolite NaA membranes: mechanisms and experimental results, *J. Membr. Sci.* 179 (2000) 185.

12. Kolsh, P., Sziladi, M., Noack, M., Caro, J., Kotsis, L., Kotsis, I., Sieber, I., Ceramic Membranes for Water Separation from Organic Solvents, *Chem. Eng. Technol.* 25 (2002) 4.
13. Matsumura, M., Kataoka, H., Separation of dilute aqueous butanol and acetone solutions by pervaporation through liquid membranes, *Biotechnol. Bioeng.* 30 (1987) 887-895.
14. Qin, Y., Sheth, J.P., Sirkar, K.K., Pervaporation membrane that are highly selective for acetic acid over water, *Ind. Eng. Chem. Res.* 42 (2003) 582-595.
15. Thongsukmak, A., Sirkar, K.K., Extractive pervaporation to separate ethanol from its dilute aqueous solutions characteristic of yeast fermentation processes, *J. Membr. Sci.* 329 (2009) 119-129.
16. Nemser, S., Applications of membranes in industry: Glassy fluoropolymer membranes, pp. 1- 20, 21st Aharon Katzir-Katchalsky Conference. September 5-8, 1993. Rehovot, Israel.
17. Majumdar, S., Stookey, D., Nemser, S., Dewatering Ethanol with Chemically and Thermally Resistant Perfluoropolymer Membranes, International Conference on Membranes. July 12-18, 2008. Honolulu, Hawaii.
18. Pinnau, I., Toy, L.G., Gas and vapor transport properties of amorphous perfluorinated copolymer membranes based on 2,2,-bistrifluoromethyl-4,5-difluoro-1,3-dioxole/tetrafluoroethylene, *J. Membr. Sci.* 109 (1996) 125-133.
19. Prabhakar, R.S., Freeman, B.D., Roman, I., Gas and vapor sorption and permeation in poly 2,2,4-trifluoro-5-trifluoromethoxy-1,3-dioxole-co-tetrafluoroethylene, *Macromolecules* 37 (2004) 7688-7697.
20. Zhao, H., Zhang, J., Wu, N., Crowley, K., Weber, S., Transport of Organic Solutes through Amorphous Teflon AF Films, *J. Am. Chem. Soc.* 127. (2005) 15112-15119.
21. Smuleac, V., Wu, J., Nemser, S., Majumdar, S., Bhattacharyya, D., Novel perfluorinated polymer-based pervaporation membranes for the separation of solvent/water mixtures, *J. Membr. Sci.* 352 (2010) 41-49.
22. Polyakov, A.M., Starannikova, L.E., Yampol'skii, Y.P., Amorphous Teflons AF as organophilic pervaporation materials transport of individual components, *J. Membr. Sci.* 216 (2003) 241-256.
23. Polyakov, A., Bondarenko, G., Tokarev, A., Yampol'skii, Y., Intermolecular interactions in target organophilic pervaporation through the films of amorphous Teflon AF2400, *J. Membr. Sci.* 277 (2006) 108-119.

24. Van Veen, H.M., Rietkirk, M.D.A., Shanahan, D.P., Van Tuel, M.M.A., Kreiter, R., Castricum, H.L., Ten Elshof, J.E., Vente, J.P., Pushing membrane stability boundaries with HybSi pervaporation membranes, *J. Membr. Sci.* 380 (2011) 124-131.
25. Personal Communication, Dr. S. Majumdar, Compact Membrane Systems Inc., April 2011.
26. Zolandz, R.R., Fleming, G.K. in *Membrane Handbook*, ed. Ho and Sirkar, Norwell, Massachusetts: Kluwer Academic Publishers (1992) 19-101.
27. Merkel, T.C., Bondar, V., Nagai, K., Freeman, B.D., Yampol'skii, Yu. P., Gas Sorption, Diffusion, and Permeation in Poly (2,2-bis(trifluoromethyl)-4,5-difluoro-1,3-dioxole-co-tetrafluoroethylene), *Macromolecules* 32 (1999) 8427-8440.
28. Vieth, W.R, Howell, J.M., Hsieh, J.H., Dual sorption theory, *J. Membr. Sci.* 1 (1976) 177-220.
29. Alentiev, A.Y., Yampol'skii, Y.P., Shantarovich, V.P., Nemser, S.M., Platé, N.A., High transport parameters and free volume of perfluorodioxole copolymers, *J. Membr. Sci.* 126 (1997) 123-132.
30. Jansen, J.C., Friess, K., Drioli, E., Organic vapour transport in glassy perfluoropolymer membranes: A simple semi-quantitative approach to analyze clustering phenomena by time lag measurements, *J. Membr. Sci.* 367 (2011) 141-151.
31. Da Silva, L. Dos Santos Politi, J.R., Gargano, R. Theoretical Study of Tetrahydrofuran: Comparative Investigation of Spectroscopic and Structural Properties Between Gas and Liquid Phases, *Int. J. Quant. Chem.* 111 (2011) 2914-2921.
32. Feng, X., Huang, R.Y.M., Pervaporation with chitosan membranes. I. Separation of water from ethylene glycol by a chitosan/polysulfone composite membrane, *J. Membr. Sci.* 116. (1996) 67-76.
33. Hu, S.Y., Zhang, Y., Lawless, D., Feng, X., Composite membranes comprising of polyvinylamine-poly(vinyl alcohol) incorporated with carbon nanotubes for dehydration of ethylene glycol by pervaporation, *J. Membr. Sci.* 417-718 (2012) 34-44.
34. Yu, C., Zhong, C., Liu, Y. Gu, X., Yang, G., Xing, W., Xu, N., Pervaporation dehydration of ethylene glycol by NaA zeolite membranes, *Chem. Eng. Research and Design* 90 (2012) 1372-1380.
35. Cohen, M.H., Turnbull, D., Molecular Transport in liquids and glasses, *J. Chem. Phys.* 31 (1959) 1164-1169.

36. Barbari, T.A., Dual-Mode Free Volume Model for Diffusion of Gas Molecules in Glassy Polymers, *J. Poly. Sci. Part B: Poly. Phys.* 35 (1997) 1737-1746.
37. Belov, N.A., Safranov, A.P., Yampolskii, Y.P., Thermodynamics of sorption of an amorphous perfluorinated copolymer AF1600 studied by inverse gas chromatography, *Macromolecules* 44 (2011) 902-912.
38. Patterson, D., Tewari, Y.B., Schreiber, H.P., Guillet, J.E., Application of gas-liquid chromatography to the thermodynamics of polymer solutions, *Macromolecules* 4 (1971) 356-359.
39. Belov, N.A., Shashkin, A.V., Safranov, A.P., Yampolskii, Y.P., Thermodynamic parameters of sorption in amorphous perfluorinated copolymers AFs below and above their glass transition temperature, *International Workshop on Membrane Distillation and Related Technologies*. October 9-12, 2011. Ravello, Italy.
40. Sarti, G.C., De Angelis, M.G., Calculation of the Solubility of Liquid Solutes in Glassy Polymers, *AIChE J.* 58 (2012) 292-301.